**UNIVERSIDADE FEDERAL FLUMINENSE**
**INSTITUTO DE FÍSICA**

Orlenys N. Troconis

# General Relativistic Study of the Structure of Highly Magnetized Neutron Stars

Niterói
May 2017

i

# Orlenys N. Troconis

# General Relativistic Study of the Structure of Highly Magnetized Neutron Stars

Tese apresentada ao Instituto de Física da Universidade Federal Fluminense, para a obtenção de Título de Doutor em Ciências, na Área de Física.

Orientador: Rodrigo P. Negreiros

**Niterói**
**February 2018**

# Comissão Julgadora:

Prof. Dr.
Manuel Malheiro

Prof. Dr.
Sérgio Duarte

Prof. Dr.
Bruno Werneck Mintz

Prof. Dr.
Raissa Mendes

Prof. Dr.
Rodrigo P. Negreiros.

*To the love of my God*
*Al amor de Dios*
*Para o amor de Deus*

# Acknowledgement

I thank the Brazilian institution CAPES for the financial assistance in the development of this work.

I thank Programa de Pós-graduação do Instituto de Física da Universidade Federal Fluminense.

I thank my supervisor Rodrigo Negreiros for his patience, motivation, and help, both in academic and personal life.

I thank my coworker Gabriel Bezerra for his patience teaching me FORTRAN and his valuable collaboration in the numerical solution. Você é um mestre!

I thank Prof. Victor Varela for his valuable contribution to understand many aspects studied in this work.

I thank the secretary of the Instituto de Física da Universidade Federal Fluminense, Fernanda, for her patience and attention with my person.

I thank my alma matter UNIVERSIDAD CENTRAL DE VENEZUELA (UCV): La casa que vence las sombras. Te amo mi UCV.

Thanks to my lovely family for their support in every step of my life. My sister Aimara Navarro, thanks for listening to me when I need and for my niece Verónica, and my brother Edgar Troconis thanks for been with me and my lovely dog Brandy every night and early morning during my undergraduating studies, for your jokes until today and for my dear nephew David. Thanks to my lovely cousin and brother Marcos González you have been an important person in all aspects of my life. Thanks to my cousin Vanessa Orel-

lana, her husband Esteban Benenatti and their children Estefano (mi bebito gerber) and Salvatore (mi grandote) and my dear nana Magi for helping me and my family. Thanks to my aunt Sonia Troconis for being a mother for me, for your love and support in my life. Thanks to my grandmother Nicolaza González (mima), I don´t have words to express my acknowledgements with you, thanks for your sweetie love and for your funny way of being. Thanks to a really wonderful woman, my dear mother Irma Troconis, thanks for you love, for your support and your incredible strength. Mami te admiro por tu gran capacidad de haber luchado por nosotros tres. Te amo mami! Thanks to my cousin Yamabari Gonzalez and my dear nieces Kissbel and Naissbel, las amo piojas!

Thank to my dear Venezuelan friends: Richard and Vanessa for your help when I arrived to Brasil the first time. Thanks to Rut Díaz and her husband Manuel Moreira for open the doors of your house. Thanks to a special person who I know few time ago and has demonstrated your friendship with me: mi panita Adriana.

Thanks to my friends: Rafael, Bruno, Gustavo and Marcos for your help, support and funny time with me during these years. Gustavo (meu vizinho lindo) obrigada pelo seu apoio e por me dar sua mão nos momentos dificeis. Marquinho eu não tenho palavras para te expresar a gratitude que sinto por você, pelas suas palavras de força quando mais precisava. Obrigada por me falar do amor do nosso senhor Deus com carinho, amor e fé. Vocês: Rafa, Brunin, Gustavo (meu vizinho) e Marquinho, moram no meu coração! Thanks to my dear doctor Rodrigo Goes for you valuable help with my health and your kindly attention to my person. Muito obrigada meu querido doutor Rodrigo.

Thanks to my best friends: Monica and Daniela Bartolini. I love you ragazzitas! You and your family are part of my heart. Thanks to my fiend and colleague Solmar Varela for your friendship and support, gracias mi Sol por siempre estar allí.

Thanks to all my students in Venezuela because I really learned from you.

Thanks to the most important person in my soul, in my life, in all I can be, you my God! Gracias mi señor Jesús por estar en cada instante de mi vida, gracias por apoyarme, guiarme, oírme, amarme. Gracias por todas las veces que me levantaste cuando estaba a punto de darme por vencida. Gracias por guiarme en este camino llamado vida, por todas las lágrimas que limpiaste con tus palabras, con tu amor, con tus señales, con las personas que colocas en mi camino. Sólo tú conoces mi corazón, mi alma y sabes lo que te amo mi Señor. Gracias por tu nuestra madre virgen María. Gracias mi señor Jesús, te amo mi pepi.

## *Resumo*

As estrelas de nêutrons são um dos objetos astrofísicos mais compactos e mais densos conhecidos na natureza. Estes resultaram da explosão da supernova de uma estrela massiva. A massa destes objetos situa-se entre uma e duas massas solares, normalmente tem raios de 10 km e muitas vezes giram rapidamente. Muitas das estrelas de nêutrons têm campos magnéticos intensos, que levam à emissão de rádio e radiação de raios-X. Essas características, juntamente com o progresso contínuo na astrofísica observacional e a observação recente de ondas gravitacionais provenientes da colisão de estrelas de nêutrons, tornam esses objetos poderosos laboratórios astrofísicos para uma ampla gama de fenômenos físicos interessantes. Este trabalho é dedicado a estudar os efeitos de campos magnéticos fortes na estrutura das estrelas de nêutrons, no âmbito da teoria da relatividade geral. O primeiro passo é estudar os aspectos formais do campo magnético na estrutura estelar e as equações do campo gravitacional usando duas abordagens diferentes, o que nos permite introduzir novas quantidades e sua possível interpretação física. O segundo passo é apresentar o teorema do virial relativista como uma integral que fornece uma verificação de consistência das soluções numéricas. Como terceiro passo, estudamos o formalismo teórico que descreve as estrelas de nêutrons com rotação não nula e altamente magnetizadas no contexto das equações de Einstein-Maxwell. Especificamente, para estrelas de nêutrons magnetizadas, estudamos campos magnéticos poloidais e configurações estáticas. São apresentadas as quantidades físicas relevantes que descrevem esses objetos e uma discussão sobre a contribuição da energia eletromagnética para a massa gravitacional. Finalmente, encontramos o espaço-tempo que descreve estrelas de nêutrons com rotação não nula e magnetizadas. A distribuição dos diferentes termos que contribuem para a massa gravitacional e a relação massa-raio é apresentada. Os resultados obtidos mostram que para estrelas com campo magnético central $\sim 10^{18}$ G os efeitos eletromagnéticos incrementam a massa em um $10.1\%$ em relação à configuração sem campo magnético. Os estudos realizados neste trabalho são fundamentais para a compreensão dos objetos astrofísicos conhecidos como Soft-Gamma Repeaters e Anomalous X-Ray Pulsars,

que são entendidos como sendo uma classe de estrelas de nêutrons chamadas de magnetares.

**Palavras-chave:** Estrelas de nêutrons, magnetars, campo magnético, estrutura.

*Abstract*

Neutron stars are one of the most compact and densest astrophysical objects known in nature, they result from the supernova explosion of a massive star. The mass of these objects lies between one and two solar masses, they typically have radii of 10 km and often spin very rapidly. Many of the neutron stars have very strong magnetic fields, which lead to the emission of radio and X-ray radiation. The density inside these objects is many times higher than the density of atomic nuclei. These features, together with the ongoing progress in observational astrophysics and the recent observation of gravitational waves coming from the collision of neutron stars, make these objects superb astrophysical laboratories for a wide range of interesting physical phenomena. This work is devoted to study the effects of strong magnetic fields in the structure of neutron stars, within the framework of the general relativity theory. The first step is to study the formal aspects of the magnetic field in the stellar structure and gravitational equations using two different approaches, which allow us to introduce new quantities and their possible physical interpretation. The second step is to present the relativistic virial theorem as an integral that provides a consistency check of numerical solutions. As third step, we study the theoretical formalism describing rotating and highly magnetized neutron stars within the context of Einstein-Maxwell's equations. Specifically, for magnetized neutron stars, we study poloidal magnetic fields and static configurations. The relevant physical quantities describing these objects are presented and a discussion about the contribution of the electromagnetic energy to the total gravitational mass. Finally, we find the spacetime describing rotating and magnetized neutron stars. The distribution of the different terms that contribute to the total gravitational mass and the mass-radius relation is presented. The results show that for stars with magnetic field $\sim 10^{18}$ G the electromagnetic effects increase the mass in $10.1\%$ with respect to the configuration without magnetic field. The studies performed in this work are key for the understanding the astrophysical objects known as a Soft-Gamma Ray Repeaters and Anomalous X-Ray Pulsars, which are understood as being one class of neutron stars called as magnetars.

x

# List of Figures

# List of Tables

# Contents

# Chapter 1

# Introduction

Neutron stars, which are the remnant of core collapse supernova, are one of the most compact objects known in nature. The first modest observation of this phenomenal explosion was in 1054 when Chinese astronomers saw and recorded the spectacular explosion of a supernova, the guest star, as the Chinese called it, was so bright that people saw it in the sky during the day for almost a month and remained visible in the evening sky for more than a year [1]. The idea of neutron stars was proposed in 1934 by Walter Baade and Fritz Zwicky, only two years after the discovery of the neutron by the English physicist Sir James Chadwick [2]. They tentatively proposed that in a supernova explosion ordinary stars are turned into stars that consist of extremely closely packed neutrons that they called neutron stars.

Compact stars are in fact the remnant of massive stars, typically have radii of 10 km and masses that lie between one and two solar masses. The density inside these objects is many times higher than the density of atomic nuclei (possibly up to 10 times denser). Neutron stars are generally associated with three classes of astrophysical objects: Pulsars [3], which are generally accepted to be rotating neutron stars, compact X-ray sources, and magnetars, which are objects with very high magnetic fields. These objects are very dense and as such, its structure must be described in the framework of Einstein´s general relativity. In this theory, gravity is seen as curvature of spacetime, caused by mass-energy. The problem of describing the structure of compact stars consists of finding the spacetime

geometry both inside and outside of the star for a given mass distribution.

It is common the use of the spherically symmetric solution to describe a wide range of astrophysical objects, this assumption implies a lot of mathematical simplifications and allows the use of Birkhoff´s theorem [4] which states that the spacetime outside of a spherical, nonrotating, gravitating body must be given by the Schwarzschild metric. This theorem led Tolman-Openheimer-Volkoff [5–7] to calculate the hydrostatic equilibrium equations describing spherically symmetric fluids, known as TOV-equations. For dissipative fluid spheres it is possible to match the interior and exterior spacetime with the Vaidya metric (known as the radiating Schwarzshild metric) [8] allowing a physical interpretation of the dynamical equations in terms of the dissipative variables [9] and a definition of the gravitational arrow of time [10].

In the study of self gravitating compact objects it is usually assumed that small deviations from spherical symmetry are likely to take place. Such small deviations are not appropriate for stars with strong magnetic fields where a full axially symmetric treatment is necessary to properly describe the system. Since the detection of soft gamma repeaters (SGRs) in 1979 and an anomalous X-ray pulsar (AXPs) in 1981, there has been great interest in neutron stars that could be powered by their strong magnetic field. In 1992 and 1993, Duncan and Thompson proposed the magnetar model [11,12] and, since then, approximately 30 SGRs and AXPs have been observed [13]. In recent years, several measurements have estimated surface magnetic fields to be of the magnitude of $10^{15}$ G for the sources 1E 1048.1-5937 and 1E 2259+586 [14]. Furthermore, the observed X-ray luminosities of the AXPs may require a field strength $B \gtrsim 10^{16}$ G [15], in addition the observational data for the source 4U 0142+61 suggests internal magnetic fields to be on the magnitude $10^{16}$ G with a possible toroidal configuration [16]. The population statistics of SGRs suggest that magnetars may constitute a significant fraction $\gtrsim 10\%$ of the neutron star population [17]. Hence it seems likely that some mechanism is capable of generating large magnetic fields in nascent neutron stars.

The above considerations motivate the study of the effects of magnetic field on neutron star properties. Such study can be carried out from three points of view: the effects

in the composition of the neutron star matter, evolution and structure. The first point is related to how magnetic fields may change the equation of state of dense matter, for example generating anisotropies, and affecting the matter composition. The second point is related to the effects on neutron stars´temporal evolution, for example the influence of a time dependent magnetic field in the true age of neutron stars. The last point is related to the structural aspects, for example how magnetic fields change the mass and radius of neutron stars.

The goal of this work is to study, within a totally general relativistic framework, the effects of magnetic fields in the structure of neutron stars, i.e. how magnetic fields affect the spacetime geometry of these compact objects. Me and my coworkers developed a complete study of the three aspects, i.e. microscopical, structural and evolutionary, such study can be found in [18].

We begin our goal studying the formal aspects of the magnetic field in the stellar structure and gravitational equations using two different approaches. The first one uses Weyl spherical coordinates from which conservation equations will be derived taking into account the magnetic field contribution. The resulting equations will be compared with a previous work where no magnetic contribution was considered and doing so, new quantities with possible physical interpretation will be introduced. The second approach is based in the study of Cook et al. [19] who considered rotating neutron stars and write the Einstein´s equations in terms of flat space elliptic operators and the source terms coming from the matter and others containing non linear quadratic terms in the metric potentials. In this section we will derive the Einstein´s equations following the method of Shapiro, but taking into account the electromagnetic contribution. These equations will be written in terms of the introduced new quantities with the idea to give the same physical interpretation and discuss the electromagnetic contribution to the gravitational mass.

The next step to achieve our goal is to study the relativistic virial theorem. The usefulness of the Newtonian virial theorem in physics and astrophysics is well known, mainly within the context of the equilibrium and stability properties of dynamical systems. The virial theorem relates the time average of kinetic energy of a generic particle with the time

average of the work executed by the forces with which the particles interact. In general relativity, it is common to use the virial theorem derived from a conservation law. In chapter III we present a relativistic version of the virial theorem as an integral identity (and not as a conservation law) for a stationary and asymptotically flat spacetime, based in the $3 + 1$ formalism. The resulting virial integral consists on terms that depend on the gravitational source, rotational properties and metric potential. The idea behind discussing this important theorem as a chapter in this thesis is because the virial theorem is used as a consistency check in numerical solutions.

In chapter IV the theoretical formalism describing rotating and highly magnetized neutron stars will be presented using a full axially symmetric treatment within the context of Einstein-Maxwell equations. The hydrostatic equilibrium equations will be derived within the assumption of infinite conductivity matter and the relevant quantities describing the structure of rotating and highly magnetized neutron stars will be presented.

In chapter V we will deal with the numerical solution of the Einstein-Maxwell equations presented in chapter IV. We first consider a rotating neutron star without magnetic field, modelled as a rotating isotropic fluid distribution. However, it is important to draw attention to the role that is played by the pressure anisotropy in selfgravitating objects as me and my coworkers showed in [20]. Second, we will study a highly magnetized neutron star modelled as a perfect fluid coupled with a poloidal magnetic field, in this last case we restrict to the static solutions (although both are stationary). As we mentioned our goal is to study only the structural consequences of the magnetic field in neutron stars and not the microscopical or evolutionary aspects, because of that we assume as the matter composition a traditional equation of state that is independent of the magnetic field at the microscopical level.

Finally, the conclusions and perspectives for future works are given in chapter VI.

# Chapter 2

# Formal aspects of the magnetic field on the structure of neutron stars

We discuss the formal aspects of the magnetic field in the stellar structure and gravitational equations in the context of Einstein's general relativity. The highly magnetized star is described as a perfect fluid coupled with a poloidal magnetic field using two different approaches, the first one uses Weyl spherical coordinates from which conservation equations will be derived. The second approach is based in the study of Shapiro et al. [19] in which Einstein field equation will be derived taking into account the electromagnetic contribution. New quantities and their possible physical interpretation will be presented in the following sections.

## 2.1 Neutron star structure using Weyl spherical coordinates

We begin by considering a bound, static and axially symmetric source. The line element may be written in cylindrical coordinates as

$$ds^2 = -A^2(dx^0)^2 + B^2[(dx^1)^2 + (dx^2)^2] + D^2(dx^3)^2, \tag{2.1}$$

where we identify $x^0 = t, x^1 = \rho, x^2 = z, x^3 = \phi$ and $A, B, D$ are positive functions of the coordinates $\rho$ and $z$. Here and throughout we set $G = c = 1$. In the Weyl spherical coordinates, the line element (2.1) is

$$ds^2 = -A^2(dt)^2 + B^2[(dr)^2 + r^2(d\theta)^2] + D^2(d\phi)^2, \tag{2.2}$$

where $\rho = rsin\theta$ and $z = rcos\theta$. We denote the coordinates as $x^\mu = (t, r, \theta, \phi)$, and note that $A(r, \theta), B(r, \theta), D(r, \theta)$ are three independent functions.

The source of curvature in Einstein's general relativity is represented by the energy-momentum tensor. For a magnetized neutron star, we describe the system as a perfect fluid coupled to a poloidal magnetic field. The perfect fluid assumption simplifies the mathematical treatment dramatically. One must note, however, that there has also been research considering spherically symmetric dissipative and anisotropic fluid distribution (see for instance refs. [9,10]). As mentioned in the introduction, highly magnetized neutron stars with poloidal fields should be modeled using an axially symmetric metric tensor which increases the complexity of the problem considerably.

The motivation behind the assumption of a poloidal magnetic field is that such assumption is compatible with the circularity of the space-time [21]. It is important to note, however, that non-negligible toroidal magnetic fields are likely to exist in neutron stars, making the study considerably more complicated. The study of toroidal magnetic fields, in addition to poloidal ones is beyond the scope of this work.

Following the scenario discussed above, the energy-momentum tensor for the system is written as that of a perfect-fluid in addition to the energy-momentum tensor of the electromagnetic field,

$$T_{\mu\nu} = T_{\mu\nu}^{PF} + T_{\mu\nu}^{EM}. \tag{2.3}$$

The perfect fluid (PF) contribution is

$$T_{\mu\nu}^{PF} = (\rho + P)u_\mu u_\nu + Pg_{\mu\nu}, \tag{2.4}$$

where $\rho$ and $P$ are, respectively, the rest-frame energy density and pressure, $u^\mu$ is the fluid

4-velocity with $u^\mu u_\mu = -1$. The electromagnetic part (EM) in (4.2) is

$$T_{\mu\nu}^{EM} = \frac{1}{4\pi} \left( F_\mu{}^\alpha F_{\nu\alpha} - \frac{1}{4} g_{\mu\nu} F^{\alpha\beta} F_{\alpha\beta} \right), \tag{2.5}$$

where the Maxwell tensor $F_{\mu\nu}$ is defined in terms of the electromagnetic 4-potential $A_\mu$ as

$$F_{\mu\nu} = A_{\nu,\mu} - A_{\mu,\nu}. \tag{2.6}$$

We are interested in describing a distribution without free-charge and with only poloidal magnetic field, thus the electromagnetic 4-potential is reduced to

$$A_\mu = (0, 0, 0, A_\phi(r, \theta)). \tag{2.7}$$

which leads to the following $F_{\mu\nu}$ (in matrix form)

$$F_{\mu\nu} = \begin{pmatrix} 0 & 0 & 0 & 0 \\ 0 & 0 & 0 & \frac{\partial A_\phi}{\partial r} \\ 0 & 0 & 0 & \frac{\partial A_\phi}{\partial \theta} \\ 0 & -\frac{\partial A_\phi}{\partial r} & -\frac{\partial A_\phi}{\partial \theta} & 0 \end{pmatrix}, \tag{2.8}$$

with the assumptions above the electromagnetic energy-momentum tensor is

$$T^{EM\mu}{}_\nu = \begin{pmatrix} T^{EM0}{}_0 & 0 & 0 & 0 \\ 0 & T^{EM1}{}_1 & T^{EM1}{}_2 & 0 \\ 0 & \frac{1}{r^2} T^{EM1}{}_2 & -T^{EM1}{}_1 & 0 \\ 0 & 0 & 0 & -T^{EM0}{}_0 \end{pmatrix}, \tag{2.9}$$

where the non-vanishin components, in terms of the electromagnetic 4-potential, are given by

$$T^{EM0}{}_0 = -\frac{1}{8\pi} g^{\phi\phi} \left[ g^{rr} \left( \frac{\partial A_\phi}{\partial r} \right)^2 + g^{\theta\theta} \left( \frac{\partial A_\phi}{\partial \theta} \right)^2 \right], \tag{2.10}$$

$$T^{EM1}{}_1 = \frac{1}{8\pi} g^{\phi\phi} \left[ g^{rr} \left( \frac{\partial A_\phi}{\partial r} \right)^2 - g^{\theta\theta} \left( \frac{\partial A_\phi}{\partial \theta} \right)^2 \right], \tag{2.11}$$

$$T^{EM1}{}_2 = \frac{1}{4\pi} g^{rr} g^{\phi\phi} \left( \frac{\partial A_\phi}{\partial r} \right) \left( \frac{\partial A_\phi}{\partial \theta} \right). \tag{2.12}$$

Now, inspired in equation (2.10) we define the following electromagnetic quantities

$$B_\theta = \sqrt{g^{rr}} \left( \frac{\partial A_\phi}{\partial r} \right), \tag{2.13}$$

$$B_r = \sqrt{g^{\theta\theta}} \left( \frac{\partial A_\phi}{\partial \theta} \right). \tag{2.14}$$

It is important to realize that these components are not exactly the components measured by the Eulerian observer, but rather convenient definitions of electromagnetic functions that allow us to write the components of $T^{EM}$ in a more intuitive manner, as

$$T^{EM0}{}_0 = -\frac{1}{8\pi} g^{\phi\phi} \left( B_r^2 + B_\theta^2 \right), \tag{2.15}$$

$$T^{EM1}{}_1 = -\frac{1}{8\pi} g^{\phi\phi} \left( B_r^2 - B_\theta^2 \right), \tag{2.16}$$

$$T^{EM1}{}_2 = \frac{1}{8\pi} 2 g^{\phi\phi} \sqrt{\frac{g^{rr}}{g^{\theta\theta}}} B_r B_\theta. \tag{2.17}$$

In here, if we want to fully comprehend the physical meaning of the components of the electromagnetic energy-momentum tensor, we must draw a parallel with its flat-space

counterpart, given (in S.I. units) as [22]

$$
T^{EM\mu\nu} = \begin{pmatrix}
\frac{1}{2}(\epsilon_0 E^2 + \frac{1}{\mu_0} B^2) & S_x/c & S_y/c & S_z/c \\
S_x/c & -\sigma_{xx} & -\sigma_{xy} & -\sigma_{xz} \\
S_y/c & -\sigma_{yx} & -\sigma_{yy} & -\sigma_{yz} \\
S_z/c & -\sigma_{zx} & -\sigma_{zy} & -\sigma_{zz}
\end{pmatrix}, \tag{2.18}
$$

where $\vec{S} = \frac{1}{\mu_0}\vec{E}\mathrm{x}\vec{B}$ is the Poynting vector and the components $\sigma_{ij}$ are given by

$$
\sigma_{ij} = \epsilon_0 E_i E_j + \frac{1}{\mu_0}B_i B_j - \frac{1}{2}\left(\epsilon_0 E^2 + \frac{1}{\mu_0}B^2\right)\delta_{ij}. \tag{2.19}
$$

The first term in (2.18) is easily identified as the electromagnetic energy density, the other terms in the diagonal, i.e. $\sigma_{xx}, \sigma_{yy}, \sigma_{zz}$ can be read as the electromagnetic pressure and the terms $\sigma_{ij}$ for $i \neq j$ represent shear stress.

Inspired in the electromagnetic energy-momentum tensor for flat space-time, we define the following quantities

$$
W \equiv \frac{1}{8\pi}g^{\phi\phi}\left(B_r^2 + B_\theta^2\right), \tag{2.20}
$$

$$
\Pi \equiv \frac{1}{8\pi}g^{\phi\phi}\left(B_r^2 - B_\theta^2\right), \tag{2.21}
$$

$$
\sigma \equiv \frac{1}{8\pi}2g^{\phi\phi}B_r B_\theta. \tag{2.22}
$$

With these definitions, the matrix form of the electromagnetic energy-momentum tensor looks like

$$
T^{EM\mu}{}_\nu = \begin{pmatrix}
-W & 0 & 0 & 0 \\
0 & -\Pi & r\sigma & 0 \\
0 & \frac{1}{r}\sigma & \Pi & 0 \\
0 & 0 & 0 & W
\end{pmatrix}. \tag{2.23}
$$

From (2.23) we can extract the following properties for $T^{\mu EM}$: it is symmetric, the component $T^{EM00}$ is positive definite and the tensor is traceless, which are the expected properties of an electromagnetic energy-momentum tensor. One must note that equation (2.23) corresponds to the mixed components of the electromagnetic energy-momentum tensor, whereas the first two properties ($T^{EM00}$ positive definite and symmetric) are related to the contravariant components.

Combining (2.4) and (2.23), the matrix form of the energy-momentum tensor describing a perfect fluid coupled with a poloidal magnetic field for the line element (2.2) is

$$T^{\mu\nu} = \begin{pmatrix} \frac{1}{A^2}(\rho + W) & 0 & 0 & 0 \\ 0 & \frac{1}{B^2}(P - \Pi) & \frac{1}{rB^2}\sigma & 0 \\ 0 & \frac{1}{rB^2}\sigma & \frac{1}{(Br)^2}(P + \Pi) & 0 \\ 0 & 0 & 0 & \frac{1}{D^2}(P + W) \end{pmatrix}. \tag{2.24}$$

The first term, i.e. $T^{00}$ in (2.24) represents the total energy density of the system which comes from the perfect fluid distribution and the electromagnetic field, through the quantity $W$; the other diagonal terms correspond to the pressure and as we can see the quantities $\Pi$ and $W$, which depend on the electromagnetic four potential, make part of the pressure of the system. Finally, the off-diagonal terms depend only on the electromagnetic four potential and represent the shear stress of the system $\sigma$.

The Einstein field equations $G^\mu_\nu = 8\pi T^\mu_\nu$ for the spacetime described by (2.2) and the source given by (2.24) are

$$G^0_0 = 8\pi T^0_0 \tag{2.25}$$

$$\Rightarrow \frac{1}{B^3}\left(B_{,rr} + \frac{1}{r}B_{,r} + \frac{1}{r^2}B_{,\theta\theta}\right) + \frac{1}{B^2D}\left(D_{,rr} + \frac{1}{r}D_{,r} + \frac{1}{r^2}D_{,\theta\theta}\right) = -8\pi(\rho + W) + \tag{2.26}$$
$$+ \frac{1}{B^4}\left[(B_{,r})^2 + \frac{1}{r^2}(B_{,\theta})^2\right],$$

$$G^1_1 = 8\pi T^1_1 \tag{2.27}$$

$$\Rightarrow \frac{1}{r^2 B^2}\left(\frac{1}{A}A_{,\theta\theta} + \frac{1}{D}D_{,\theta\theta}\right) + \frac{1}{rB^2}\left(\frac{1}{A}A_{,r} + \frac{1}{D}D_{,r}\right) = 8\pi(P - \Pi) + \tag{2.28}$$

$$- \frac{1}{AB^3}\left(A_{,r}B_{,r} - \frac{1}{r^2}A_{,\theta}B_{,\theta}\right) +$$

$$- \frac{1}{AB^2 D}\left(A_{,r}D_{,r} + \frac{1}{r^2}A_{,\theta}D_{,\theta}\right) +$$

$$- \frac{1}{B^3 D}\left(B_{,r}D_{,r} - \frac{1}{r^2}B_{,\theta}D_{,\theta}\right),$$

$$G^2_2 = 8\pi T^2_2, \tag{2.29}$$

$$\Rightarrow \frac{1}{B^2}\left(\frac{1}{A}A_{,rr} + \frac{1}{D}D_{,rr}\right) = 8\pi(P + \Pi) + \tag{2.30}$$

$$+ \frac{1}{AB^3}\left(A_{,r}B_{,r} - \frac{1}{r^2}A_{,\theta}B_{,\theta}\right) +$$

$$- \frac{1}{AB^2 D}\left(A_{,r}D_{,r} + \frac{1}{r^2}A_{,\theta}D_{,\theta}\right) +$$

$$+ \frac{1}{B^3 D}\left(B_{,r}D_{,r} - \frac{1}{r^2}B_{,\theta}D_{,\theta}\right),$$

$$G^3_3 = 8\pi T^3_3, \tag{2.31}$$

$$\Rightarrow \frac{1}{AB^2}\left(A_{,rr} + \frac{1}{r}A_{,r} + \frac{1}{r^2}A_{,\theta\theta}\right) + \frac{1}{B^3}\left(B_{,rr} + \frac{1}{r}B_{,r} + \frac{1}{r^2}B_{,\theta\theta}\right) = 8\pi(P + W) + \tag{2.32}$$

$$+ \frac{1}{B^4}\left[(B_{,r})^2 + \frac{1}{r^2}(B_{,\theta})^2\right],$$

$$G^1_2 = 8\pi T^1_2, \tag{2.33}$$

$$\Rightarrow \frac{1}{r^2 B^2}\left(\frac{1}{A}A_{,\theta} + \frac{1}{D}D_{,\theta}\right) = 8\pi\sigma - \frac{1}{rAB^3}(A_{,r}B_{,\theta} + A_{,\theta}B_{,r}) + \tag{2.34}$$

$$- \frac{1}{rDB^3}(B_{,r}D_{,\theta} + B_{,\theta}D_{,r}) + \frac{1}{rB^2}\left(\frac{1}{A}A_{,r\theta} + \frac{1}{D}D_{,r\theta}\right),$$

where the subscript $f_{,r} = \frac{\partial f}{\partial r}$, $f_{,\theta} = \frac{\partial f}{\partial \theta}$ and $f_{,rr} = \frac{\partial^2 f}{\partial r^2}$, $f_{,\theta\theta} = \frac{\partial^2 f}{\partial \theta^2}$.

With the goal of providing a physical interpretation to the quantities $W, \Pi$ and $\sigma$ we now derive the conservation equations for a perfect fluid coupled with a poloidal magnetic field and compare these equations with those obtained in [23] where no electromagnetic contribution was considered.

The non-vanishing components of the conservation equations $T^{\mu\nu}_{\;;\nu} = 0$ which represent energy-momentum conservation for the energy-momentum tensor (2.24) are

For $\mu = 0$

$$\dot{\rho} + \dot{W} = 0 \tag{2.35}$$

where the dot denotes derivative with respect to $t$. Equation (2.35) is a consequence of the staticity.

The other non-vanishing components are

$\mu = 1$

$$(P - \Pi)_{,r} + \frac{A_{,r}}{A}(\rho + W + P - \Pi) \quad - \quad \frac{B_{,r}}{B}2\Pi - \frac{D_{,r}}{D}(W + \Pi) + \tag{2.36}$$
$$+ \quad \frac{1}{r}\left[\sigma_{,\theta} + \left(\frac{A_{,\theta}}{A} + 2\frac{B_{,\theta}}{B} + \frac{D_{,\theta}}{D}\right)\sigma - 2\Pi\right] = 0,$$

$\mu = 2$

$$(P + \Pi)_{,\theta} + \frac{A_{,\theta}}{A}(\rho + W + P + \Pi) \quad + \quad \frac{B_{,\theta}}{B}2\Pi - \frac{D_{,\theta}}{D}(W - \Pi) + \tag{2.37}$$
$$+ \quad r\left[\sigma_{,r} + \left(\frac{A_{,r}}{A} + 2\frac{B_{,r}}{B} + \frac{D_{,r}}{D}\right)\sigma\right] + 2\sigma = 0,$$

Equations (2.36) and (2.37) represent the hydrostatic equilibrium conditions. In the special case of no magnetic field and an isotropic fluid, these equations reduce to the Tolman-Openheimer-Volkoff equations [5–7].

At this point it is important to refer to the work of Herrera et al. [23] in which axially symmetric, anisotropic bound sources were studied. The matter content considered

by the authors in locally Minkowski coordinates $(\tau, x, y, z)$ is given by

$$
\hat{T}_{\alpha\beta} = \begin{pmatrix} \mu & 0 & 0 & 0 \\ 0 & P_{xx} & P_{xy} & 0 \\ 0 & P_{yx} & P_{yy} & 0 \\ 0 & 0 & 0 & P_{zz} \end{pmatrix},
\tag{2.38}
$$

where $\mu, P_{xx}, P_{yy}, P_{zz}, P_{xy} = P_{yx}$ denote the energy density, pressure and shear stress, respectively, measured by a locally Minkowskian observer. In a spacetime described by (2.2), the energy-momentum tensor is

$$
T_{\alpha\beta} = (\mu + P)V_\alpha V_\beta + P g_{\alpha\beta} + \Pi_{\alpha\beta},
\tag{2.39}
$$

with

$$
\begin{aligned}
\Pi_{\alpha\beta} &= (P_{xx} - P_{zz})\left(K_\alpha K_\beta - \frac{h_{\alpha\beta}}{3}\right) \\
&+ (P_{yy} - P_{zz})\left(L_\alpha L_\beta - \frac{h_{\alpha\beta}}{3}\right) + 2P_{xy}K_{(\alpha}L_{\beta)},
\end{aligned}
\tag{2.40}
$$

$$
P = \frac{P_{xx} + P_{yy} + P_{zz}}{3}, \quad h_{\alpha\beta} = g_{\alpha\beta} + V_\alpha V_\beta,
\tag{2.41}
$$

where $V_\alpha$, $K_\alpha$ and $L_\alpha$ are 4-vectors in the time, radial and angular directions, respectively.

$$
V_\alpha = (-A, 0, 0, 0), \quad K_\alpha = (0, B, 0, 0), \quad L_\alpha = (0, 0, Br, 0).
\tag{2.42}
$$

The conservation equations calculated in ref. [23] are

$$
\begin{aligned}
P_{xx,r} + \frac{A_{,r}}{A}(\mu + P_{xx}) \quad + \quad & \frac{B_{,r}}{B}(P_{xx} - P_{yy}) + \frac{D_{,r}}{D}(P_{xx} - P_{zz}) + \\
+ \quad & \frac{1}{r}\left[P_{xy,\theta} + \left(\frac{A_{,\theta}}{A} + 2\frac{B_{,\theta}}{B} + \frac{D_{,\theta}}{D}\right)P_{xy} + P_{xx} - P_{yy}\right] = 0,
\end{aligned}
\tag{2.43}
$$

$$P_{yy,\theta} + \frac{A_{,\theta}}{A}(\mu + P_{yy}) \quad + \quad \frac{B_{,\theta}}{B}(P_{yy} - P_{xx}) + \frac{D_{,\theta}}{D}(P_{yy} - P_{zz}) + \tag{2.44}$$
$$+ \quad r\left[P_{xy,r} + \left(\frac{A_{,r}}{A} + 2\frac{B_{,r}}{B} + \frac{D_{,r}}{D}\right)P_{xy}\right] + 2P_{xy} = 0.$$

Comparing equations (2.36) and (2.37), which describe a perfect fluid coupled with a poloidal magnetic field, with the hydrostatic equations (2.43) and (2.44), calculated in ref. [23], which describe an anisotropic fluid (without electromagnetic contribution), we can read the quantity $\rho + W$ as the total energy density of our distribution. In fact, the definition of $W$ given by eq. (2.20) reminds us of the typical definition of the electromagnetic energy density. The quantity $2\Pi$ can be read as the anisotropy of the distribution, and it is a direct consequence of the poloidal magnetic field. The quantity $\sigma$ given by (2.22) can be identified as the shear stress experienced by the fluid. The quantities $W + \Pi$ and $W - \Pi$ can be read as an anisotropy defined with respect to z-axis and $P + \Pi$ and as terms related to the pressure. In conclusion, if we apply the Bondi approach [24] then a locally Minkowskian observer measures, for the perfect fluid coupled with a poloidal magnetic field, $\rho + W$ as the total energy density, $2\Pi$ as the anisotropy caused by the different components of the magnetic field and $\sigma$ as the shear stress of the distribution.

## 2.2   Neutron star structure using Shapiro's approach

Shapiro et. al. [19] studied the spin-up of a rapidly rotating star by angular momen-
tum loss. In this section we use the same metric tensor used by Shapiro et al. but instead
of rotational effects, we consider magnetic field effects on the neutron star structure. The
goal is to write the general relativistic field equations determining the metric potentials in
terms of the quantities introduced in the previous section, i.e. $W, \Pi$ and $\sigma$ and give the same
physical interpretation as before.

The space-time considered by Shapiro et al. is written for rotating equilibrium
models considered as stationary and axisymmetric and given by the following metric tensor,

$$ds^2 = -e^{(\gamma+\rho)}(dt)^2 + e^{2\alpha}[(dr)^2 + r^2(d\theta)^2] + e^{(\gamma-\rho)}r^2 sin^2\theta(d\phi - \omega dt)^2, \qquad (2.45)$$

where the coordinates are $x^\mu = (t, r, \theta, \phi)$ and the metric functions $\gamma$, $\rho$, $\alpha$ and $\omega$ depend
only on the coordinates $(r, \theta)$.

We consider a perfect fluid distribution coupled with a poloidal magnetic field with-
out rotation, i.e. in the equations of [25] the metric potential $\omega = 0$. The energy momentum
tensor $T^{\mu\nu}$ is

$$T^{\mu\nu} = T^{PF\mu\nu} + T^{EM\mu\nu}, \qquad (2.46)$$

with

$$T^{PF\mu\nu} = (\rho_0 + \rho_i + P)u^\mu u^\nu + Pg^{\mu\nu} \qquad (2.47)$$

where $\rho_0$ is the rest energy density, $\rho_i$ is the internal energy density, $P$ is the pressure and
$u^\mu$ is the matter four velocity with $u^\mu u_\mu = -1$. The term $T^{EM}$ is given by eq. (2.5).

The Einstein field equations $G^{\mu\nu} = 8\pi T^{\mu\nu}$ for the distribution described by the
energy-momentum tensor (2.46) using (2.45) following the Cook-Shapiro-Teulkosky approach
(which is inspired by the method of Komatsu-Eriguchi-Hachisu [25]) in which all nonlinear
and coupling terms from $G^{\mu\nu}$ (hence terms associated with geometry) are considered as part

of the source, named as effective source $S_\gamma$ and $S_\rho$.

$$\left(\nabla^2 + \frac{1}{r}\partial_r - \frac{\mu}{r^2}\partial_\mu\right)(\gamma e^{\gamma/2}) = S_\gamma(r,\mu) \tag{2.48}$$

$$\nabla^2\left(\rho e^{\gamma/2}\right) = S_\rho(r,\mu) \tag{2.49}$$

where $\nabla^2$ is the flat-space, spherical coordinate Laplacian, $\mu = cos\theta$. The effective source terms are given by

$$S_\gamma(r,\mu) = e^{\gamma/2}\left[16\pi e^{2\alpha}P + \frac{\gamma}{2}\left(16\pi e^{2\alpha}P - \frac{1}{2}\nabla\gamma.\nabla\gamma\right)\right], \tag{2.50}$$

$$\begin{aligned}
S_\rho(r,\mu) &= e^{\gamma/2}\left[8\pi e^{2\alpha}(\rho_0 + \rho_i + P) + \frac{\gamma_{,r}}{r} - \frac{\mu}{r^2}\gamma_{,\mu} + \frac{\rho}{2}\left(16\pi e^{2\alpha}P - \frac{1}{2}\nabla\gamma.\nabla\gamma - \frac{\gamma_{,r}}{r} + \frac{\mu}{r^2}\gamma_{,\mu}\right)\right] \\
&+ e^{\gamma/2}\frac{e^{-(\gamma-\rho)}}{r^2(1-\mu^2)}2\nabla A_\phi.\nabla A_\phi,
\end{aligned} \tag{2.51}$$

where $f_{,r} = \frac{\partial f}{\partial r}$ and $f_{,\mu} = \frac{\partial f}{\partial \mu}$ and $\nabla f.\nabla f = (f_{,r})^2 + \frac{(1-\mu^2)}{r^2}(f_{,\mu})^2$.

Comparing equation (2.51) with expression (6) in [19] (with $\omega = 0$) we realize the source $S_\rho$ for a perfect-fluid coupled with a poloidal magnetic field can be written as

$$S_\rho(r,\mu) = S_\rho^{PF} + S_\rho^{EM} \tag{2.52}$$

where $S_\rho^{PF}$ corresponds to the perfect fluid contribution and $S_\rho^{EM}$ is the electromagnetic source for the metric potential $\rho$. They are given by

$$S_\rho^{PF} = e^{\gamma/2}\left[8\pi e^{2\alpha}(\rho_0 + \rho_i + P) + \frac{\gamma_{,r}}{r} - \frac{\mu}{r^2}\gamma_{,\mu} + \frac{\rho}{2}\left(16\pi e^{2\alpha}P - \frac{1}{2}\nabla\gamma.\nabla\gamma - \frac{\gamma_{,r}}{r} + \frac{\mu}{r^2}\gamma_{,\mu}\right)\right], \tag{2.53}$$

$$S_\rho^{EM}(r,\mu) = e^{\gamma/2}\frac{e^{-(\gamma-\rho)}}{r^2(1-\mu^2)}2\nabla A_\phi.\nabla A_\phi. \tag{2.54}$$

Hence we can see the effective source for the metric potential $\rho$ is the superposition

of the source corresponding to the perfect fluid distribution plus the influence of the poloidal

magnetic field which depends on $A_\phi$, while comparing $S_\gamma$ source (2.50) with expression (7)

in [19] we realize no magnetic contribution is present in the $\gamma$ effective source.

The third field equation determines the metric potential $\alpha$ and is given by

$$
\begin{aligned}
\alpha_{,\mu} = & -\frac{1}{2}(\gamma_{,\mu} + \rho_\mu) - \{(1 + r\gamma_{,r})^2(1 - \mu^2) + \left[\mu - (1 - \mu^2)\gamma_{,\mu})\right]^2\}^{-1}\times \\
& \times \left[ -\frac{1}{2}\{3\mu^2 - 4\mu(1 - \mu^2)\gamma_{,\mu} + (1 - \mu^2)^2(\gamma_{,\mu})^2\}(\gamma_{,\mu} + \rho_{,\mu}) + \right. \\
& -\frac{1}{2}r\gamma_{,r}(1 + r\gamma_{,r})(1 - \mu^2)(\gamma_{,\mu} + \rho_{,\mu}) + \frac{1}{2}\mu r(1 + r\gamma_{,r})(\gamma_{,r} - \rho_{,r}) + \\
& - r(1 + r\gamma_{,r})(1 - \mu^2)(\gamma_{,r\mu} + \gamma_{,r}\gamma_{,\mu}) + \frac{1}{2}r(1 + r\gamma_{,r})(1 - \mu^2)(\gamma_{,r}\gamma_{,\mu} - \rho_{,r}\rho_{,\mu}) + \\
& + \frac{1}{2}[\mu - (1 - \mu^2)\gamma_{,\mu}](3\mu\rho_{,\mu} + r\rho_{,r}) - \frac{1}{2}[\mu - (1 - \mu^2)\gamma_{,\mu}][r^2\gamma_{,rr} - (1 - \mu^2)\gamma_{,\mu\mu}] + \\
& \left. -\frac{1}{4}r^2[\mu - (1 - \mu^2)\gamma_{,\mu}]\left\{\nabla\gamma.\nabla\gamma + \nabla\rho.\nabla\rho - \frac{2(1 - \mu^2)}{r^2}[(\gamma_{,\mu})^2 + (\rho_{,\mu})^2]\right\} \right] + \\
& + \{(1 + r\gamma_{,r})^2(1 - \mu^2) + \left[\mu - (1 - \mu^2)\gamma_{,\mu})\right]^2\}^{-1}\times \\
& \times e^{-(\gamma-\rho)}\left\{\frac{[\mu - (1 - \mu^2)\gamma_{,\mu}]}{(1 - \mu^2)}\left[\nabla A_\phi.\nabla A_\phi - \frac{2(1 - \mu^2)}{r^2}(A_{\phi,\mu})^2\right] + \frac{2(1 + r\gamma_{,r})}{r}(A_{\phi,r})(A_{\phi,\mu})\right\}.
\end{aligned}
$$
$$(2.55)$$

If we consider no magnetic dipole influence, i.e. $A_\phi = 0$ then equation (2.55) is equation

(11) in [19] with $\omega = 0$.

A possible physical interpretation for quantities related to energy, anisotropy and

shear stress named as $W$, $\Pi$, $\sigma$, respectively, was given in [18] as we discussed in the previous

section. Now, we write Einstein-Maxwell field equations for each metric potential in terms

of these quantities and give them a similar interpretation. We begin writing these quantities

as follow

$$
\begin{aligned}
W & = \frac{1}{8\pi}g^{\phi\phi}(B_r^2 + B_\theta^2) \\
& = \frac{1}{8\pi}g^{\phi\phi}\left(g^{\theta\theta}(A_{\phi,\theta})^2 + g^{rr}(A_{\phi,r})^2\right) \\
& = \frac{1}{8\pi}\frac{e^{-(\gamma-\rho)}e^{-2\alpha}}{r^2(1 - \mu^2)}\nabla A_\phi.\nabla A_\phi,
\end{aligned}
$$
$$(2.56)$$

$$
\begin{aligned}
\Pi &= \frac{1}{8\pi} g^{\phi\phi}(B_r^2 - B_\theta^2) \\
&= \frac{1}{8\pi} g^{\phi\phi} \left( g^{\theta\theta}(A_{\phi,\theta})^2 - g^{rr}(A_{\phi,r})^2 \right) \\
&= -\frac{1}{8\pi} \frac{e^{-(\gamma-\rho)}e^{-2\alpha}}{r^2(1-\mu^2)} \left[ \nabla A_\phi . \nabla A_\phi - \frac{2(1-\mu^2)}{r^2}(A_{\phi,\mu})^2 \right],
\end{aligned}
\tag{2.57}
$$

$$
\begin{aligned}
\sigma &= \frac{1}{8\pi} 2g^{\phi\phi} B_r B_\theta \\
&= \frac{1}{8\pi} 2g^{\phi\phi} \sqrt{g^{\theta\theta}} \sqrt{g^{rr}} (A_{\phi,r})(A_{\phi,\theta}) \\
&= -\frac{1}{8\pi} \frac{2e^{-(\gamma-\rho)}}{r} \frac{e^{-2\alpha}}{r^2(1-\mu^2)^{1/2}}(A_{\phi,r})(A_{\phi,\mu}).
\end{aligned}
\tag{2.58}
$$

Comparing expressions (2.54) with (2.56), we can write for the source of the metric potential $\rho$

$$
S_\rho^{EM}(r,\mu) = e^{\gamma/2}16\pi e^{2\alpha}W.
\tag{2.59}
$$

Therefore the field equation for the metric potential $\rho$ can be written in terms of the quantity $W$

$$
\nabla^2(\rho e^{\gamma/2}) = e^{\gamma/2}\left[ 8\pi e^{2\alpha}(\rho_0 + \rho_i + P + 2W) + \frac{\rho}{2}\left( 16\pi e^{2\alpha}P - \frac{1}{2}\nabla\gamma.\nabla\gamma - \frac{\gamma_{,r}}{r} + \frac{\mu}{r^2}\gamma_{,\mu} \right) \right]
\tag{2.60}
$$

We can see the electromagnetic influence in the term $2W$ and that appears as a sum of the energy density and pressure associated to the perfect fluid distribution, hence this result allows us to take this term as part of the total energy density and pressure, specifically electromagnetic energy density in agreement with the interpretation given in the previous section and as me and my coworkers shown in [18] where the authors use a metric tensor different from (2.45). The factor two in (2.60) is not entirely unexpected since this factor is known to occur in relating electromagnetic to mechanical energy as Papapetrou and Bonnor showed [26, 27] and as we will show later in chapter IV when we write the total gravitational mass expression and the factor two appears with the electromagnetic energy density. This factor presumably arises from the fact that non-Maxwellian stresses are present

in addition to purely electromagnetic ones, and these contribute to the gravitational mass.

Writing equation (2.55) for the metric potential $\alpha$ in terms of the introduced quantities we find,

$$
\begin{aligned}
\alpha_{,\mu} =\ & -\frac{1}{2}(\gamma_{,\mu} + \rho_{,\mu}) - \left\{(1 + r\gamma_{,r})^2(1 - \mu^2) + \left[\mu - (1 - \mu^2)\gamma_{,\mu}\right]^2\right\}^{-1} \times \\
& \times\ \Bigg[ -\frac{1}{2}\{3\mu^2 - 4\mu(1 - \mu^2)\gamma_{,\mu} + (1 - \mu^2)^2(\gamma_{,\mu})^2\}(\gamma_{,\mu} + \rho_{,\mu}) + \\
& -\ \frac{1}{2}r\gamma_{,r}(1 + r\gamma_{,r})(1 - \mu^2)(\gamma_{,\mu} + \rho_{,\mu}) + \frac{1}{2}\mu r(1 + r\gamma_{,r})(\gamma_{,r} - \rho_{,r}) + \\
& -\ r(1 + r\gamma_{,r})(1 - \mu^2)(\gamma_{,r\mu} + \gamma_{,r}\gamma_{,\mu}) + \frac{1}{2}r(1 + r\gamma_{,r})(1 - \mu^2)(\gamma_{,r}\gamma_{,\mu} - \rho_{,r}\rho_{,\mu}) + \\
& +\ \frac{1}{2}[\mu - (1 - \mu^2)\gamma_{,\mu}](3\mu\rho_{,\mu} + r\rho_{,r}) - \frac{1}{2}[\mu - (1 - \mu^2)\gamma_{,\mu}][r^2\gamma_{,rr} - (1 - \mu^2)\gamma_{,\mu\mu}] + \\
& -\ \frac{1}{4}r^2[\mu - (1 - \mu^2)\gamma_{,\mu}]\left\{\nabla\gamma.\nabla\gamma + \nabla\rho.\nabla\rho - \frac{2(1 - \mu^2)}{r^2}[(\gamma_{,\mu})^2 + (\rho_{,\mu})^2]\right\} \Bigg] + \\
& -\ \left\{(1 + r\gamma_{,r})^2(1 - \mu^2) + \left[\mu - (1 - \mu^2)\gamma_{,\mu}\right]^2\right\}^{-1} \times \\
& \times\ \left\{8\pi r^2 e^{2\alpha}\left\{\left[\mu - (1 - \mu^2)\gamma_{,\mu}\right]\Pi + (1 - \mu^2)^{1/2}(1 + r\gamma_{,r})\sigma\right\}\right\}. \qquad (2.61)
\end{aligned}
$$

From (2.61) we realize when we write the equation for the metric potential $\alpha$ in terms of the introduced quantities the factor $e^{2\alpha}$ appears in the right side of equation making the solution associated to this metric potential more difficult than (2.55), where $\alpha$ only appears in the left side of the equation.

The physical interpretation of $\Pi$ and $\sigma$ is related to anisotropy and the shear stress, respectively. In equation (2.61) the magnetic contribution appears in the last term through the quantities $\Pi$ and $\sigma$ and these two quantities only appear in the equation related to the metric potential $\alpha$, which is the factor associated to the coordinates $r$ and $\theta$ in our metric (2.45), through $e^{2\alpha}$, and these two coordinates, i.e. radial and polar, are the directions where the symmetry is broken.

In our system the breaking of spherical symmetry is due to the poloidal magnetic field which has two components $B_r$ and $B_\theta$, quantities $\Pi$ and $\sigma$ are written in terms of these components.

We can understand that $\Pi$ is related to anisotropy (two different components of the magnetic field) and $\sigma$ is related to the shear stress. These two quantities are responsible for

breaking the symmetry of the system. This interpretation of $\Pi$ and $\sigma$ is in agreement with the interpretation given in the previous section and in [18] where the metric tensor is written in the Weyl spherical coordinates and another approach was used.

In conclusion, the electromagnetic contribution has been studied modelling a highly magnetized neutron star as a perfect fluid coupled with a poloidal magnetic field, using two different coordinates describing axially-symmetric spacetimes. The two approaches used in order to give possible physical interpretation for three introduced quantities, named as $W, \Pi$ and $\sigma$, are in agreement on understanding these quantities as electromagnetic energy, anisotropy and shear stress, respectively.

# Chapter 3

# The $3+1$ formalism and the virial

# theorem

The utility of the virial theorem in different areas of physics is well known. In many studies of astrophysics and general relativity it is common to use the virial theorem derived from a conservation law. This chapter is devoted to present a relativistic version of the virial theorem as an integral identity (and not as a conservation law) for a stationary and asymptotically flat spacetime, based on the $3+1$ formalism. The derived identity will be use in chapter V as a consistency check of numerical solution of Einstein equations for a rotating and magnetized neutron star.

## 3.1    The $3+1$ formalism

It is common to assume stationary models as an initial (unstable) condition in axisymmetric collapse problems [21], in this case the chosen coordinates must be adapted to the dynamical evolution which is expressed within the $3+1$ formalism.

The $3+1$ formalism supposes that the spacetime is foliated into a family of spacelike hypersurfaces $\Sigma_t$, levelled by a scalar function: the time coordinate, in that way the real parameter $t$ may be considered as a coordinate associated to the Killing vector $\xi$: $\xi = \partial/\partial t$ (a stationary spacetime). The time-like 4 vector field orthogonal to the hypersurface $\Sigma_t$ and

oriented in the direction of increasing $t$ is given by

$$n_\alpha = -Nt_{,\alpha} \tag{3.1}$$

where $n_\alpha n^\alpha = -1$ (normalized) and $N$ is the lapse function, which is positive for spacelike hypersurfaces and is interpreted as the proper time measured by an Eulerian observer $\mathcal{O}_o$ whose 4-velocity is $n^\alpha$

$$d\tau = Ndt. \tag{3.2}$$

The positive definite 3-metric induced by $g$ on $\Sigma_t$ is

$$h_{\alpha\beta} = g_{\alpha\beta} + n_\alpha n_\beta. \tag{3.3}$$

The metric tensor $\mathbf{h}$ and the normal vector $\mathbf{n}$ provide two useful tools to decompose any 4-dimensional tensor into a purely spacelike part (hence in $\Sigma_t$) and a purely timelike part (orthogonal to $\Sigma_t$ and aligned with $\mathbf{n}$).

In general, the Killing vector is not orthogonal to the hypersurface $\Sigma_t$; leading to the definition of shift vector $N^\alpha$ which means the orthogonal projection of $\xi$ onto $\Sigma_t$ and is interpreted as a measure of the changes in the spatial coordinates $x^i_{t_0 + \delta t} = x^i_{t_0} - N^i dt$, where

$$N^\alpha := -h^\alpha_\sigma \xi^\sigma, \tag{3.4}$$

a non zero shift vector means that the Eulerian observer does not follow the $x^i =$const. lines The relationship between these vectors is

$$\xi^\alpha = Nn^\alpha - N^\alpha. \tag{3.5}$$

The components of the 4-metric tensor $g$ can be written as

$$ds^2 = -(N^2 - N_i N^i)dt^2 - 2N_i dt dx^i + h_{ij} dx^i dx^j. \tag{3.6}$$

The $3 + 1$ formalism consists of writing the Einstein equations, which form a system

of second order partial differential equations (PDE′s) into a system of first order (with respect to the coordinate $t$) PDE′s, in the form of a Cauchy evolution problem, subject to certain constraints. The method consists in projecting the Einstein equations into the hypersurface $\Sigma_t$ which means

$$h^{\alpha\beta}\left(R_{\alpha\beta} - \frac{1}{2}Rg_{\alpha\beta}\right) = 8\pi h^{\alpha\beta}T_{\alpha\beta} \tag{3.7}$$

and using (3.3)

$$R_{\alpha\beta}n^\alpha n^\beta - \frac{1}{2}R = 8\pi S^\alpha_\alpha, \tag{3.8}$$

where the stress energy tensor in the hypersurface $\Sigma_t$ is

$$S^{\alpha\beta} = h^\alpha{}_\mu h^\beta{}_\nu T^{\mu\nu}. \tag{3.9}$$

Due to the Einstein tensor projection into $\Sigma_t$ we will have a 3-dimensional Riemann and Ricci tensor, $R^{\tilde\alpha}_{\beta\gamma\delta}$ and $\tilde{R}_{\alpha\beta}$, respectively, which are purely spatial (spatial derivatives of the spatial metric $h$) whereas the 4-dimensional Riemann and Ricci tensors contain also time derivatives of the metric $g$.The information present in $R^\alpha_{\beta\gamma\delta}$ and missing in $R^{\tilde\alpha}_{\beta\gamma\delta}$ can be found in another spatial and symmetric tensor $K_{\alpha\beta}$ called extrinsic curvature which is defined as:

$$K_{\alpha\beta} = -h^\mu_\alpha h^\nu_\beta n_{(\nu;\mu)} = -n_{\beta;\alpha} - n_\alpha a_\beta, \tag{3.10}$$

where $a_\beta = n^\alpha n_{\beta;\alpha}$ is the acceleration of normal observers. The extrinsic curvature measures the changes in the normal vector under parallel transport, hence it measures how the 3-dimensional hypersurface $\Sigma_t$ is bent with respect to the 4-dimensional spacetime. The trace of the extrinsic curvature tensor is linked to the covariant divergence of the 4-velocity through

$$K = -n^\alpha_{;\alpha}. \tag{3.11}$$

Gauss equation enable one to express the Ricci tensor $R_{\alpha\beta}$ of the metric $g$, in terms

of the Ricci tensor $\tilde{R_{\alpha\beta}}$ of the 3-metric $h_{\alpha\beta}$, the lapse function $N$ and the extrinsic curvature tensor $K_{\alpha\beta}$ of the hypersurface $\Sigma_t$ [28]

$$h^{ij}\nu_{;ij} - \frac{1}{4}\tilde{R} + h^{ij}\nu_{;j}\nu_{;i} - \frac{3}{4}(K_{ij}K^{ij} - K^2) + (Kn^{\alpha})_{;\alpha} = 4\pi S_i{}^i \qquad (3.12)$$

where $\nu = \ln N$.

In collapse problems, it is common [29] to choose maximal slicing hypersurfaces $\Sigma_t$ which are defined by the requirement of a trace-free extrinsic curvature tensor

$$K = 0. \qquad (3.13)$$

The world lines of *Eulerian observers* are normal to the maximal hypersurfaces $\Sigma_t$, they coincide with the *locally nonrotating observers* introduced by Bardeen [30] in the stationary axisymmetric case, the well known *zero-angular momentum observers* (**ZAMO**) [31].

## 3.2   The Virial theorem

The term "virial" comes from the latin *vires* which means strength, force or energy. The virial theorem relates the time average of kinetic energy of a generic particle with the time average of the works executed by the forces with which the particles interact. This important theorem is thanks to Clausius who in 1870 delivered the lecture "On a Mechanical Theorem Applicable to Heat" to the Association for Natural and Medical Sciences of the Lower Rhine, following a 20-years study of thermodynamics.

The Newtonian version of the virial theorem is widely used in astrophysics, mainly within the context of the equilibrium and stability properties of dynamical systems. One example of this usefulness is the fact that the virial theorem has been used to derive the Chandrasekhar limit for the stability of white dwarf stars [32]. On another hand, in astronomy the virial theorem, and related concepts, provide an often convenient means by which to quantify the mass and size of a galaxy [33], which are often defined in terms of the "virial

radius" and "virial mass", respectively.

Bonazzola [34] has derived a general relativistic version of the virial theorem in the stationary axisymmetric case. The Bonazzola identity proved to be very useful as a consistency check for numerical computation of steady-state rotating star models [21, 35] and it will be the validity criteria to find numerical solutions in the present work, as we will see in chapter V. In the case of spherical symmetry, a general relativistic formulation of the non-stationary virial theorem has been found by Vilain [36] and applied to stability problems. Katz [37] proposed a general formulation of the relativistic virial theorem without supposing any symmetry. His formulation involves "virial vector fields" which are defined with respect to a given flat background metric. His original goal was to obtain the virial theorem as a surface integral at infinity, so that it would have been independent of the choice of the virial vector fields. The result was "0 = 0" and the conclusion is the virial theorem has to be formulated as a space integral, involving some extra structure, like the virial vector fields. In the next section we are going to present a brief discussion about the relativistic version of the virial theorem.

## 3.2.1 The relativistic virial theorem

We consider a stationary and asymptotically flat spacetime. As mentioned in the previous section, stationary means that there exists a Killing vector field, $\xi$, which is time-like. This vector is defined up to scale factor, which is fixed by the requirement that the scalar product $\xi_\mu \xi^\mu = -1$. Asymptotically flat spacetime means:

- A spacetime with spatial sections $\Sigma_t$ containing a compact region $B$ such that $\Sigma_t - B$ is diffeomorphic to $\mathbb{R}^3 - 0$. For an ordinary star, $B$ may be reduced to one point, whereas for a black hole, $B$ shall enclose the event horizon.

- On each $\Sigma_t$, there exists a coordinate system $x^i$ such that the components $g_{\alpha\beta}$ of the metric differ from $diag(-1, 1, 1, 1)$ only by terms $O(1/r)$ as $r \to \infty$ and the first derivatives $g_{\alpha\beta,\gamma}$ are $O(1/r^2)$.

The relativistic Virial Theorem is based on the 3+1 formalism described in the previous section [38,39]; the starting point consists in integration over the space-like hypersurface $\Sigma_t$ of equation (3.12)

$$
\int_{\Sigma_t} \sqrt{h} d^3 x \left[ 4\pi S^i_{\ i} \ - \ h^{ij} \nu_{;j} \nu_{;i} + \frac{3}{4} (K_{ij} K^{ij} - K^2) \right] = \tag{3.14}
$$
$$
= \int_{\Sigma_t} \sqrt{h} d^3 x (K n^\alpha)_{;\alpha} + \int_{\Sigma_t} \sqrt{h} d^3 x h^{ij} \nu_{;ij} - \frac{1}{4} \int_{\Sigma_t} \sqrt{h} d^3 x \tilde{R}.
$$

If we consider the stationary case, the term of the first integral of the right hand side of (3.14) can be write as

$$
(K n^\alpha)_{;\alpha} = \frac{1}{N} (K N^i)_{;i} = \frac{1}{N} K N^i \nu_{;i} + \left( K \frac{N^i}{N} \right)_{;i}, \tag{3.15}
$$

and with the use of the Gauss theorem,

$$
\int_{\Sigma_t} \sqrt{h} d^3 x (K n^\alpha)_{;\alpha} = \int_{\Sigma_t} \sqrt{h} d^3 x \frac{1}{N} K N^i \nu_{;i} + \lim_{S \to \infty} \oint_S dS_i \frac{K}{N} N^i = \int_{\Sigma_t} \sqrt{h} d^3 x \frac{1}{N} K N^i \nu_{;i}, \tag{3.16}
$$

where the asymptotic flatness condition was considered.

For the second integral of the right hand side of (3.14) we use Gauss theorem and then write this integral in terms of the total energy in the hypersurface $\Sigma_t$ which is known as the Komar mass [40] defined for a stationary spacetime,

$$
m := \frac{1}{8\pi} \lim_{S \to \infty} \oint_S dS_{\alpha\beta} \xi^{[\alpha;\beta]}, \tag{3.17}
$$

since the space is asymptotically flat (see appendix of [41] for further details)

$$
\int_{\Sigma_t} \sqrt{h} d^3 x h^{ij} \nu_{;ij} = \lim_{S \to \infty} \oint dS_i h^{ij} \nu_{;j} = 4\pi m. \tag{3.18}
$$

The last integral in (3.14) consists in the integration of the Ricci scalar of the hypersurface $\Sigma_t$. This integral can be computed using the bimetric formalism which consists in introducing into the hypersurface a flat background metric $\gamma$ (for further details see [41]

and references therein). The introduced metric is flat everywhere in the case of ordinary stars and coincide at infinity with the non-flat 3-metric $h$ by virtue of the asymptotic flatness hypothesis. Using this bimetric formalism, the Ricci scalar integral can be written as [42]

$$\int_{\Sigma_t} \sqrt{h} d^3 x \tilde{R} = 16\pi M_{ADM} + \int_{\Sigma_t} \sqrt{h} d^3 x h^{ij} [\Delta^l{}_{im} \Delta^m{}_{jl} - \Delta^l{}_{lm} \Delta^m{}_{ij}], \tag{3.19}$$

with

$$\Delta^i{}_{jk} = \frac{1}{2} h^{ij} [h_{lk\|j} + h_{jl\|k} - h_{jk\|l}], \tag{3.20}$$

where the double vertical stroke $\|$ denotes covariant derivation associated with the metric $\gamma$ [42] and $M_{ADM}$ is the Arnowitt-Deser-Misner mass-energy [39].

Taking into account that in the case of stationary and asymptotically flat spacetime, Komar mass and ADM mass do coincide [43, 44], expression (3.14) is

$$\int_{\Sigma_t} \sqrt{h} d^3 x \left[ 4\pi S^i{}_i - h^{ij} \nu_{;j} \nu_{;i} + \frac{1}{4} h^{ij} (\Delta^l{}_{im} \Delta^m{}_{jl} - \Delta^l{}_{lm} \Delta^m{}_{ij}) + \right. \tag{3.21}$$
$$\left. + \frac{3}{4} (K_{ij} K^{ij} - K^2) - \frac{K}{N} N_i h^{ij} \nu_{;j} \right] = 0.$$

Equation (3.21) is the general relativistic virial theorem, named in that way because in the Newtonian limit this expression reduces to the classical virial theorem. The Virial theorem integral can be read as containing terms related to the gravitational source, second derivatives of the metric potential $\nu$ and terms associated to the extrinsic curvature tensor.

# Chapter 4

# Neutron star structure

The theoretical formalism describing a rotating and highly magnetized neutron star is presented in this chapter. As mentioned in the introduction, in order to properly describe this kind of astrophysical objects it is necessary a full axially symmetric treatment within the context of Einstein-Maxwell equations. First, we describe the spacetime and the Einstein-Maxwell equations within the approach used by Bonazzola et al. [21] which allows us to write these equations in terms of a flat space elliptic operator and the source terms containing matter, electromagnetic and non linear quadratic terms in the metric potentials. Secondly, the hydrostatic equilibrium equations will be derived within the assumption of infinite conductivity matter. Finally, the relevant physical quantities describing the system will be presented.

## 4.1   Structure equations

In this study we assume that spacetime is stationary, axis-symmetric and circular, which means the current 4-vector and fluid 4-velocity are parallel to a general combination of the Killing vectors [45]. Most authors studying rapid rotation based their works in the approach of Bardeen et. al. [46] which explicitly assumes an isotropic stress tensor and is thus incompatible with electromagnetic fields. The authors of [21,35,47] present a formula-

tion which allows such spacetime for the most general energy-momentum tensor. The metric
that describes such spacetime is given by

$$ds^2 = -e^{2\nu}dt^2 + e^{2(\zeta-\nu)}(dr^2 + r^2 d\theta^2) + e^{-2\nu}G^2 r^2 sin^2\theta(d\phi - N^\phi dt)^2, \tag{4.1}$$

where the coordinates are $x^\mu = (x^0, x^1, x^2, x^3) = (t, r, \theta, \phi)$ and the metric functions $\nu, \zeta, G$
and $N^\phi$ depend on the coordinates $(r, \theta)$.

The energy-momentum tensor describing a perfect fluid coupled with electromag-
netic field is

$$T^{\mu\nu} = T^{PF\mu\nu} + T^{EM\mu\nu}, \tag{4.2}$$

the perfect fluid (PF) and the electromagnetic (EM) contributions are given by

$$T^{PF\mu\nu} = (\epsilon + P)u^\mu u^\nu + Pg^{\mu\nu}, \tag{4.3}$$

$$T^{EM\mu\nu} = \frac{1}{4\pi}\left(F^{\mu\alpha}F^\nu{}_\alpha - \frac{1}{4}g^{\mu\nu}F^{\alpha\beta}F_{\alpha\beta}\right), \tag{4.4}$$

where $\epsilon$ and $P$ are the rest frame energy density and pressure, respectively, $u^\mu$ is the fluid
4-velocity, $g_{\mu\nu}$ is the metric tensor and

$$F_{\mu\nu} = A_{\nu,\mu} - A_{\mu,\nu} \tag{4.5}$$

is the Maxwell tensor where $A_\mu$ is the electromagnetic 4-potential. Stationarity, axisym-
metry and circularity properties for the spacetime described by (4.1) imply that the non
vanishing components of the current 4-vector are $j^\mu = (j^t, 0, 0, j^\phi)$ and consequently the
electromagnetic potential components are $A_\mu = (A_t, 0, 0, A_\phi)$ [45].

We are going to use the Bonazzola approach [21] which is based on the 3+1 formalism
discussed in chapter III. From the Einstein field equations, Bonazzola et al. derive a Poisson
equation for each of the metric variables. The determination of the gravitational field is
reduced to the integration of a system of four coupled elliptic partial differential equations

(hereafter PDE) of the form

$$\Delta_f u = \sigma_u^{matter} + \sigma_u^{quad} \tag{4.6}$$

where $\Delta_f$ is a flat space elliptic operator (namely a two or a three dimensional flat space Laplacian), $u$ a metric potential, $\sigma_u^{matter}$ is the source term involving all matter terms (such as fluid, electromagnetic fields, etc.) and $\sigma_u^{quad}$ is an expression containing only non linear terms in the metric potentials. We use the Bonazzola's formalism to derive equations governing the equilibrium of rotating neutron stars with strong magnetic fields. This approach may be useful in the study of systems based on other types of anisotropic stress-energy tensor different of (4.2) such as the energy momentum tensor studied in [10].

The equations that describe a perfect fluid coupled with electromagnetic field are the Einstein-Maxwell equations

$$G_{\mu\nu} = 8\pi T_{\mu\nu}. \tag{4.7}$$

$$F_{\alpha\beta;\gamma} + F_{\gamma\alpha;\beta} + F_{\beta\gamma;\alpha} = 0, \tag{4.8}$$

$$F^{\alpha\beta}{}_{;\beta} = 4\pi j^\alpha, \tag{4.9}$$

where equations (4.8) and (4.9) are the homogeneous (Faraday´s law and non-magnetic monopole) and inhomogeneous (Gauss and Ampere-Maxwell laws) Maxwell equations.

Using the approach suggested by (4.6) for the metric tensor defined in (4.1) and considering the matter defined by the energy-momentum tensor (4.2), Einstein-Maxwell equations are written as [48]

$$\Delta_3 \nu = \sigma_\nu, \tag{4.10}$$

$$\tilde{\Delta}_3 \tilde{N}^\phi = \sigma_{\tilde{N}^\phi}, \tag{4.11}$$

$$\Delta_2 \tilde{G} = \sigma_{\tilde{G}}, \tag{4.12}$$

$$\Delta_2 \zeta = \sigma_\zeta, \tag{4.13}$$

$$\Delta_3 A_t = \sigma_{A_t}, \tag{4.14}$$

$$\tilde{\Delta}_3 \tilde{A}_\phi = \sigma_{\tilde{A}_\phi}, \tag{4.15}$$

where

$$\tilde{N}^\phi \equiv r sin\theta N^\phi, \tag{4.16}$$

$$\tilde{G} \equiv r sin\theta G, \tag{4.17}$$

$$\tilde{A}^\phi \equiv \frac{A_\phi}{r sin\theta}, \tag{4.18}$$

and $\Delta_2, \Delta_3$ and $\tilde{\Delta}_3$ are respectively the two-dimensional flat space Laplacian, the three-dimensional flat space Laplacian, and the $\phi$ component of the three-dimensional flat space vector Laplacian and they are given by

$$\Delta_2 \equiv \frac{\partial^2}{\partial r^2} + \frac{1}{r}\frac{\partial}{\partial r} + \frac{1}{r^2}\frac{\partial^2}{\partial \theta^2}, \tag{4.19}$$

$$\Delta_3 \equiv \frac{\partial^2}{\partial r^2} + \frac{2}{r}\frac{\partial}{\partial r} + \frac{1}{r^2}\frac{\partial^2}{\partial \theta^2} + \frac{1}{r^2 \tan\theta}\frac{\partial}{\partial \theta}, \tag{4.20}$$

$$\tilde{\Delta}_3 \equiv \Delta_3 - \frac{1}{r^2 sin^2\theta}. \tag{4.21}$$

The source terms $\sigma_u^{matter}$ are given by

$$\sigma_\nu = 4\pi e^{2(\zeta-\nu)}(E + S_i^i) + \frac{1}{2}e^{-4\nu}G^2r^2sin^2\theta(\partial N^\phi)^2 - \partial\nu\partial(\ln G), \tag{4.22}$$

$$\sigma_{\tilde{N^\phi}} = -\frac{16\pi e^{2\zeta+\nu}}{G^2}\frac{I_\phi}{rsin\theta} - rsin\theta\partial N^\phi\partial[\ln(e^{-4\nu}G^3)], \tag{4.23}$$

$$\sigma_{\tilde{G}} = 8\pi e^{2(\zeta-\nu)}Grsin\theta(S_r^r + S_\theta^\theta), \tag{4.24}$$

$$\sigma_\zeta = 8\pi e^{2(\zeta-\nu)}S_\phi^\phi + \frac{3}{4}e^{-4\nu}G^2r^2sin^2\theta(\partial N^\phi)^2 - (\partial\nu)^2, \tag{4.25}$$

$$\sigma_{A_t} = -4\pi e^{2(\zeta-\nu)}(g_{tt}j^t + g_{t\phi}j^\phi) + e^{-2\nu}g_{t\phi}\partial A_t\partial N^\phi - (2 + e^{-2\nu}g_{tt})\partial A_\phi\partial N^\phi$$
$$- (\partial A_t + 2N^\phi\partial A_\phi)\partial[\ln(e^{-2\nu}G)] - \frac{2N^\phi}{r}\left(A_{\phi,r} + \frac{1}{r\tan\theta}A_{\phi,\theta}\right), \tag{4.26}$$

$$\sigma_{\tilde{A_\phi}} = -4\pi e^{2\zeta-4\nu}G^2rsin\theta(j^\phi - N^\phi j^t) + e^{-4\nu}G^2rsin\theta\partial N^\phi(\partial A_t + N^\phi\partial A_\phi)$$
$$+ \frac{1}{rsin\theta}\partial A_\phi\partial[\ln(e^{-2\nu}G)]. \tag{4.27}$$

In these expressions the notation $\partial f\partial g$ denotes

$$\partial f\partial g \equiv \nabla f.\nabla g \equiv f_{,r}g_{,r} + \frac{1}{r^2}f_{,\theta}g_{,\theta}. \tag{4.28}$$

The contributions from the energy-momentum tensor are

$$E = T_{\mu\nu}n^\nu n^\mu, \tag{4.29}$$

$$I_\mu = -h_{\mu\nu}n_\gamma T^{\nu\gamma}, \tag{4.30}$$

$$S_{\mu\nu} = h_{\mu\gamma}h_{\nu\rho}T^{\gamma\rho}, \tag{4.31}$$

where the physical meaning of $n^\mu$ and $h_{\mu\nu} = g_{\mu\nu} + n_\mu n_\nu$ are the same as presented in chapter III. In the coordinates $x^\mu = (t, r, \theta, \phi)$ the components of the timelike four vector are $n_\mu = (-N, 0, 0, 0)$ where $N = e^\nu$ is the lapse function. For the energy-momentum tensor (4.2) we have

$$E = E^{PF} + E^{EM}, \tag{4.32}$$

$$I_\mu = I_\mu^{PF} + I_\mu^{EM}, \tag{4.33}$$

$$S_{\mu\nu} = S_{\mu\nu}^{PF} + S_{\mu\nu}^{EM}. \tag{4.34}$$

For the perfect fluid we have

$$E^{PF} = \Gamma^2(\epsilon + P) - P, \tag{4.35}$$

$$(I^{PF})_\phi = e^{-\nu}Grsin\theta(E^{PF} + P)U, \tag{4.36}$$

$$(S^{PF})_r^r = P, \quad (S^{PF})_\theta^\theta = P, \quad (S^{PF})_\phi^\phi = P + (E^{PF} + P)U^2, \tag{4.37}$$

where $\Gamma$ is the Lorentz factor linking the Eulerian observer $\mathcal{O}_o$ and the fluid comoving observer $\mathcal{O}_1$ with velocity $u^\mu$,

$$\Gamma = -n_\alpha u^\alpha \Rightarrow \Gamma^2 = \frac{1}{1 - U^2}, \tag{4.38}$$

being $U$ the physical fluid velocity in the $\phi$ direction, as measured by the Eulerian observer,

and it is given by

$$U = \frac{1}{\Gamma}\vec{e_\phi}.\vec{u},$$ (4.39)

where $\vec{e_\phi}$ is the unit spatial vector in the $\phi$ direction.

The non-vanishing components of the four velocity are related by

$$u^\phi = \Omega u^t,$$ (4.40)

where $\Omega$ is the angular velocity as seen by an inertial observer at infinity, who is at rest with respect to the star's center. We obtain for $U$

$$U = e^{-2\nu}Grsin\theta(\Omega - N^\phi).$$ (4.41)

Note that if the fluid were at rest with respect to the local Eulerian observer, then $U = 0$ and $\Omega = N^\phi \neq 0$, hence it would not be at rest for an inertial observer at infinity: this is the well known phenomena of *dragging of the inertial frame* [49–52].

For the electromagnetic part of the energy-momentum tensor we have

$$E^{EM} = \frac{1}{8\pi}(E_iE^i + B_iB^i),$$ (4.42)

$$(I^{EM})_\phi = \frac{1}{4\pi}e^{2\zeta-3\nu}Gr^2sin\theta(E^rB^\theta - E^\theta B^r),$$ (4.43)

$$(S^{EM})^r_r = \frac{1}{8\pi}(E_\theta E^\theta - E_r E^r + B_\theta B^\theta - B_r B^r),$$ (4.44)

$$(S^{EM})^\theta_\theta = -(S^{EM})^r_r,$$ (4.45)

$$(S^{EM})^\phi_\phi = E^{EM}.$$ (4.46)

Note that the only non vanishing component of the Poynting vector is $(I^{EM})_\phi$, which is consistent with the circularity assumption. In the above expressions $E_i$ and $B_i$ are the components of the electric and magnetic fields as measured by the Eulerian observer $\mathcal{O}_o$ [38], and given by

$$
\begin{aligned}
E_\alpha &= n^\beta F_{\alpha\beta} \\
&= \left[0, e^{-\nu}(A_{t,r} + N^\phi A_{\phi,r}), e^{-\nu}(A_{t,\theta} + N^\phi A_{\phi,\theta}), 0\right],
\end{aligned}
\tag{4.47}
$$

$$
\begin{aligned}
B_\alpha &= -\frac{1}{2}\epsilon_{\alpha\beta\rho\sigma}n^\beta F^{\rho\sigma} \\
&= \left[0, \frac{e^\nu}{Gr^2 sin\theta}A_{\phi,\theta}, -\frac{e^\nu}{G sin\theta}A_{\phi,r}, 0\right],
\end{aligned}
\tag{4.48}
$$

where $\epsilon_{\alpha\beta\rho\sigma}$ is the Levi-Civita tensor associated with the metric $g_{\mu\nu}$ given by (4.1).

The theorem of Cowling [53] states that an axisymmetric magnetic field cannot be generated or maintained by the motion of a fluid, since finite resistivity involves dissipation, leading to magnetic field decay. Hence stationary models of neutron stars in magnetic fields require a separation of dynamical and dissipative timescales, encoded in an assumption of infinite conductivity (magnetic fields "frozen in" and carried with the fluid, a common assumption in astrophysics [54]). In the case of neutron stars matter studies indicate [54] that ohmic dissipation timescale is larger than the age of the universe [55], so the infinite conductivity assumption is well justified.

According to Ohm's law, and assuming that the matter has infinite conductivity, the electric field as measured by the fluid observer must be zero. This condition leads to the following relation between the two components of the potential 4-vector inside the star [21]

$$
A_{t,i} = -\Omega A_{\phi,i}.
\tag{4.49}
$$

From this equation we have either $\Omega = const$, or $A_\phi = A_\phi(\Omega)$, but the latter condition cannot be fulfilled in general since $A_\phi$ has to satisfy the Maxwell-Ampere equation, thus we retain only the case $\Omega = const$ and conclude that a stationary configuration with some

magnetic field is necessarily rigidly rotating. Equation (4.49) is integrated and yields

$$A_t = -\Omega A_\phi + constant \tag{4.50}$$

where the constant is determined by the total electric charge of the star.

## 4.2  Hydrostatic equilibrium equations

The hydrostatic equilibrium equations are provided by the conservation of the energy-momentum tensor

$$T^{\mu\nu}{}_{;\nu} = 0. \tag{4.51}$$

Applying the above equation to the energy-momentum tensor of our system we obtain

$$\frac{1}{(\epsilon + P)}P_{,i} + \nu_{,i} - (\ln\Gamma)_{,i} - \frac{1}{(\epsilon + P)}f_i = 0, \tag{4.52}$$

from left to right, the above equation can be understood as (by analogy with the Newtonian case) the pressure force, gravitational force, centrifugal force and Lorentz force given by

$$f_i = F_{i\alpha}j^\alpha = j^t A_{t,i} + j^\phi A_{\phi,i}. \tag{4.53}$$

Considering a one parameter EoS, $\epsilon = \epsilon(n)$, $P = P(n)$, where $n$ is the baryon density, the first integral of the first term in equation (4.52) is identified as the heat function $H$

$$H(n) = \int_0^n \frac{1}{(\epsilon(n') + P(n'))}\frac{dP(n')}{dn'}dn', \tag{4.54}$$

which is a regular function of $n$ when $\epsilon$ and $P$ tend to zero. For example, at zero temperature and in chemical equilibrium, the first law of thermodynamics allows to write $H(n) = \ln g(n)$, where $g$ is the enthalpy per baryon $g := \frac{(\epsilon+P)}{n}$ or the total of possible states [56, 57]. In the

case of cold stars, the EoS parameter $n$ is the proper baryon density, at zero temperature. The star surface corresponds to $H(0) = 0$ which will be an important condition in order to find numerical solutions as we will see in the next chapter.

Introducing (4.49), (4.53) and (4.54) in (4.52), we have

$$(H + \nu - \ln \Gamma)_{,i} - \frac{1}{(\epsilon + P)}(j^\phi - \Omega j^t)A_{\phi,i} = 0. \tag{4.55}$$

The above equation suggests that there exists a function $M(r, \theta)$ such that

$$-\frac{1}{(\epsilon + P)}(j^\phi - \Omega j^t)A_{\phi,i} = M_{,i}. \tag{4.56}$$

with the adoption of a current function

$$f(A_\phi) = \frac{1}{(\epsilon + P)}(j^\phi - \Omega j^t) \tag{4.57}$$

we can write

$$-f(A_\phi)A_{\phi,i} = M_{,i}, \tag{4.58}$$

and hence equation (4.55) can be written as

$$(H + \nu - \ln \Gamma + M)_{,i} = 0. \tag{4.59}$$

The first integral of motion is

$$H(r, \theta) + \nu(r, \theta) - \ln \Gamma(r, \theta) + M(r, \theta) = C = constant \tag{4.60}$$

with

$$M(r, \theta) = M(A_\phi(r, \theta)) = -\int_0^{A_\phi(r,\theta)} dx f(x). \tag{4.61}$$

Besides there is a freedom of choice for function $f(A_\phi)$, the integrability condition

(4.57) represents a significant restriction on the form of the electromagnetic current that allows the existence of stationary solutions. The constant $C$ is determined by an input parameter, e.g. the pressure specified at some point in the star.

The electric and magnetic fields are linked by the infinite conductivity assumption (4.50), so equations (4.42)-(4.46) can be written in terms of the electromagnetic potential $A_\phi$ and the fluid velocity $U$

$$E^{EM} = \frac{1}{8\pi} \frac{e^{4\nu-2\zeta}}{G^2 r^2 sin^2\theta} (1+U^2) \left( (A_{\phi,r})^2 + \frac{1}{r^2}(A_{\phi,\theta})^2 \right),$$  (4.62)

$$I_\phi^{EM} = \frac{1}{4\pi} \frac{e^{3\nu-\zeta}}{Grsin\theta} U \left( (A_{\phi,r})^2 + \frac{1}{r^2}(A_{\phi,\theta})^2 \right),$$  (4.63)

$$(S^{EM})_r^r = \frac{1}{8\pi} \frac{e^{4\nu-2\zeta}}{G^2 r^2 sin^2\theta} (1-U^2) \left( (A_{\phi,r})^2 - \frac{1}{r^2}(A_{\phi,\theta})^2 \right),$$  (4.64)

$$(S^{EM})_\theta^\theta = - (S^{EM})_r^r$$
$$= -\frac{1}{8\pi} \frac{e^{4\nu-2\zeta}}{G^2 r^2 sin^2\theta} (1-U^2) \left( (A_{\phi,r})^2 - \frac{1}{r^2}(A_{\phi,\theta})^2 \right),$$  (4.65)

$$(S^{EM})_\phi^\phi = E^{EM}$$
$$= \frac{1}{8\pi} \frac{e^{4\nu-2\zeta}}{G^2 r^2 sin^2\theta} (1+U^2) \left( (A_{\phi,r})^2 + \frac{1}{r^2}(A_{\phi,\theta})^2 \right).$$  (4.66)

In summary, the formalism of stationary neutron stars with poloidal magnetic fields consists of a closed system of:

- Eleven variables:

  - Four metric variables: $\nu, G, N^\phi, \zeta$.

  - Energy density: $\epsilon$.

  - Pressure: $P$.

  - Two components of the electromagnetic potential: $A_t, A_\phi$.

  - Two components of the electromagnetic current: $j^t, j^\phi$.

  - The heat function: $H(r,\theta)$.

- Eleven equations:

  - Four Poisson equations for the metric variables: (4.10)-(4.13).

  - Two Poisson equations for the components of the electromagnetic potential: (4.14) and (4.15).

  - The relation between the components of the electromagnetic potential (infinity conductivity assumption): equation (4.50).

  - The equation of state: $P = P(\epsilon)$.

  - The relation between the heat function $H$, $\epsilon$ and $P$.

  - The first integral of the equations of hydrostatic equilibrium: equation (4.60).

  - The restriction on the electromagnetic current: equation (4.57).

- Three input parameters:

  - Angular velocity $\Omega$.

  - Total electric charge $Q$.

  - Central density $\epsilon_c$ or central pressure $P_c$.

- One input function: $f(A_\phi)$.

- The relevant boundary conditions.

## 4.3   Physical quantities describing the system

In this section we calculate some relevant physical quantities that describe the rotating or magnetized neutron star, these quantities are the circumferential radius, total gravitational mass, angular momentum and the magnetic moment.

The stellar equator is defined as the closed line at the surface of the star defined by $t = const$ and $\theta = \pi/2$ (equatorial plane). It has a constant value of the coordinate $r$, that

we identified as $r_{eq}$. A characterization of the stellar equator is the circumferential radius defined as [58]

$$R := \frac{l}{2\pi} \tag{4.67}$$

where $l$ is the circumference of the star in the equatorial plane, i.e. the proper length of the equator as given by the metric tensor. For the line element (4.1) that means

$$ds^2 = e^{-2\nu} G^2 r^2 \sin^2 \theta d\phi^2 \Rightarrow l = \int_0^{2\pi} e^{-\nu} G r_{eq} d\phi, \tag{4.68}$$

considering the symmetry in the $\phi$ direction

$$R = e^{-\nu_{eq}} G_{eq} r_{eq}, \tag{4.69}$$

where $\nu_{eq} = \nu(r_{eq}, \pi/2)$ and $G_{eq} = G(r_{eq}, \pi/2)$. As we can see, differently from the spherically symmetric case, for an axially symmetric spacetime the coordinate $r$ does not coincide with the circumferential radius.

For a static matter distribution or in slow evolution regime [10], the energy (mass) concept is well defined. For the spherically symmetric and non dissipative case, the exterior spacetime is described by the Schwarzshild metric and as a consequence of the coupling conditions, the total energy of the system is equal to the Schwarzschild parameter $M$ [59].

However, the definition of the energy distribution of a part of the fluid is not unique. This ambiguity in the energy localization, that is present even in classical electrodynamics [60], has been object of several discussions leading to different energy definitions, for example for spherically symmetric relativistic fluids is common the use of the mass function [59] to calculate the numerical solution of relativistic gravitational collapse [61]. However, another interesting energy definition for static or sloswly evolving distribution is the Tolman-Whittaker mass [62,63] which plays the role of the active gravitational mass (see [64] for more details).

The Komar mass [40] is another definition of the mass and it is commonly used for

stationary asymptotically flat spacetimes as we mentioned in chapter III. Because we are interested in describing a rotating or magnetized neutron star we will use the Komar mass expression to calculate the mass of the system.

The Komar mass $m$ is given by [65]

$$m = \int_{\Sigma_t} (T_i^i - T_t^t)\sqrt{-g}dx^1 dx^2 dx^3. \tag{4.70}$$

In the following, we will calculate $m$ for two different cases: first, for a rotating fluid without magnetic field and second, for a perfect fluid (without rotation) coupled with a poloidal field.

## 4.3.1   Mass and angular momentum for a rotating star

For a rotating fluid without magnetic field the extrinsic curvature is part of the Komar mass,

$$m = \int_0^\infty dr \int_0^\pi d\theta \int_0^{2\pi} d\phi r^2 sin\theta e^{2(\zeta-\nu)} G\left[(E + S_i^i) + \frac{1}{2\pi}(\kappa_1^2 + \kappa_2^2)\right]. \tag{4.71}$$

where the components of the extrinsic curvature $K_{\alpha\beta}$ for the metric tensor (4.1) are

$$\kappa_1 = -\frac{1}{2}e^{-(\zeta+\nu)}Grsin\theta N_{,r}^\phi \quad \kappa_2 = -\frac{1}{2}e^{-(\zeta+\nu)}Gsin\theta N_{,\theta}^\phi. \tag{4.72}$$

Considering (4.37) we have,

$$S_i^i = \Gamma^2(\epsilon + P)U^2 + 3P \tag{4.73}$$

hence

$$E + S_i^i = \Gamma^2(\epsilon + P)(1 + U^2) + 2P. \tag{4.74}$$

Then, considering the above equations, the total gravitational mass for a rotating fluid

(without magnetic field) is

$$m = \int_0^\infty dr \int_0^\pi d\theta \int_0^{2\pi} d\phi r^2 sin\theta e^{2(\zeta-\nu)} G \left[ \Gamma^2(\epsilon + P)(1 + U^2) + 2P + \frac{1}{2\pi}(\kappa_1^2 + \kappa_2^2) \right]. \quad (4.75)$$

so part of the energy of a rotating neutron star without magnetic field arises from a term which is not associated to the components of the extrinsic curvature tensor (later in chapter V we will call as a perfect fluid contribution, because it coincides with the energy density associated with a perfect fluid in the nonrotating case), and a term coming from the extrinsic curvature contribution.

To compute the total angular momentum of the rotating star we use the fact that the spacetime is asymptotically flat which, mathematically, means when $r \to \infty$

$$\nu(r, \theta) \to 0, \quad (4.76)$$

$$N^\phi(r, \theta) \to 0, \quad (4.77)$$

$$\zeta(r, \theta) \to 0, \quad (4.78)$$

$$G(r, \theta) \to 1. \quad (4.79)$$

The solution of (4.11) satisfying these conditions has a leading term when $r \to \infty$ of the form

$$N^\phi(r, \theta) \sim \frac{2J}{r^3} \quad (4.80)$$

where $J$ is a constant independent of $r$ and $\theta$ and is identified as the total angular momentum of the star [66]. Integrating equation (4.11) on a sphere of large radius, transforming the left hand side into a surface flux integral of $\nabla N^\phi$, thanks to Gauss theorem, using the asymptotic behavior of $N^\phi$ (4.80) (see [21] for more details) the expression for $J$ corresponding to the

metric (4.1) is

$$J = \int_0^\infty dr \int_0^\pi d\theta \int_0^{2\pi} d\phi\, r^2 sin\theta G e^{2\zeta - 3\nu} I_\phi \tag{4.81}$$

and taking into account (4.35) and (4.36), we have

$$J = 2\pi \int_0^\infty dr \int_0^\pi d\theta\, r^3 sin^2\theta G^2 e^{2(\zeta - 2\nu)} \Gamma^2 (\epsilon + P) U \tag{4.82}$$

where the symmetry in the $\phi$ direction was considered.

In the next chapter the mass, angular momentum and the angular velocity will be used to describe a rotating neutron star without magnetic field.

## 4.3.2 Mass and magnetic moment for a magnetized star

For a perfect fluid coupled with a poloidal magnetic field we have for the energy-momentum tensor (4.70),

$$T^i{}_i = T^{PFi}{}_i + T^{EMi}{}_i, \qquad T^t{}_t = T^{PFt}{}_t + T^{EMt}{}_t \tag{4.83}$$

For the perfect fluid contribution, considering $u^\mu = (u^0, 0, 0, 0)$ and $u^\mu u_\mu = -1$, we have

$$T^{PFi}{}_i = 3P, \qquad T^{PFt}{}_t = -\epsilon \tag{4.84}$$

For the electromagnetic field contribution,

$$T^{EMi}{}_i = \frac{1}{4\pi}\left( F^{i\rho}F_{i\rho} - \frac{1}{4}\delta^i_i F^{\rho\sigma}F_{\rho\sigma} \right), \tag{4.85}$$

taking into account that $A_\mu = (0, 0, 0, A_\phi(r, \theta))$,

$$F^{\rho\sigma}F_{\rho\sigma} = F^{i\rho}F_{i\rho} = 2\frac{e^{4\nu - 2\zeta}}{G^2 r^2 sin^2(\theta)}\left[ (A_{\phi,r})^2 + \frac{1}{r^2}(A_{\phi,\theta})^2 \right] \tag{4.86}$$

hence,

$$T^{EMi}{}_i = \frac{1}{8\pi}\frac{e^{4\nu-2\zeta}}{G^2 r^2 sin^2(\theta)}\left[(A_{\phi,r})^2 + \frac{1}{r^2}(A_{\phi,\theta})^2\right] = E^{EM} \tag{4.87}$$

$$T^{EMt}{}_t = -\frac{1}{16\pi}F^{\rho\sigma}F_{\rho\sigma} = -E^{EM} \tag{4.88}$$

The expression in parenthesis in (4.70) is,

$$T^i{}_i = 3P + E^{EM} \qquad T^t{}_t = -(\epsilon + E^{EM}) \tag{4.89}$$

For the line element (4.1) the factor $\sqrt{-g} = e^{2(\zeta-\nu)}Gr^2 sin\theta$, and the Komar mass is

$$m = \int_0^\infty dr \int_0^\pi d\theta \int_0^{2\pi} d\phi r^2 sin\theta e^{2(\zeta-\nu)}G(\epsilon + 3P + 2E^{EM}). \tag{4.90}$$

It is worth noting that in this chapter we are using different coordinates and metric tensor compared with chapter II, where we used the Cook-Shapiro-Teukolsky metric tensor and again we realize the presence of the factor 2 multiplying the electromagnetic energy density in the expression of the total gravitational mass, hence we verify the conclusion of Papapetrou [26], this factor appears as a fundamental property of electro-gravitational field and hence is independent on the coordinates choice. This result is a consequence of the fact that there is no possibility of formulating the law of conservation of energy without using the potential energy of gravitation.

Another important point to mention is the fact that comparing expressions (4.90) and (4.75) we notice an analogy between the roles of the electromagnetic energy and the total extrinsic curvature, however the distributions of these energies through the star are different as we will show in the next chapter.

The magnetic moment of the star is defined in terms of the asymptotic behaviour of the magnetic field as measured by the Eulerian observer $O_o$ [48], and considering the poloidal

nature of the field

$$\tilde{B}_r = \frac{2\mu cos\theta}{r^3},$$ (4.91)

considering that this is the r-component of $\vec{B}$ in the orthonormal basis associated to $(r, \theta, \phi)$. The relation between $\tilde{B}_r$ and $B_r$, which is the $r$-component of $B_\alpha$, is

$$B_r = e^{\zeta-\nu}\tilde{B}_r,$$ (4.92)

using equation (4.48), we have

$$\left(e^{\zeta-\nu}\frac{2\mu cos\theta}{r^3}\right) = B_r \mid_{r\to\infty} = \left(\frac{e^\nu}{Gr^2 \sin\theta}\right)(A_{\phi,\theta}) \mid_{r\to\infty},$$ (4.93)

and hence

$$\mu = \frac{e^{2\nu-\zeta}}{2G} \frac{r}{sin\theta cos\theta}(A_{\phi,\theta}) \mid_{r\to\infty} .$$ (4.94)

In the next chapter the mass, magnetic dipole moment, magnetic field at the pole and in the center will be used to describe the numerical solution of a magnetized neutron star without rotation.

# Chapter 5

# Numerical procedure and Results

Numerical relativity is one of the branches of the general relativity theory that allows physicists to solve the non linear equations that describe systems like the highly magnetized neutron stars. This chapter deals with the numerical solution of the Einstein-Maxwell equations presented in chapter IV. In this study we consider a rotating neutron star without magnetic field and highly magnetized neutron star modelled as a perfect fluid coupled with a poloidal magnetic field, in this last case we restrict to the static configuration (although both are stationary). In terms of the potential observability of the effects of large magnetic fields, relevant situations appear to be for nonrotating or slowly rotating neutron stars, for example on June 2016 a team of researchers led by Antonino D'Alì from Italy's National Institute of Astrophysics [67] picked up strange X-ray bursts coming from the supernova remnant RCW 103, known as 1E 1613, based on their data another team of researchers lead by Nanda Rea [68] from the University of Amsterdam in the Netherlands concluded that this object is likely a magnetar which is rotating once every 6.67 hours, much slower than the slowest magnetars known, which spins around once every 10 seconds.

## 5.1   Equation of state of the matter considered

The link between the microscopic and macroscopic properties of a system is given by the equation of state (EoS), $P = P(\epsilon)$, which is derived from a microscopic model of the matter that hypothetically composes the system.

The goal of this work is to study the effects of the magnetic field in the structure of neutron stars and not at the microscopic level, because of that we consider as the matter composition a traditional model of EoS known as G300 [69], which is based on a relativistic quantum field theory describing the nuclear matter present in the neutron star using the relativistic mean field approximation, where the fields are replaced by their mean values.

The model supposes that the neutron stars are composed by hadrons and studies the system in the framework of field theory of interacting nucleons, hyperons and mesons. The parameters of the theory are adjusted to reproduce the bulk properties of the nuclear matter, summarized in table 5.1

| Saturation Energy | $E/N$ | -16 MeV |
|---|---|---|
| Saturation Density | $\rho_0$ | 0.16 fm$^{-3}$ |
| Compressibility | $K$ | 265 MeV |
| Symmetry Energy | $a_{sym}$ | 32.5 MeV |
| Nucleon Effective Mass | $m^*/m_N$ | 0.796 |

Table 5.1: Bulk nucleus properties used to constrain neutron star matter model, $m_N = 938$MeV is the average nucleon mass

The method stars from a Lagrangian model which is written in terms of a group of coupling parameters, the barions and mesons are the fermionic and bosonic fields, respectively [69, 70]. The next step is to make use of the Euler-Lagrange equations for each field and with the use of some approximations, the expected value of the energy momentum tensor in the fundamental state is calculated in terms of the Lagrangian. Finally, the energy-momentum tensor of a perfect fluid in a flat spacetime is used and the result is the desired relationship between pressure and energy density $P = P(\epsilon)$. Figure 5.1 shows this relationship.
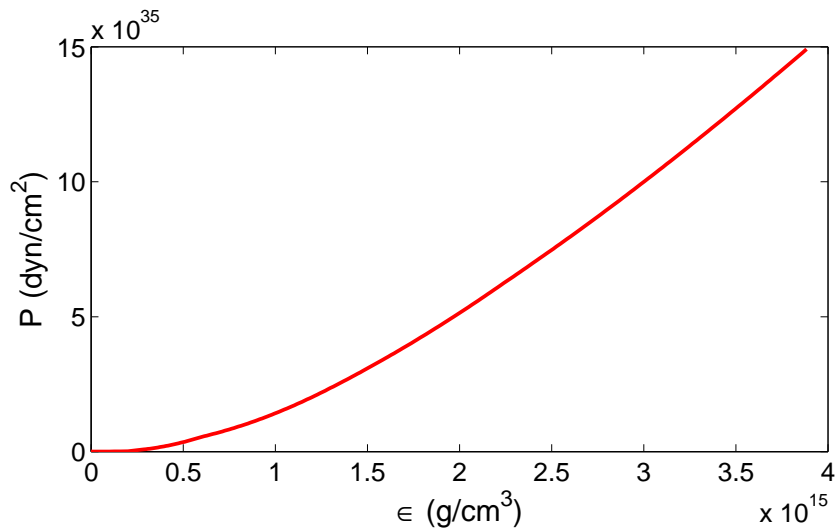
Figure 5.1: Pressure as a function of energy density for the G300 model

## 5.2   Numerical solution for the metric potentials.

To solve the Poisson equations for the metric potentials (4.10 - 4.15) we use Green's functions, similar to the method of Komatsu, Eriguchi and Hachisu (KEH) [25] and Cook, Shapiro and Teukolsky [19], but with a different treatment to find the solution for the metric potential $\alpha$, this point will be discussed in more details in the next subsection.

Equations (4.10), (4.11) and (4.15), for the metric potentials $\nu, N^\phi$ and $A_\phi$, respectively, are of the form

$$\Delta_3 u = \sigma_u, \tag{5.1}$$

where $\Delta_3$ is the three-dimensional flat space Laplacian and $\sigma_u$ is the source of the function $u$. The solution of this equation is

$$u(\vec{r}) = \int dV' \sigma_u(\vec{r'}) G_{3D}(\vec{r}, \vec{r'}), \tag{5.2}$$

where $dV$ is the volume element. The Green's function $G_{3D}$ is given by

$$G_{3D}(\vec{r}, \vec{r'}) = -\frac{1}{4\pi} \frac{1}{\mid \vec{r} - \vec{r'} \mid} \tag{5.3}$$

Equations defining the metric potentials $G$ and $\zeta$ are of the form

$$\Delta_2 u = \sigma_u, \tag{5.4}$$

where $\Delta_2$ is the two-dimensional flat space Laplacian, the solution of this equation is

$$u(\vec{r}) = \int dA' \sigma_u(\vec{r}') G_{2D}(\vec{r}, \vec{r}'), \tag{5.5}$$

where $dA$ is the area element and $G_{2D}$ the two-dimensional Green´s function given by

$$G_{2D}(\vec{r}, \vec{r}') = \frac{1}{2\pi} \ln | \vec{r} - \vec{r}' | \tag{5.6}$$

To find numerical solution for the metric potentials the radial domain $0 \le r \le \infty$ is compactified using the following change of variable

$$r = R\left(\frac{s}{1-s}\right) \tag{5.7}$$

where $R$ is some length scale and the new domain is then $0 \le s \le 1$, hence $s$ maps radial infinity to the finite coordinate location $s = 1$. The computational domain is divided into "inner" and "outer" grids, where the equatorial surface is located at the radial position $s = 0.5$, hence the equatorial radius is set at $r = R$.

For the angular variable, one can choose the coordinate change presented in chapter II where $\mu = \cos\theta$, however in the next equations we will make use of the variable $\theta$ for writing the solution of the metric potentials.

Taking into account the azimuthal and equatorial symmetries present in the configurations, imposing the boundary conditions [all metric functions finite at the origin and $(\nu, N^\phi, \zeta, A_\phi) |_{r\to\infty} \to 0, G |_{r\to\infty} \to 1$], and using the expansion series for the Green´s function given by equations (28) - (32) in reference [25], the solution of the elliptical field equations

(4.10), (4.11), (4.12) and (4.15) in terms of variables $(s, \theta)$ are

$$
\begin{aligned}
\nu(s, \theta) = &- \sum_{n=0}^{\infty} P_{2n}(\cos \theta) \\
&\times \left[ \left( \frac{1-s}{s} \right)^{2n+1} \int_0^s ds' \frac{s'^{2n}}{(1-s')^{2n+2}} \int_0^{\pi/2} d\theta' \sin \theta' P_{2n}(\cos \theta') \tilde{\sigma}_\nu(s', \theta') \right] \\
&+ \left[ \left( \frac{s}{1-s} \right)^{2n} \int_s^1 ds' \frac{(1-s')^{2n}}{s'^{2n+1}} \int_0^{\pi/2} d\theta' \sin \theta' P_{2n}(\cos \theta') \tilde{\sigma}_\nu(s', \theta') \right],
\end{aligned}
\tag{5.8}
$$

$$
\begin{aligned}
N^\phi(s, \theta) = &- \frac{1}{R} \sum_{n=1}^{\infty} \frac{P_{2n-1}^1(\cos \theta)}{2n(2n-1) \sin \theta} \\
&\times \left[ \left( \frac{1-s}{s} \right)^{2n+1} \int_0^s ds' \frac{s'^{2n-1}}{(1-s')^{2n+1}} \int_0^{\pi/2} d\theta' \sin \theta' P_{2n-1}^1(\cos \theta') \tilde{\sigma}_{\tilde{N}^\phi}(s', \theta') \right] \\
&+ \left[ \left( \frac{s}{1-s} \right)^{2n-2} \int_s^1 ds' \frac{(1-s')^{2n-2}}{s'^{2n}} \int_0^{\pi/2} d\theta' \sin \theta' P_{2n-1}^1(\cos \theta') \tilde{\sigma}_{\tilde{N}^\phi}(s', \theta') \right],
\end{aligned}
\tag{5.9}
$$

$$
\begin{aligned}
G(s, \theta) = &1 - \frac{2}{\pi} \sum_{n=1}^{\infty} \frac{\sin[(2n-1)\theta]}{(2n-1) \sin \theta} \\
&\times \left[ \left( \frac{1-s}{s} \right)^{2n} \int_0^s ds' \frac{s'^{2n-1}}{(1-s')^{2n+1}} \int_0^{\pi/2} d\theta' \sin[(2n-1)\theta'] \tilde{\sigma}_{\tilde{G}}(s', \theta') \right] \\
&+ \left[ \left( \frac{s}{1-s} \right)^{2n-2} \int_s^1 ds' \frac{(1-s')^{2n-3}}{s'^{2n-1}} \int_0^{\pi/2} d\theta' \sin[(2n-1)\theta'] \tilde{\sigma}_{\tilde{G}}(s', \theta') \right],
\end{aligned}
\tag{5.10}
$$

$$
\begin{aligned}
A_\phi(s, \theta) = &- R \sum_{n=1}^{\infty} \frac{P_{2n-1}^1(\cos \theta)}{2n(2n-1)} \sin \theta \\
&\times \left[ \left( \frac{1-s}{s} \right)^{2n-1} \int_0^s ds' \frac{s'^{2n-1}}{(1-s')^{2n+1}} \int_0^{\pi/2} d\theta' \sin \theta' P_{2n-1}^1(\cos \theta') \tilde{\sigma}_{\tilde{A}_\phi} \right] \\
&+ \left[ \left( \frac{s}{1-s} \right)^{2n} \int_s^1 ds' \frac{(1-s')^{2n-2}}{s'^{2n}} \int_0^{\pi/2} d\theta' \sin \theta' P_{2n-1}^1(\cos \theta') \tilde{\sigma}_{\tilde{A}_\phi} \right],
\end{aligned}
\tag{5.11}
$$

where $\tilde{\sigma}_f = r^2 \sigma_f = R^2 \left( \frac{s}{1-s} \right)^2 \sigma_f$, is the dimensionless source of the potential $f$, $P_n$ is the Legendre polynomial and $P_n^m$ is the associated Legendre function. The solution for the component $A_t$ is not presented in this chapter because we will deal only with the static configuration for a magnetized star.

## 5.2.1   Special case: solution of the metric potential $\zeta$

In the chapter II we studied a perfect fluid coupled with a poloidal magnetic field inspired in the work of Shapiro et al. [19]. As we have seen the equations defining the metric potentials $\rho$ and $\gamma$ are of the form of (5.1) and (5.4), respectively, but the equation defining the metric potential $\alpha$ is of the form

$$\frac{\partial \alpha}{\partial \theta} = \mathfrak{S}(r, \theta) \tag{5.12}$$

where $\mathfrak{S}$ is a complicated expression containing first and second order derivatives, quadratic terms of these derivatives and even terms like $\gamma_{,r\mu}$ [see equation (2.55)].

In the current formalism the role of the metric potential $\alpha$ is taken by $\zeta$, but the equation defining it is of the form $\Delta_2 \zeta = \sigma_\zeta$, which looks simpler than equation (5.12). The solution of the metric potential $\zeta$ however, should be handled with care because its may result in a logarithmic divergence at infinity during iteration procedure. To avoid this problem we use the virial theorem discussed in the chapter III.

The starting point is to remember that the Green's function of the 2D Laplacian is given by equation (5.6) hence the solution for the metric potential $\zeta$ is

$$\zeta(r, \theta) = \frac{1}{2\pi} \int_{r'}^{\infty} r' dr' \int_0^{2\pi} d\theta' \sigma_\zeta(r', \theta') \ln |\, \vec{r} - \vec{r'}\, | \tag{5.13}$$

where the source $\sigma_\zeta$ is given by equation (4.25). Since the regularity conditions at $r = 0$ imply that all scalar functions may be expanded into a series of $\cos(n\theta)$, the analytical continuation satisfies

$$\forall \theta \in [\pi, 2\pi], \qquad \sigma_\zeta(r, \theta) = \sigma_\zeta(r, 2\pi - \theta). \tag{5.14}$$

On the other hand, when $r \to \infty$, the term $\ln |\, \vec{r} - \vec{r'}\, | \sim \ln r$, so that $\zeta(r, \theta) \sim I \ln r$, where

$$I := \frac{1}{2\pi} \int_{r'}^{\infty} r' dr' \int_0^{2\pi} d\theta' \sigma_\zeta(r', \theta'). \tag{5.15}$$

Taking into account the asymptotic flatness condition at infinity $\zeta = 0$, the integral should be zero

$$\frac{1}{2\pi} \int_{r'}^{\infty} r' dr' \int_{0}^{2\pi} d\theta' \sigma_{\zeta}(r', \theta') = 0 \tag{5.16}$$

Using the expression of $\sigma_{\zeta}$ given by equation (4.25),

$$\int_{r'}^{\infty} r' dr' \int_{0}^{2\pi} d\theta' \left[ 8\pi e^{2(\zeta' - \nu')} S_{\phi}^{\phi} + \frac{3}{4} e^{-4\nu'} G'^2 r'^2 \sin^2 \theta' (\partial N^{\phi'})^2 - (\partial \nu')^2 \right] = 0. \tag{5.17}$$

where the primes over the metric function $u$ means $u = u(r', \theta')$, for example $\nu' = \nu(r', \theta')$.

The above equality corresponds to the virial theorem expressed by equation (3.21), taking into account that for the present study we choose the hypersurface $\Sigma_t$ to be maximal slicing [29], usually used in numerical relativity, so that the trace of the extrinsic curvature tensor is zero $K = 0$. The term $(\partial N^{\phi'})^2$ is related to the components of the extrinsic curvature, through equations

$$\kappa_1 = -\frac{1}{2} e^{-(\zeta + \nu)} G r \sin \theta N_{,r}^{\phi} \quad \kappa_2 = -\frac{1}{2} e^{-(\zeta + \nu)} G \sin \theta N_{,\theta}^{\phi}. \tag{5.18}$$

As we can see, the integral (5.17) has three terms, one related to the source, second associated to the extrinsic curvature and the last term containing second derivatives of the metric potential $\nu$, just the structure of the virial integral (3.21) presented in chapter III.

The source $\sigma_{\zeta}$ can be written as

$$\sigma_{\zeta} = \sigma_{\zeta}^m + \sigma_{\zeta}^f, \tag{5.19}$$

where the prescriptions $m$ and $f$ mean matter and field, so $\sigma_{\zeta}^m$ contains the "matter terms" (those involving components of the stress-energy tensor) and $\sigma_{\zeta}^f$ contains the "field terms" (those involving only the metric variables), in agreement with equation (4.6). Considering this, the integral $I$ for $\sigma_{\zeta}$ can be written as $I = I^m + I^f = 0$, which in terms of the

compactified variable $s$ is

$$\int_0^1 ds \frac{s}{(1-s)^3} \sigma_{\zeta,0}^m(s) + \int_0^1 ds \frac{s}{(1-s)^3} \sigma_{\zeta,0}^f(s) = 0 \tag{5.20}$$

where

$$\sigma_{\zeta,0}(s) = \int_0^{2\pi} d\theta \sigma_\zeta(s,\theta). \tag{5.21}$$

Equation (5.20) is a solution of Einstein´s equations, however it may blow up, due to the logarithm factor, spoiling convergence. In order to avoid the logarithmic divergence caused by the violation of (5.20) and to guarantee the convergence of the iteration, the technique is to write the equation for the metric potential $\zeta$ as [35]

$$\Delta_2 \zeta = \sigma_\zeta^m + \lambda \sigma_\zeta^f \tag{5.22}$$

where the parameter $\lambda$ is

$$\lambda = -\frac{\int_0^1 ds \frac{s}{(1-s)^3} \sigma_{\zeta,0}^m(s)}{\int_0^1 ds \frac{s}{(1-s)^3} \sigma_{\zeta,0}^f(s)}. \tag{5.23}$$

At the end of the iteration process $\lambda$ must approach to 1 for the computed metric functions to represent a valid solution to Einstein's equations.

Finally, the solution of the metric potential $\zeta$ is then given by

$$\begin{aligned}
\zeta(s,\theta) =& \frac{2}{\pi} \left[ \ln r(s) \int_0^s ds' \frac{1}{(1-s')^2} \int_0^{\pi/2} d\theta' \tilde{\sigma}_\zeta(s',\theta') + \int_s^1 ds' \frac{1}{(1-s')^2} \ln r(s') \int_0^{\pi/2} d\theta' \tilde{\sigma}_\zeta(s',\theta') \right] \\
&- \frac{2}{\pi} \sum_{n=1}^\infty \frac{\cos(2n\theta)}{2n} \left[ \left( \frac{1-s}{s} \right)^{2n} \int_0^s ds' \frac{s'^{2n}}{(1-s')^{2n+2}} \int_0^{\pi/2} d\theta' \cos(2n\theta') \tilde{\sigma}_\zeta(s',\theta') \right. \\
&\left. + \left( \frac{s}{1-s} \right)^{2n} \int_s^1 ds' \frac{(1-s')^{2n-2}}{s'^{2n}} \int_0^{\pi/2} d\theta' \cos(2n\theta') \tilde{\sigma}_\zeta(s',\theta') \right],
\end{aligned} \tag{5.24}$$

where the source $\tilde{\sigma}_\zeta = Rr(\sigma_\zeta^m + \lambda \sigma_\zeta^f) = R^2(\frac{s}{1-s})(\sigma_\zeta^m + \lambda \sigma_\zeta^f)$. At the end of the iteration the quantity $|\, 1 - \lambda \,|$ appears to be a good indicator of the discrepancy between the achieved

solution and the exact one.

A valid question would be why one does not use the virial theorem for the metric function $\tilde{G}$ as equation (4.12) also involves the two dimensional Laplacian in a similar way than the equation defining the metric potential $\zeta$? Such procedure is not needed since the $\sin\theta$ factor present in the source $\sigma_{\tilde{G}}$ guarantees that the $\ln r$ term vanishes. The key issue here is that the analytical continuation on $[\pi, 2\pi]$ of the source term $\sigma_{\tilde{G}}$ is not satisfied, since

$$\sigma_{\tilde{G}} = \sigma_G r sin\theta \Rightarrow \sigma_{\tilde{G}}(r, \theta) \neq \sigma_{\tilde{G}}(r, 2\pi - \theta) \tag{5.25}$$

but, instead, the source $\sigma_G$ satisfies the analytical continuation and hence,

$$\forall \theta \in [\pi, 2\pi], \quad \sigma_{\tilde{G}}(r, \theta) = \sigma_G(r, 2\pi - \theta) r sin\theta. \tag{5.26}$$

The integral $I$ for the source $\sigma_{\tilde{G}}$ is

$$I := \frac{1}{2\pi} \int_{r'}^{\infty} r' dr' \int_{0}^{2\pi} d\theta' \sigma_{\tilde{G}}(r', \theta'). \tag{5.27}$$

Now using the analytical continuation (5.26)

$$\int_{r'}^{\infty} r' dr' \int_{0}^{2\pi} d\theta' \sigma_{\tilde{G}}(r', \theta') = \int_{r'}^{\infty} r' dr' \int_{0}^{2\pi} d\theta' \sigma_G(r', 2\pi - \theta') r' sin\theta', \tag{5.28}$$

hence the integral $I = 0$ everywhere.

## 5.3  Results

In the following we show the results corresponding to the solution for rotating neutron stars without magnetic field and for nonrotating neutron stars with a poloidal magnetic field. The terms that allow us to calculate the virial factor $\lambda$, i.e. $\sigma_{\zeta}^m$ and $\sigma_{\zeta}^f$ will be written in terms of the physical variables and the coordinate $s$ for each case. The results for the mass, radius, angular momentum, magnetic field at the pole and center as well the magnetic moment will be presented. The contour plots of some quantities like the extrinsic

curvature and electromagnetic energy density will shed light on how the high rotation or high magnetic field affect the system. Finally, the mass-radius relation will be shown for the case of magnetized neutron stars with different central densities and magnetic field.

### 5.3.1   Results for a rotating neutron star without magnetic field

A rotating neutron star without magnetic field is studied for three values of the angular velocity, defined in terms of the relation between the polar and equatorial radius $r_{ratio} = r_{pole}/r_{eq}$. The first value corresponds to $r_{ratio} = 1.00$ which defines the spherically symmetric case, the second value is $r_{ratio} = 0.80$ which generates an intermediate deformation and the last one $r_{ratio} = 0.70$ generating the largest deformation with an acceptable value of the virial parameter $\lambda$ for a star with central density $\epsilon_c = 500$ MeV/fm$^3$. In table 5.2 we show the results for the total gravitational mass $m$, the circumferential radius $R$, the perfect fluid [1] contribution to the mass $M^{PF}$, the contribution of the extrinsic curvature to the total mass $M^\kappa$, the angular velocity $\Omega$, the total angular momentum $J$ and the virial factor $\mid 1 - \lambda \mid$.

The perfect fluid and the extrinsic curvature contributions to the gravitational mass of the system in table 5.2 are given by

$$M^{PF} = 4\pi R^3 \int_0^1 ds \frac{s^2}{(1-s)^4} \int_0^{\pi/2} d\theta sin\theta e^{2(\epsilon-\nu)} G\left[\Gamma^2(\epsilon+P)(1+U^2)+2P\right], \quad (5.29)$$

$$M^\kappa = 4\pi R^3 \int_0^1 ds \frac{s^2}{(1-s)^4} \int_0^{\pi/2} d\theta sin\theta e^{2(\epsilon-\nu)} G\left[\frac{1}{2\pi}(\kappa_1^2+\kappa_2^2)\right]. \quad (5.30)$$

The terms for calculate the virial factor $\lambda$ in this case are given by

$$\sigma_\zeta^m = 8\pi G_N e^{2(\zeta-\nu)}\left[P+(\epsilon+P)\frac{U^2}{1-U^2}\right] \quad (5.31)$$

$$\sigma_\zeta^f = \frac{3}{4}e^{-4\nu}G^2 sin^2\theta[s^2(1-s)^2(N_{,s}^\phi)^2+(N_{,\theta}^\phi)^2]-\frac{(1-s)^2}{R^2}\left[(1-s)^2(\nu_{,s})^2+\frac{1}{s^2}(\nu_{,\theta})^2\right] \quad (5.32)$$

---

[1] we use this name because this term remember us the expression of the total gravitational mass of the perfect fluid for a nonrotating star

Figures 5.2 - 5.9 show the distribution of each term that contributes to the gravitational mass, i.e. $M^{PF}$ and $M^{\kappa}$ and the pressure contour, for a star with a fixed central density $\epsilon_c = 500$ MeV/fm$^3$ and different values of the angular velocity corresponding to the table 5.2. The red solid line shows the star surface. The values reported in the table for $M^{PF}$ and $M^{\kappa}$, correspond to equations (5.29) and (5.30), respectively, while the values showed in the legend of the figures 5.2 - 5.6 correspond to expressions within the brackets in these equations, i.e. the contour plots of the perfect fluid contribution to the total mass in figures 5.2 -5.4 are the contour plots of the term within the brackets in equation (5.29),while the contour plots of the extrinsic curvature contribution to the total mass in figures 5.5 and 5.6 are the contour plots of the term within the brackets in equation (5.30), in units of energy density $g/cm^3$.

Comparing the graphics that show the energy density coming from $M^{PF}$, pressure and the extrinsic curvature contribution, for the different values of $r_{ratio}$, we realize the rotational effects in the shape of the star surface and the distribution of the extrinsic curvature energy, while the distribution of the energy associated to $M^{PF}$ is concentrated around the center of the star, as we can see from figure 5.2, 5.3 and 5.4, the energy coming from $M^{\kappa}$ has its biggest values near to the star's surface, as show figures 5.5 and 5.6, actually we can see values between $(0.5 - 1.5) \times 10^{12}$ g/cm$^3$ outside of the star´s surface. In the sense of the maximum values reached by the perfect fluid contribution to the energy density (figures 5.2, 5.3 and 5.4) and the maximum pressure (figures 5.7, 5.8 and 5.9), there are no difference between the three cases, i.e. the maximum energy density or the maximum pressure reached for stars with different angular velocities remain the same, but for the plots showing the extrinsic curvature contribution, the maximum value grows up from zero (the spherical symmetric configuration) to $\sim 4.5 \times 10^{12}$g/cm$^3$ corresponding to a star with angular velocity $\Omega = 0.585 \times 10^4$s$^{-1}$, i.e a star for which $r_{pole} = 70\% r_{eq}$.

| $r_{ratio}$ | $m$ | $R$ | $M^{PF}$ | $M^{\kappa}$ | $\Omega$ | $J$ | $\mid 1 - \lambda \mid$ |
|---|---|---|---|---|---|---|---|
| | $M_{\odot}$ | km | $M_{\odot}$ | $(10^{-2})M_{\odot}$ | $(10^{4})\ s^{-1}$ | $(10^{71})$ erg.s | $(10^{-2})$ |
| 1.00 | 1.543 | 12.841 | 1.543 | 0.000 | 0.000 | 0.000 | 1.454 |
| 0.80 | 1.645 | 14.205 | 1.632 | 1.302 | 0.493 | 4.642 | 2.356 |
| 0.70 | 1.728 | 15.331 | 1.706 | 2.259 | 0.585 | 6.428 | 4.368 |

Table 5.2: Properties for rotating neutron stars with central energy density $\epsilon_c = 500$ MeV/fm$^3$
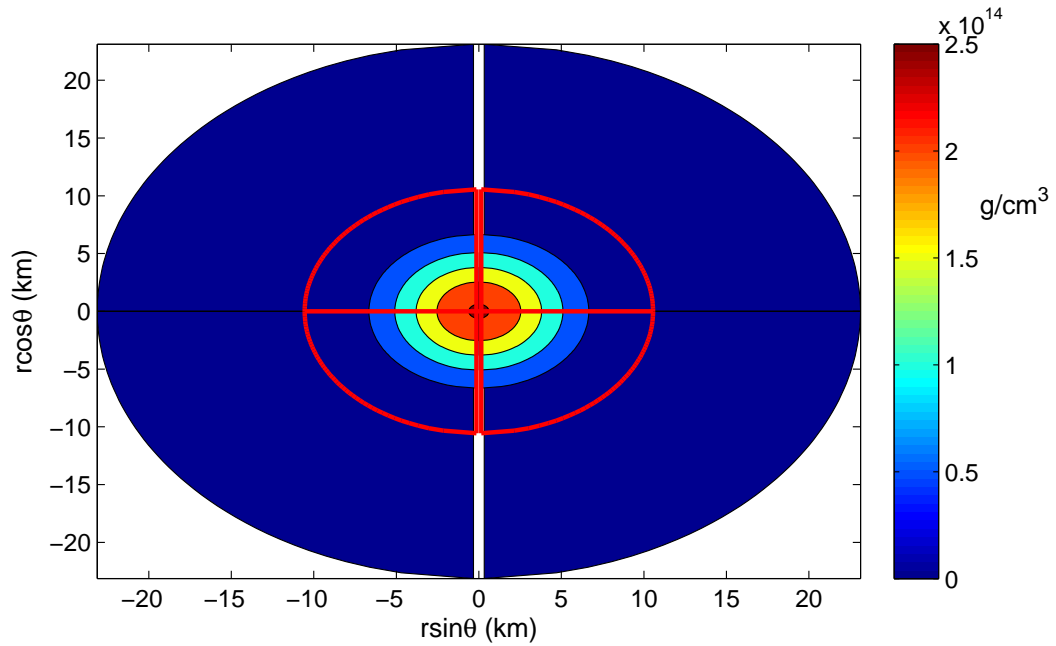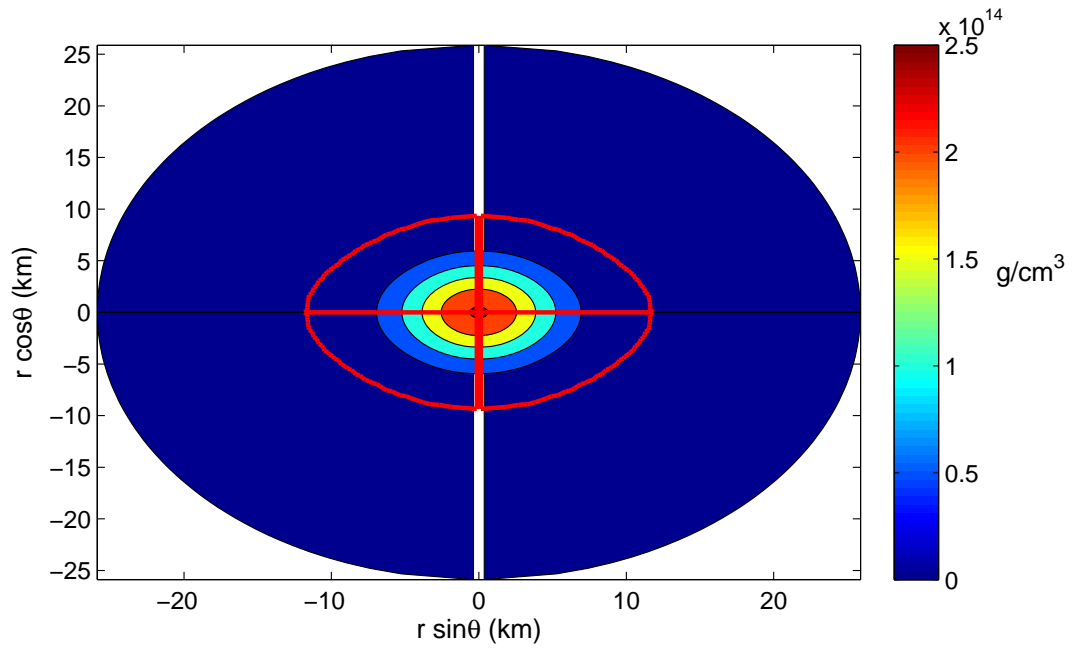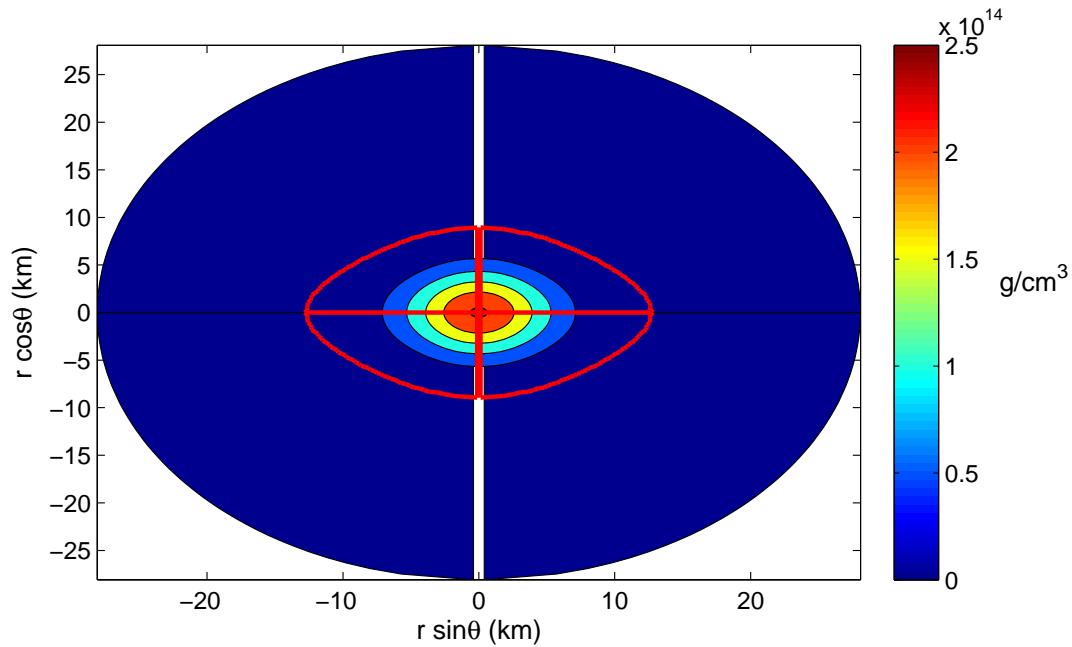


Figure 5.2: Contour plot of the energy density coming from the perfect fluid contribution to the total mass for a star with $r_{ratio} = 1.00$ and $\epsilon_c = 500$ MeV/fm$^3$. The figure shows the distribution of the term within the brackets in equation (5.29). The red solid line represents the star's surface.

Figure 5.3: Contour plot of the energy density coming from the perfect fluid contribution to the total mass for a star with $r_{ratio} = 0.80$ and $\epsilon_c = 500$ MeV/fm$^3$. The figure shows the distribution of the term within the brackets in equation (5.29). The red solid line represents the star's surface.



Figure 5.4: Contour plot of the energy density coming from the perfect fluid contribution to the total mass for a star with $r_{ratio} = 0.70$ and $\epsilon_c = 500$ MeV/fm$^3$. The figure shows the distribution of the term within the brackets in equation (5.29). The red solid line represents the star's surface.
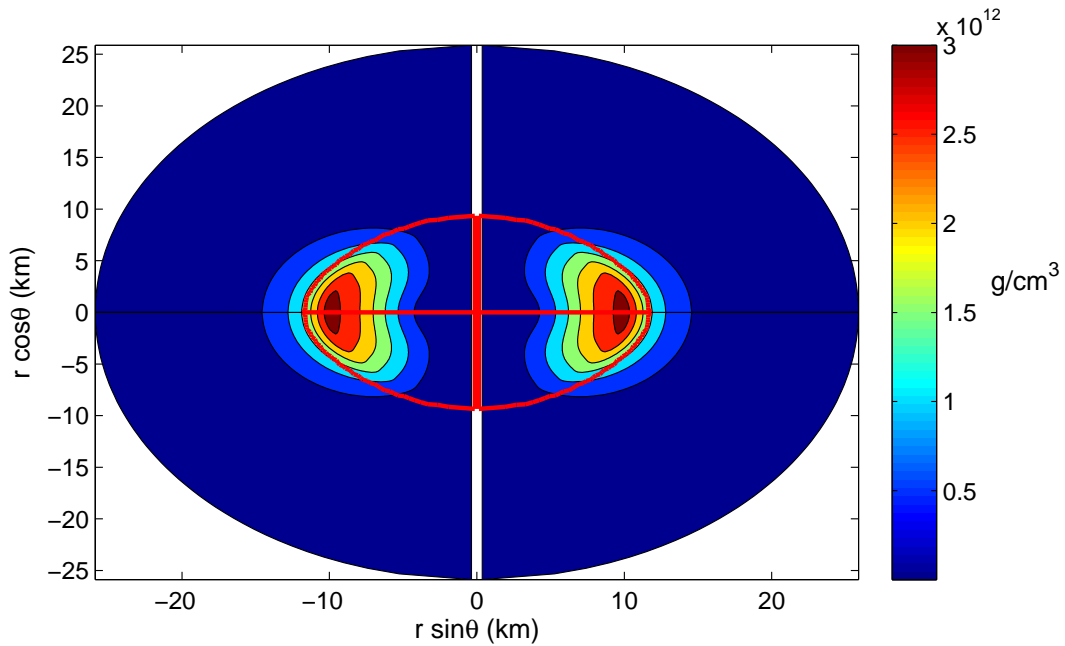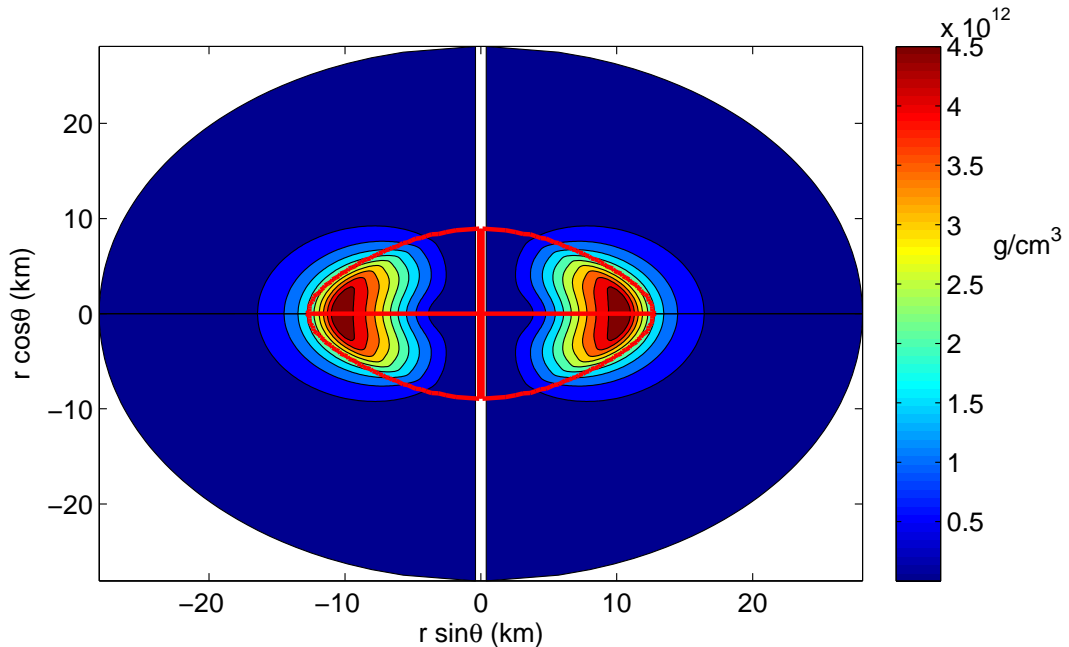
Figure 5.5: Contour plot of the energy density coming from the extrinsic curvature contribution to the total mass for a star with $r_{ratio} = 0.80$ and $\epsilon_c = 500$ MeV/fm$^3$. The figure shows the distribution of the term within the brackets in equation (5.30). The red solid line represents the star's surface.



Figure 5.6: Contour plot of the energy density coming from the extrinsic curvature contribution to the total mass for a star with $r_{ratio} = 0.70$ and $\epsilon_c = 500$ MeV/fm$^3$. The figure shows the distribution of the term within the brackets in equation (5.30). The red solid line represents the star's surface.
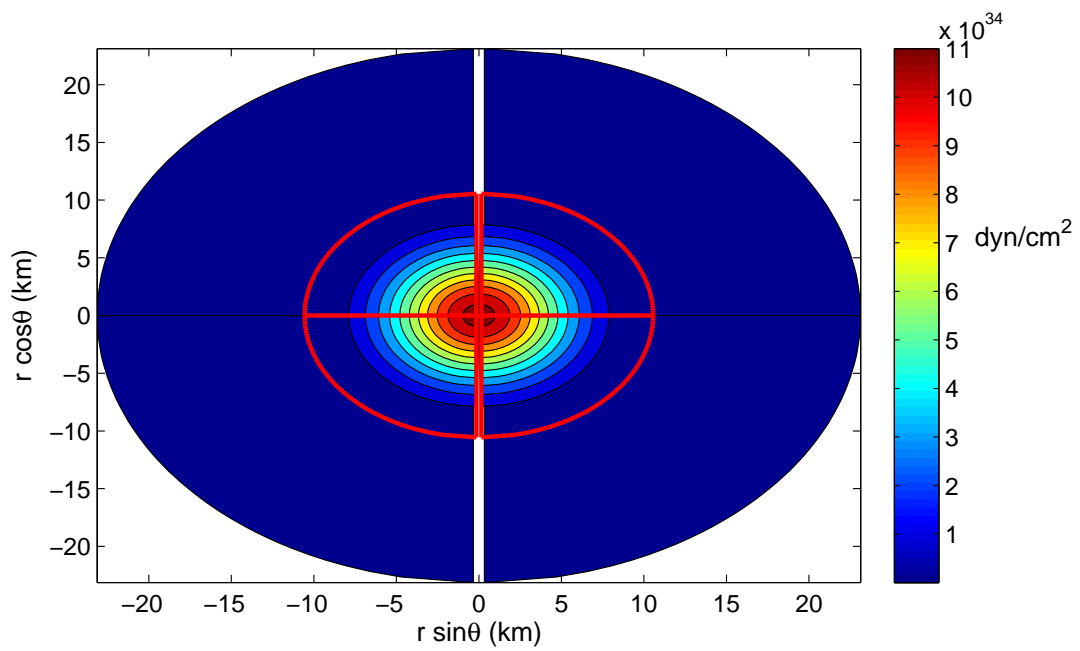
Figure 5.7: Contour plot of the pressure for a star with $r_{ratio} = 1.00$ and $\epsilon_c = 500$ MeV/fm$^3$. The red solid line represents the star's surface.



Figure 5.8: Contour plot of the pressure for a star with $r_{ratio} = 0.80$ and $\epsilon_c = 500$ MeV/fm$^3$. The red solid line represents the star's surface.
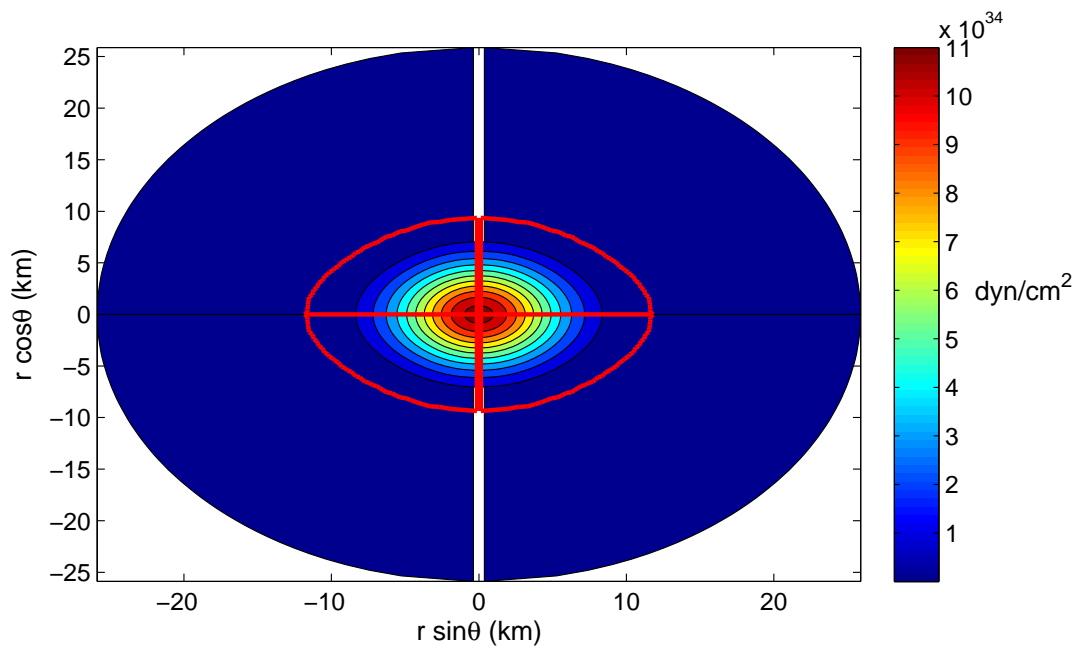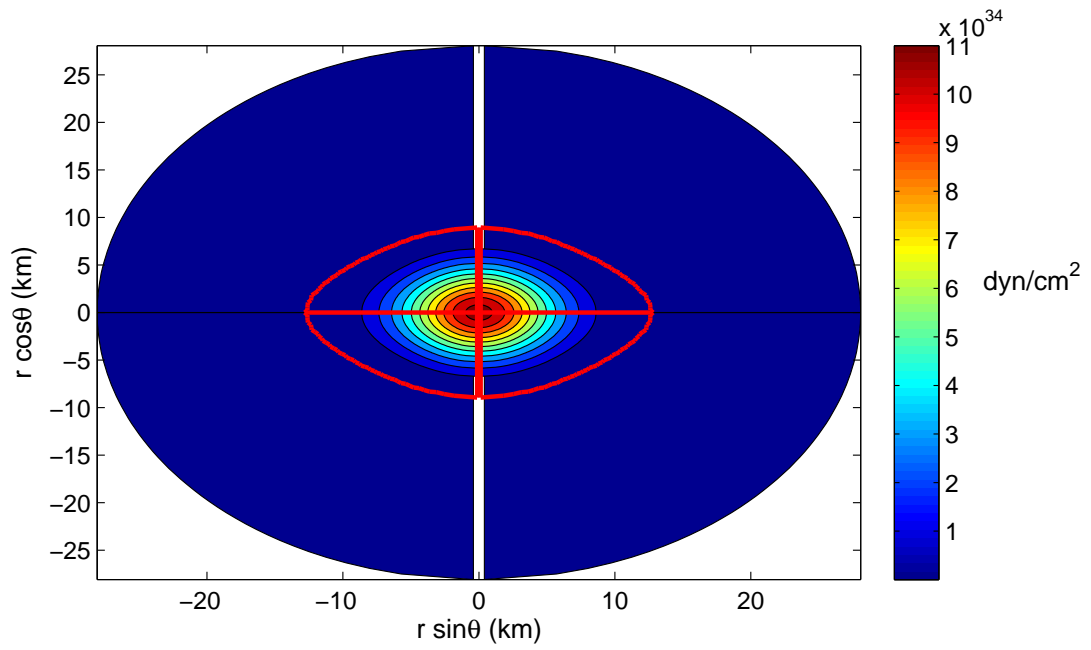
Figure 5.9: Contour plot of the pressure for a star with $r_{ratio} = 0.70$ and $\epsilon_c = 500$ MeV/fm$^3$. The red solid line represents the star's surface.

### 5.3.2   Results for a highly magnetized neutron star

As we mentioned in the introduction of this chapter we restrict attention to static configurations, which involves a number of simplifications, including the vanishing of $N^\phi$, $A_t$, and $J^t$, and the absence of surface charges. Moreover, we have chosen the current function defined by equation (4.57) to be a constant $f(A_\phi) = f_o$, hence the 4-current density has only one component given by

$$j^\phi = (\epsilon + P)f_o, \tag{5.33}$$

hence the azimutal component of $j^\mu$ in an orthonormal basis is

$$\tilde{j}^\phi = e^{-\nu}Gr\sin\theta(\epsilon + P)f_o, \tag{5.34}$$

In the following, neutron stars with a poloidal magnetic field are studied for different values of the current function $f_0$ which will help us to study from the spherical symmetric configuration ($f_o = 0.00$) as well as a highly magnetized star ($f_o = 3.26$) in which the strong magnetic field affects the matter distribution in the system, as we will see. In table 5.3 we show the results for the total gravitational mass $m$, the circumferential radius $R$, the perfect fluid [2] contribution to the mass $M^{PF}$, the electromagnetic contribution to the mass $M^{EM}$, the magnetic field magnitude at the center $B_c$ and at the pole $B_{pole}$, the magnetic moment $\mu$ at $\theta = \pi/4$ and the virial factor $\mid 1 - \lambda \mid$ for stars with a fixed central density $\epsilon_c = 350$ MeV/fm$^3$.

The perfect fluid and the electromagnetic contributions to the gravitational mass are given by

$$M^{PF} = 4\pi R^3 \int_0^1 ds \frac{s^2}{(1-s)^4} \int_0^{\pi/2} d\theta sin\theta e^{2(\epsilon - \nu)}G(\epsilon + 3P), \tag{5.35}$$

---

[2]we use this name because this term remember us the expression of the gravitational mass of the perfect fluid for a nonmagnetized star

$$M^{EM} = 4\pi R^3 \int_0^1 ds \frac{s^2}{(1-s)^4} \int_0^{\pi/2} d\theta sin\theta e^{2(\epsilon-\nu)} G(2E^{EM}). \tag{5.36}$$

In terms of the coordinates $(s,\theta)$ the expression (4.94) for the magnetic moment is

$$\mu(s,\theta) = \frac{e^{2\nu-\zeta}}{2Gcos\theta sin\theta} R \frac{s}{1-s} (A_{\phi,\theta}) \mid_{s\to1} . \tag{5.37}$$

For the case of a perfect fluid coupled with a poloidal magnetic field, the terms that allow us to calculate the virial quantity $\lambda$ are

$$\sigma_\zeta^m = 8\pi G_N e^{2(\zeta-\nu)} P + G_N \frac{e^{2\nu}}{R^4 G^2 sin^2\theta} \frac{(1-s)^4}{s^2} \left[ (1-s)^2 (A_{\phi,s})^2 + \frac{1}{s^2}(A_{\phi,\theta})^2 \right], \tag{5.38}$$

and

$$\sigma_\zeta^f = -\frac{(1-s)^2}{R^2} \left[ (1-s)^2 (\nu_{,s})^2 + \frac{1}{s^2}(\nu_{,\theta})^2 \right]. \tag{5.39}$$

Figures 5.10 - 5.23 show the distribution of each term that contributes to the gravitational mass, i.e. $M^{PF}$ and $M^{EM}$, the contour of the pressure and the electromagnetic potential $A_\phi$ with magnetic field lines, for stars with a fixed central energy density $\epsilon_c = 350$ MeV/fm$^3$ and different values of the current function corresponding to the table 5.3. The red solid line shows the star surface. The values reported in the table for $M^{PF}$ and $M^{EM}$, correspond to equations (5.35)and (5.36), respectively, while the values showed in the legend of the figures 5.10 - 5.16 correspond to the expressions within the parenthesis in these equations, i.e. the contour plots of the perfect fluid contribution to the total mass in figures 5.10 - 5.13 are the contour plots of the term within parenthesis in equation (5.35), while the contour plots of the electromagnetic contribution to the total mass in figures 5.14 - 5.16 are the contour plots of the term within parenthesis in equation (5.36), in units of energy density $g/cm^3$.

Comparing the graphics that show the energy distribution associated to the perfect fluid contribution for $f_o = 1.00$ with the spherically symmetric configuration (figures 5.11 and 5.10, respectively), we see no significantly differences, however when the current fucntion

is $f_o = 2.50$ the shape of the star's surface shows a deviation from the spherically symmetric configuration (figure 5.12) showing the effects of the increase of magnetic field.  The same observations are valid for figures that show the contour plot of the pressure, figures 5.17, 5.18 and 5.19, where the maximum values reached for $P$ remains in   5.5 dyn/cm$^2$, but for $f_o = 2.50$ as before the increase of the magnetic field affects the shape of the star. The electromagnetic effects become more dramatic when the magnetic field increases from $B_c = 1.844 \times 10^{17}$ G to $B_c = 1.240 \times 10^{18}$ G which corresponds to $f_o = 3.26$, the effects of this higher magnetic field are reflected not only in the shape of the star but also in the matter distribution, for this value of $f_o$ the magnetic forces push the matter off-center, showing the transition to a toroidal topology (figures 5.13 and 5.20), similar results were reported by Lattimer et. al. [71]. The electromagnetic energy at the center experiments a growth from $\sim 14 \times 10^{11}$ g/cm$^3$ for $f_o = 1.00$, $\sim 12 \times 10^{12}$ g/cm$^3$ for $f_o = 2.50$ to the highest value $\sim 6 \times 10^{13}$ g/cm$^3$ for $f_o = 3.26$ as we can see in figures 5.14,5.15 and 5.16, respectively. The increase in the magnetic field is shown in figures 5.21, 5.22 and 5.23 where we can see the change in the order of magnitude of $A_\phi$ between the different values of the current function, from $A_{\phi,max} \sim 4.5 \times 10^{28}$ G.cm to $A_{\phi,max} \sim 6.0 \times 10^{29}$ G.cm.  The red line changes from spherical to ellipsoidal, showing the effects in the shape of the star of the growing magnetic field. From these figures we can conclude that the only component of the 4-current density is $j^\phi$ which vanishes at the center and in the surface of the star. The current measured by a local observer in the equatorial plane $\tilde{j}^\phi$ peaks somewhere inside the star and vanishes at the origin and the surface, as equation (5.34) suggests, generating the poloidal magnetic field. Another conclusion that these figures allow us to draw is the fact that the highest magnitude of the magnetic field is at the center of the star in contrast to figure 1 of Lattimer et. al. [71] in which the magnetic field strength can not be deduced from the lines distribution. After the value $f_o = 3.26$ for a star with $\epsilon_c = 350$ MeV/fm$^3$, convergence cannot be achieved. In that sense, the transition to a toroidal topology is suggestive of possible dynamical outcomes that may be considered for future works.

It is important to draw attention to the fact that the maximum values of the pressure in the case of a rotating stars without magnetic field (figures 5.7, 5.8 and 5.9) are $\sim 11 \times$

$10^{34}$ dyn/cm$^2$ and for magnetized stars without rotation (figures 5.17, 5.18 and 5.19) the maximum pressure values are $\sim 5.5 \times 10^{34}$ dyn/cm$^2$, the first value mentioned corresponds to a star with central density $\epsilon_c = 500$ MeV/fm$^3$ while the second one corresponds to $\epsilon_c = 350$ MeV/fm$^3$, but when the current function is set at $f_o = 3.26$ these maximum values become similar as we can see in figure 5.20. It would be interesting for future works, to compare the effects of high central densities for rotating neutron stars and high magnetic fields in the magnitude of the total pressure.

Another important point to be mentioned is that besides the expressions for the gravitational mass for the rotating star with no magnetic field and the magnetized star without rotation, equations (4.75) and (4.90), respectively, suggest an analogy between the roles of the energy density coming from the extrinsic curvature and the electromagnetic contribution in the gravitational mass, figures 5.5 and 5.6 for a rotating star and figures 5.14, 5.15 and 5.16 for a magnetized star, show that the distribution in the star of these energies are different, while the energy associated to the extrinsic curvature tensor is concentrated near to the surface of the star, the electromagnetic energy has its maximum values near to the center. Another difference between these two curvature sources is associated to the maximum values they reach, while for the extrinsic curvature its maximum value is $\sim 4.5 \times 10^{12}$g/cm$^3$ for the electromagnetic energy the maximum value is $\sim 6 \times 10^{13}$g/cm$^3$, being only one order of magnitude less than the maximum values reached for the perfect fluid contribution.

| $f_0$ | $m$ | $R$ | $M^{PF}$ | $M^{EM}$ | $B_c$ | $B_{pole}$ | $\mu$ | $\mid 1 - \lambda \mid$ |
|---|---|---|---|---|---|---|---|---|
| | $M_\odot$ | km | $M_\odot$ | $(10^{-3})M_\odot$ | $(10^{17})$ G | $(10^{17})$ G | $(10^{35})$ Gaussian | $(10^{-3})$ |
| 0.000 | 1.275 | 13.257 | 1.275 | 0.000 | 0.000 | 0.000 | 0.000 | 7.164 |
| 1.000 | 1.303 | 13.367 | 1.300 | 2.342 | 1.844 | 0.242 | 3.028 | 9.744 |
| 2.500 | 1.562 | 14.211 | 1.535 | 26.714 | 5.535 | 0.879 | 10.089 | 10.938 |
| 3.260 | 2.986 | 15.541 | 2.745 | 241.7 | 12.400 | 2.995 | 32.797 | 130.600 |

Table 5.3: Properties of magnetized stars with central energy density $\epsilon_c = 350$ MeV/fm$^3$
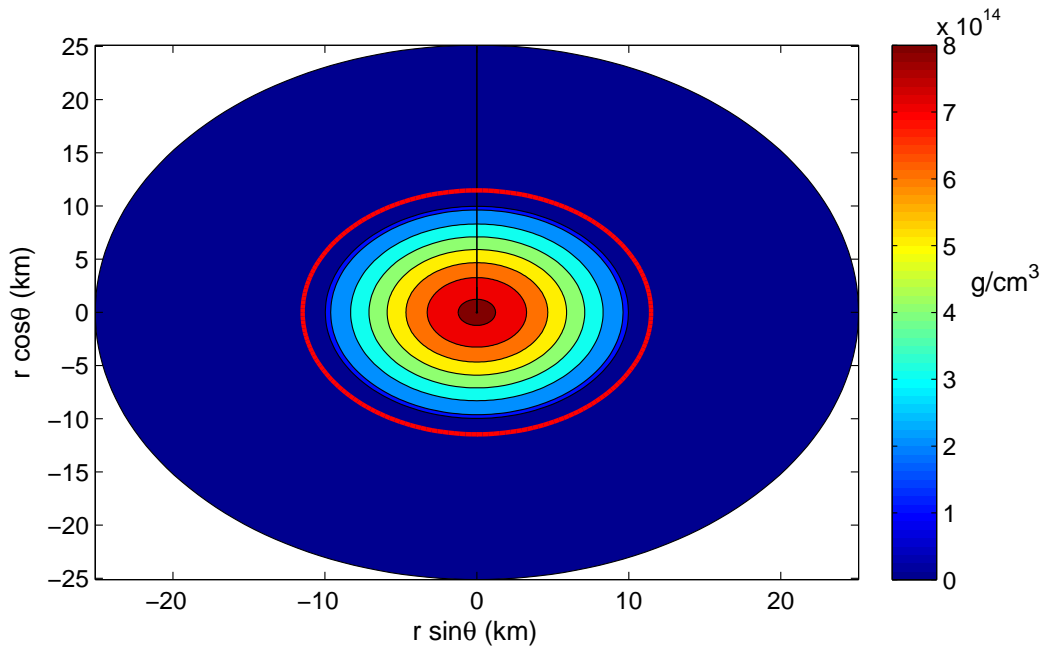
Figure 5.10: Contour plot of the energy density coming from the perfect fluid contribution to the total mass for a star with $f_o = 0.00$ and $\epsilon_c = 350$ MeV/fm$^3$. The figure shows the distribution of the term within the parenthesis in equation (5.35). The red solid line represents the star's surface.
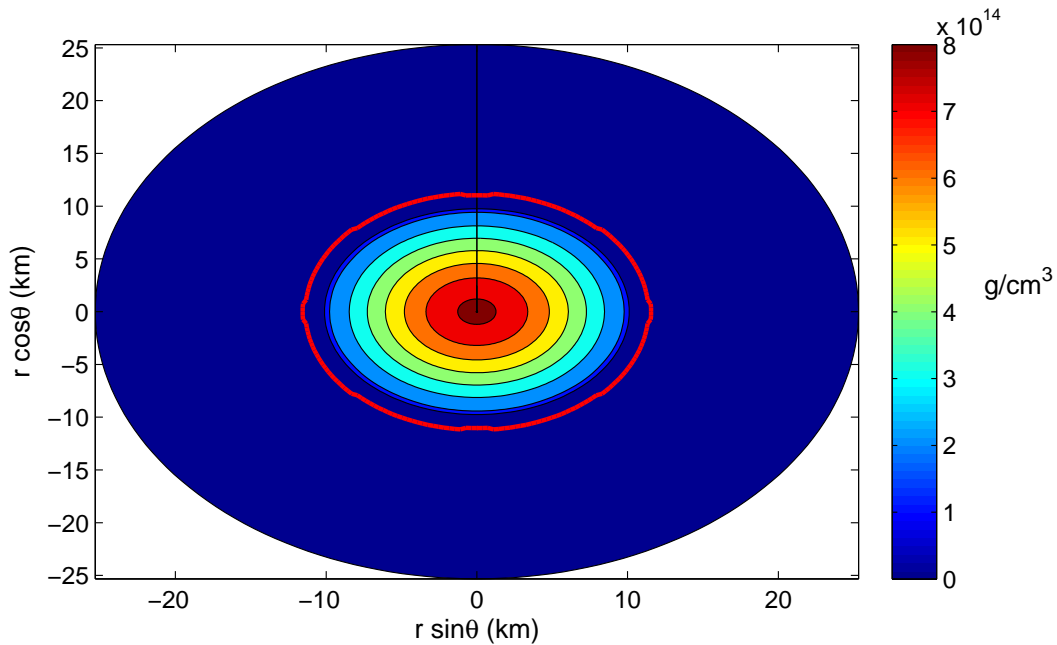


Figure 5.11: Contour plot of the energy density coming from the perfect fluid contribution to the total mass for a star with $f_o = 1.00$ and $\epsilon_c = 350$ MeV/fm$^3$. The figure shows the distribution of the term within the parenthesis in equation (5.35). The red solid line represents the star's surface.
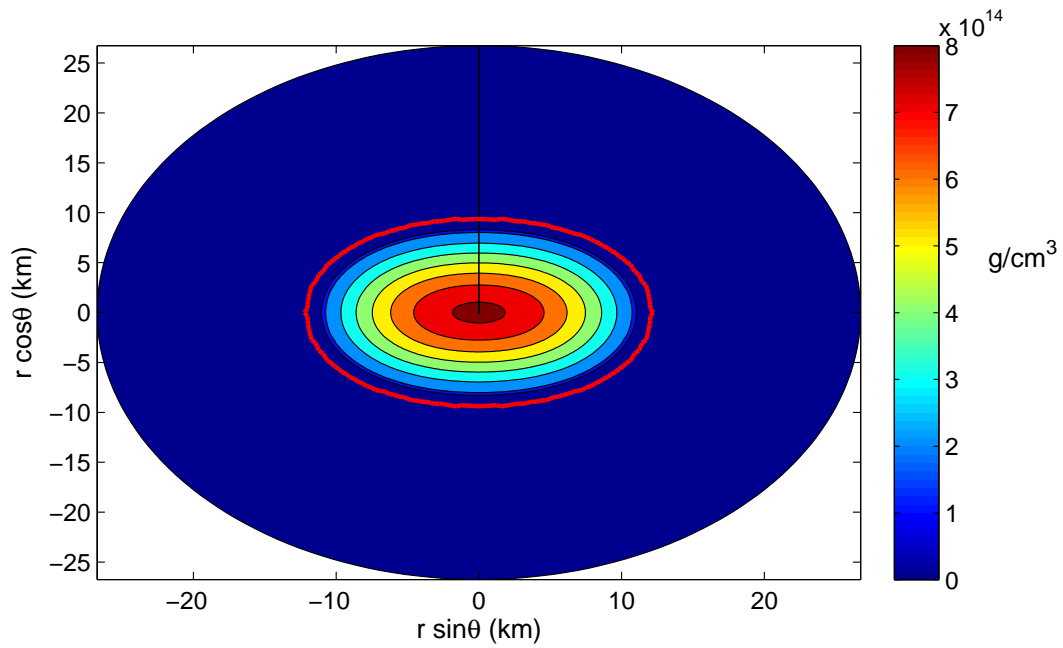
Figure 5.12: Contour plot of the energy density coming from the perfect fluid contribution to the total mass for a star with $f_o = 2.50$ and $\epsilon_c = 350$ MeV/fm$^3$. The figure shows the distribution of the term within the parenthesis in equation (5.35). The red solid line represents the star's surface.
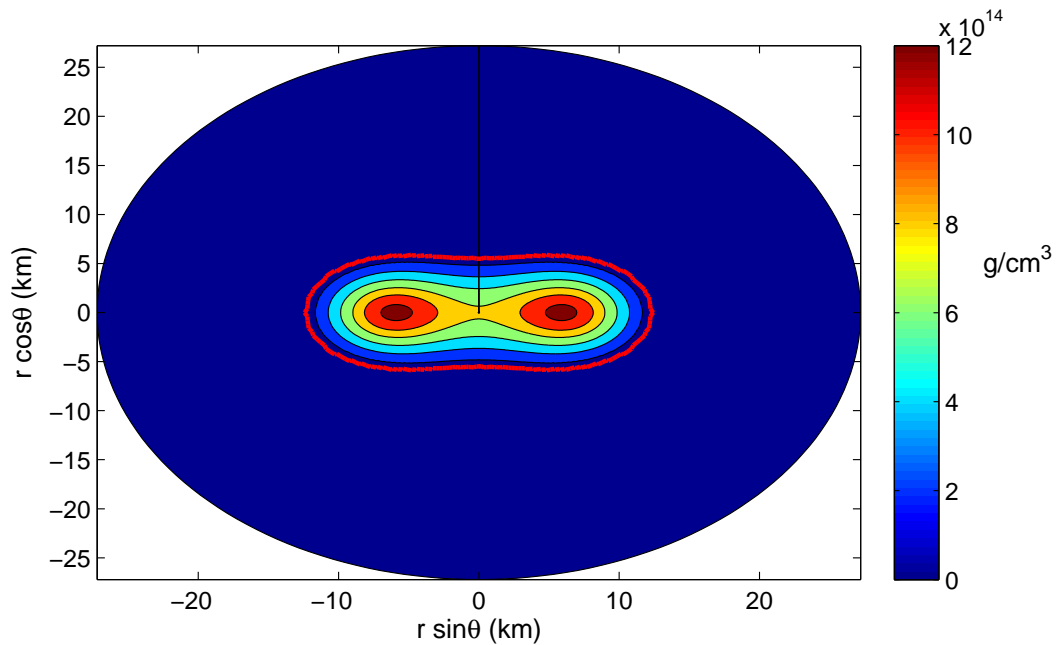


Figure 5.13: Contour plot of the energy density coming from the perfect fluid contribution to the total mass for a star with $f_o = 3.26$ and $\epsilon_c = 350$ MeV/fm$^3$. The figure shows the distribution of the term within the parenthesis in equation (5.35). The red solid line represents the star's surface.

Figure 5.14: Contour plot of the energy density coming from the electromagnetic contribution to the total mass for a star with $f_o = 1.00$ and $\epsilon_c = 350$ MeV/fm³. The figure shows the distribution of the term within the parenthesis in equation (5.36). The red solid line represents the star's surface.
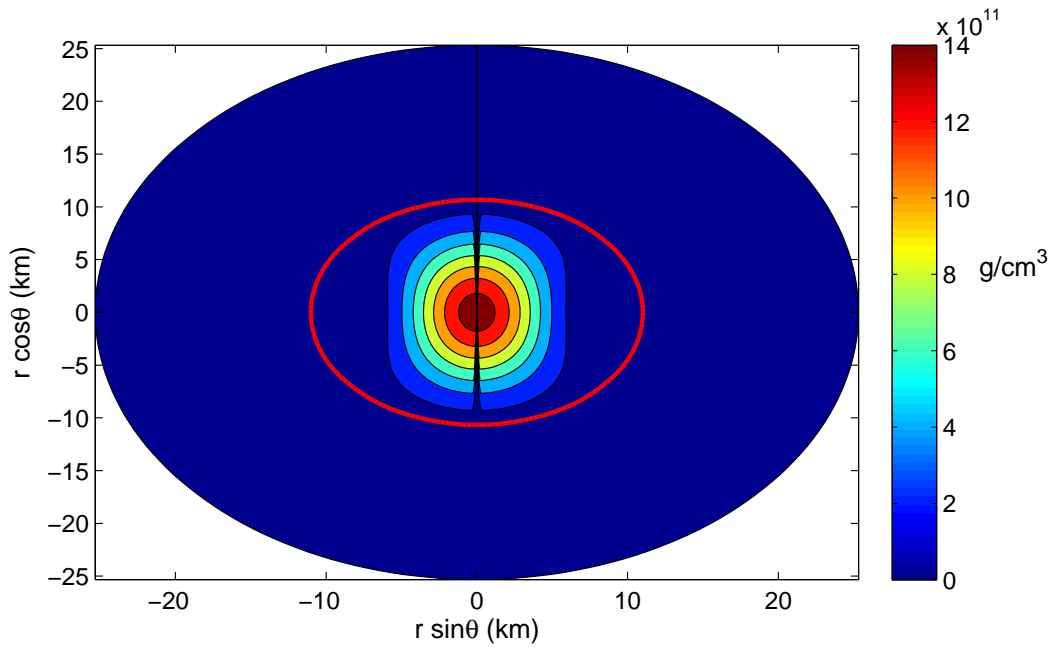


Figure 5.15: Contour plot of the energy density coming from the electromagnetic contribution to the total mass for a star with $f_o = 2.50$ and $\epsilon_c = 350$ MeV/fm³. The figure shows the distribution of the term within the parenthesis in equation (5.36). The red solid line represents the star's surface.
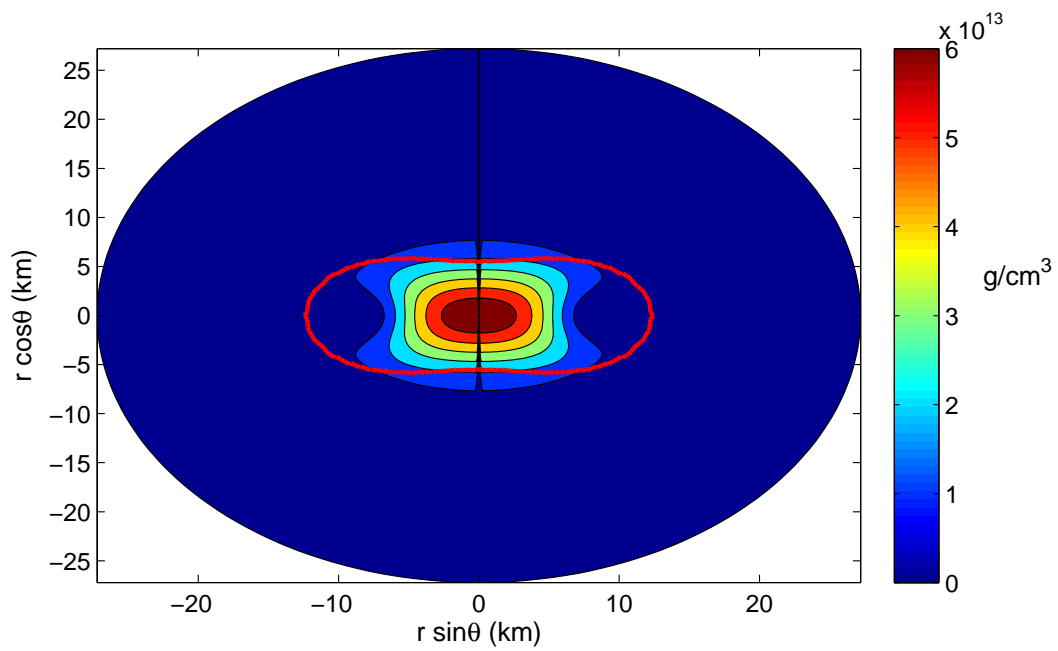
Figure 5.16: Contour plot of the energy density coming from the electromagnetic contribution to the total mass for a star with $f_o = 3.26$ and $\epsilon_c = 350$ MeV/fm³. The figure shows the distribution of the term within the parenthesis in equation (5.36). The red solid line represents the star's surface.
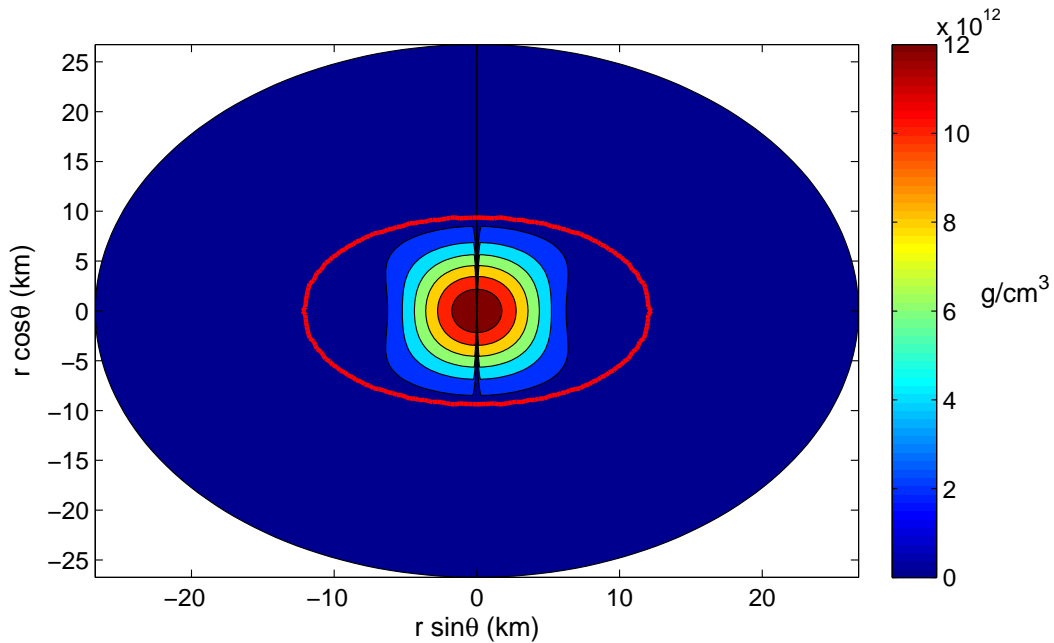
Figure 5.17: Contour plot of the pressure for a star with $f_o = 0.00$ and $\epsilon_c = 350$ MeV/fm$^3$. The red solid line represents the star's surface.
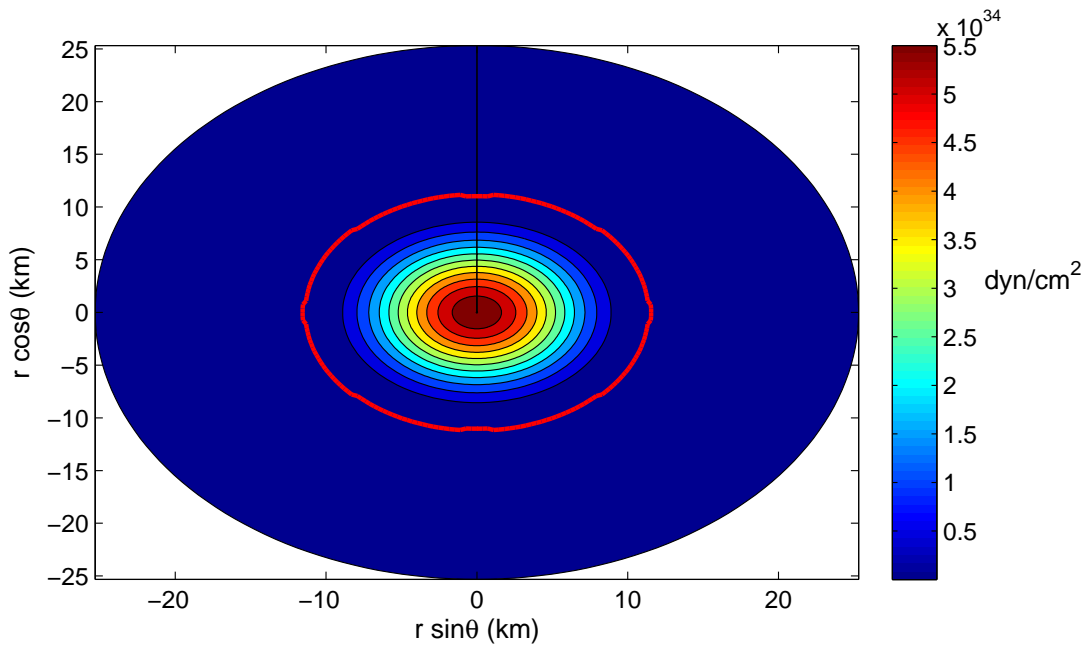


Figure 5.18: Contour plot of the pressure for a star with $f_o = 1.00$ and $\epsilon_c = 350$ MeV/fm$^3$. The red solid line represents the star's surface.
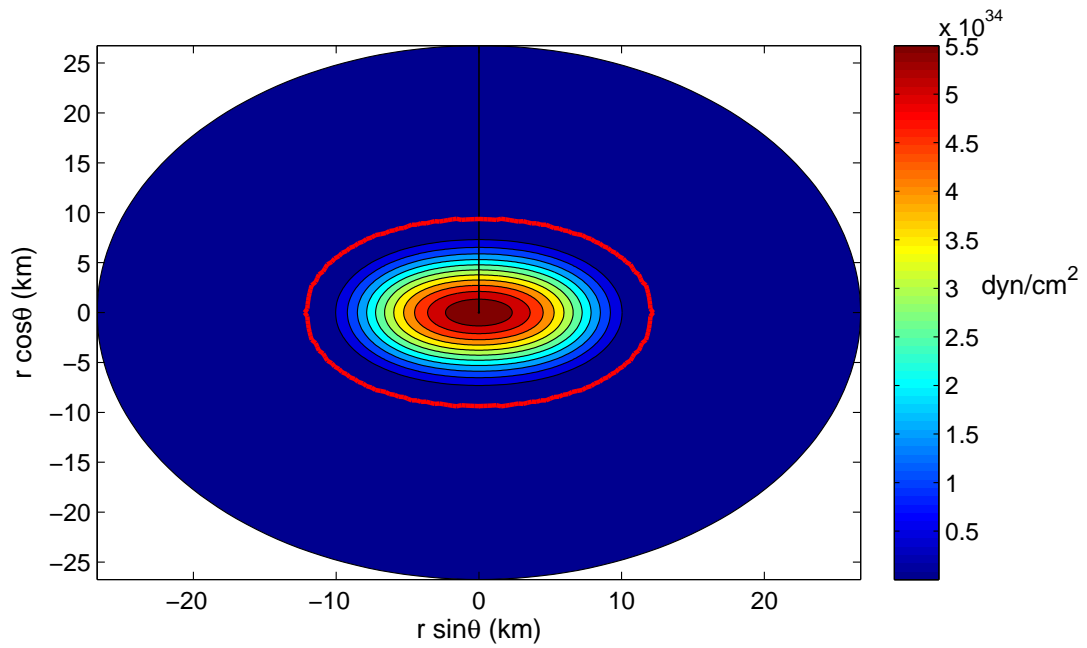
Figure 5.19: Contour plot of the pressure for a star with $f_o = 2.50$ and $\epsilon_c = 350$ MeV/fm$^3$. The red solid line represents the star's surface.



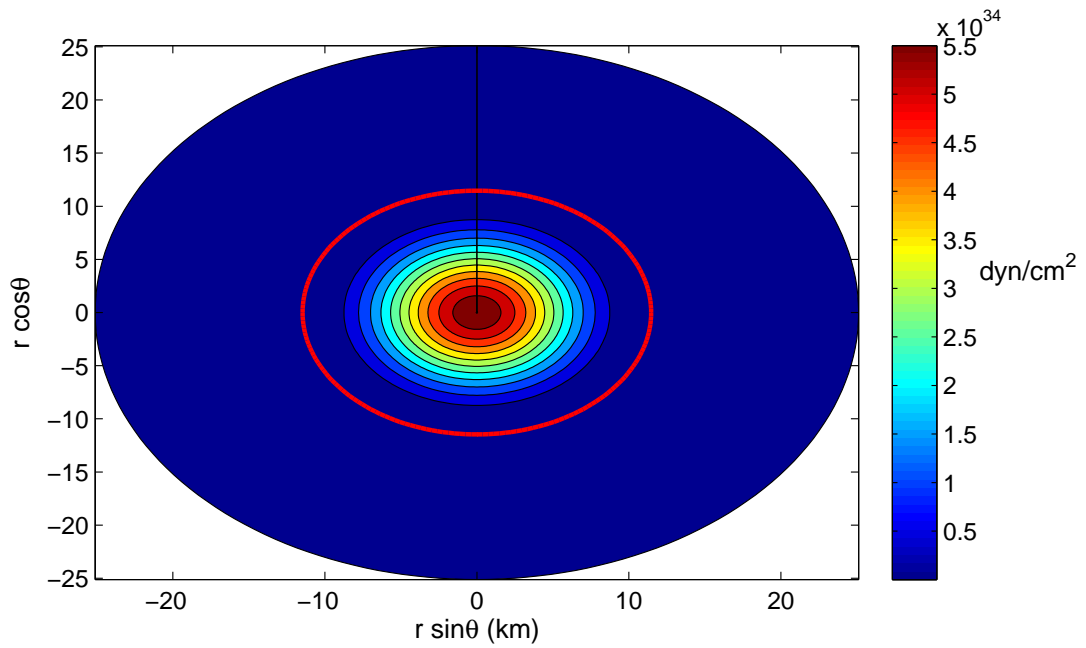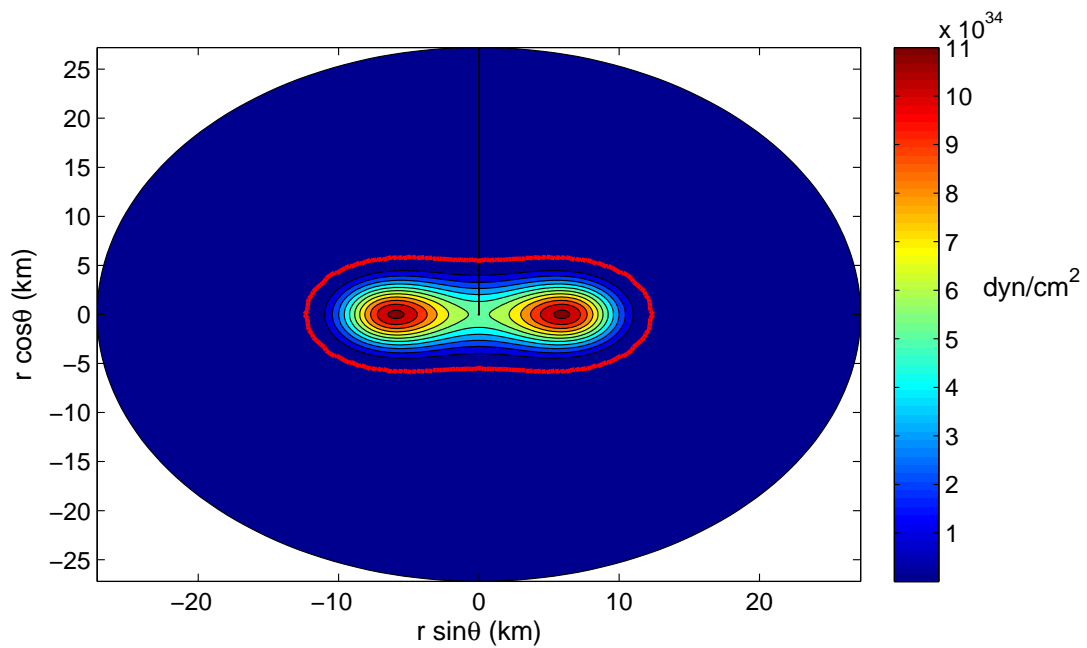Figure 5.20: Contour plot of the pressure for a star with $f_o = 3.26$ and $\epsilon_c = 350$ MeV/fm$^3$. The red solid line represents the star's surface.

Figure 5.21: Contour plot of the electromagnetic potential for a star with $f_o = 1.00$ and $\epsilon_c = 350$ MeV/fm$^3$. The white lines show the magnetic field (in Gauss) and the red solid line represents the star's surface.



Figure 5.22: Contour plot of the electromagnetic potential for a star with $f_o = 2.50$ and $\epsilon_c = 350$ MeV/fm$^3$. The white lines show the magnetic field (in Gauss) and the red solid line represents the star's surface.
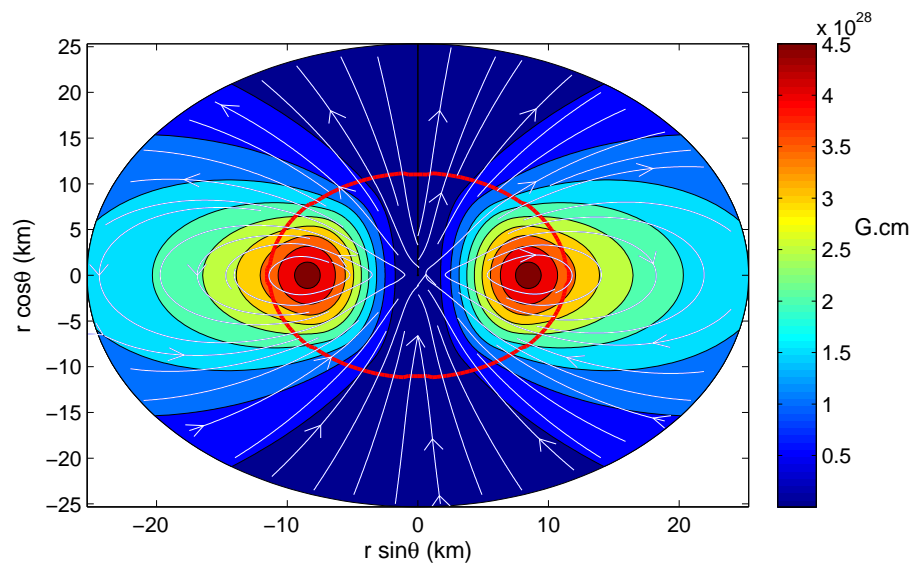
Figure 5.23: Contour plot of the electromagnetic potential for a star with $f_o = 3.26$ and $\epsilon_c = 350$ MeV/fm$^3$. The white lines show the magnetic field (in Gauss) and the red solid line represents the star's surface.

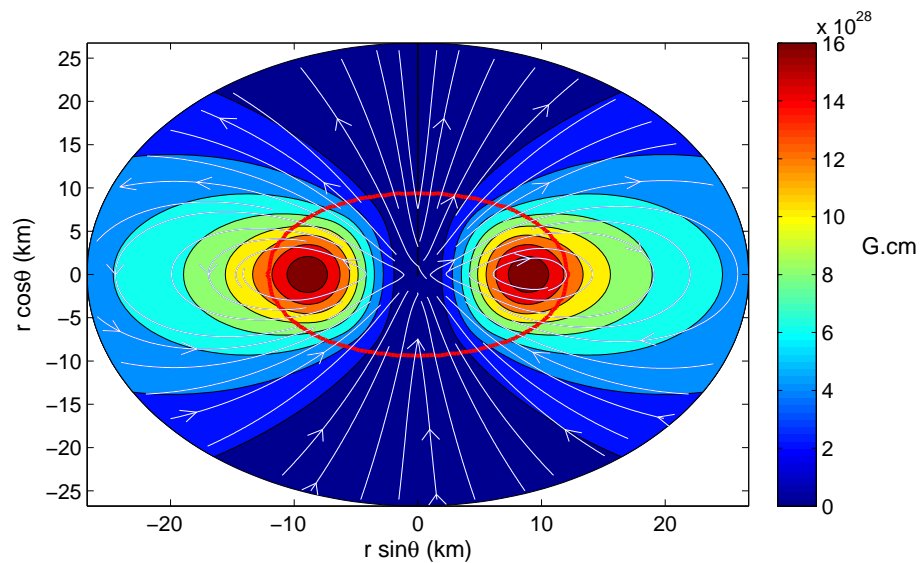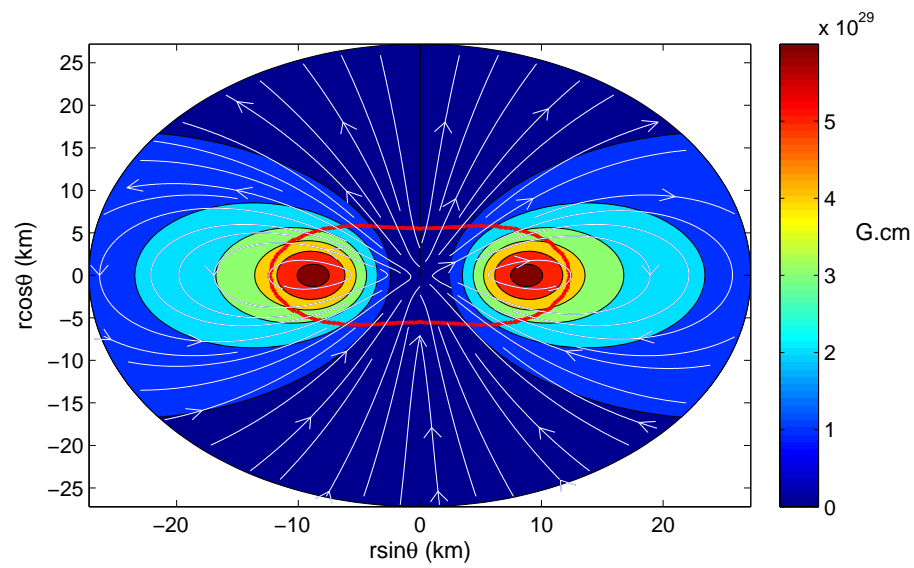### 5.3.3 Stellar sequences

Figures 5.24 and 5.25 show the gravitational mass as a function of the circumferential radius and the mass as a function of the central density, respectively, for static stars each of them with constant current functions. The range considered for the central energy density is between $(120 - 1860)$ MeV/fm$^3$ which allow us to study stars with low and high values of $\epsilon_c$. The lower line represents the spherically symmetric configuration with $f_o = 0.00$ (no magnetic field) with the lowest value of the virial factor $\mid 1 - \lambda \mid \sim 10^{-4}$ corresponding to a central density $\epsilon_c = 186.273$ MeV/fm$^3$ (see table 5.5). The black curve corresponds to $f_o = 1.00$ which has similar values of the spherically symmetric configuration as the figures show, this fact allow us to conclude that stars with this value of the current function can be studied as a perturbation of the spherically symmetric configuration.

The effects of higher magnetic field are shown by the red and violet curves which exhibit more differences than the blue and black ones. When the current function grows to $f_o = 2.00$ or $f_o = 2.50$ the effects of the magnetic field are considerable, as we concluded for a star with a fixed value of the central energy density in the previous section. In fact, for the value of $\epsilon_c = 400$ MeV/fm$^3$ for example, the mass of the star changes from $m = 1.534 \text{M}_\odot$ to $m = 1.662 \text{M}_\odot$ and the magnetic field at the pole changes from the order of $B_{pole} \sim 10^{16}$G to $B_{pole} \sim 10^{17}$ G. The largest value of the magnetic field at the center reported in table 5.5 corresponds to a mass of $m = 2.016 \text{M}_\odot$ and $R = 10.351$km with $B_c = 1.065 \times 10^{18}$ G, for $\epsilon_c = 1498.705$ MeV/fm$^3$. Note that for this last value reported for $\epsilon_c$ the radius of the star decreases with the growing of the current function value, but each of them being higher than its corresponding spherical star.

Figure 5.26 shows the circumferential radius as a function of the central density. For a range of $\epsilon_c \in (200-1350)$ MeV/fm$^3$ the radius of the star grows with the magnetic field, but for $\epsilon_c \sim 1400$ MeV/fm$^3$ this situation begins to be different for ultra relativistic situations, as figure 5.27 shows for high values of the central density, stars with higher values of $f_o$ have smaller radii, even for $\epsilon_c \in (1500 - 1860)$ MeV/fm$^3$ the red and violet curves corresponding to $f_o = 2.00$ and $f_o = 2.50$, respectively, are below the blue one which corresponds to the spherically symmetric configuration, similar results were reported by Bocquet et. al. [48]. In

this section we have not studied the stellar sequence for $f_o = 3.26$ because for this value of the current function convergence cannot be achieved for densities around $\sim 400$ MeV/fm$^3$.

The maximum mass configuration properties for static stars with a poloidal magnetic field are summarized in table 5.4. The mass increases with the magnetic field, reaching maximum values similar to that reported by Lattimer et al. [71] for the EoS taken from Prakash, Cooke and Lattimer (PCLhyp) [72] which is based on a relativistic field-theoretical description of dense matter starting from the Lagrangian proposed by Zimanyi and Moszkowski [73] with the inclusion of hyperons. The mass reported by Lattimer et. al. [71] is $m = 2.04$M$_\odot$ with a radius $R = 11.8$ km, corresponding to a central density $\epsilon_c = 20.09 \times 10^{14}$ g/cm$^3$ which are very similar to that reported in table 5.4 where the maximum mass is $m = 2.038$M$_\odot$ with $R = 11.094$km corresponding to $\epsilon_c = 20.41 \times 10^{14}$ g/cm$^3$. However, the values of the magnetic field at the center and in the pole reported by Lattimer et. al. $B_c = 23.5 \times 10^{17}$ G and $B_{pole} = 13.0 \times 10^{17}$ G, are higher than the one computed with our code. A possible explanation for this result is the fact that in the EoS PCLhyp the authors consider the presence of quarks as part of the microscopical composition of the neutron star.

A final point to be mentioned is the fact that the magnetic field values reported in this work are smaller than the limit value estimation of Lattimer et. al. [71]

$$B_{lim} \simeq 8 \times 10^{18} \left( \frac{1.4\text{M}_\odot}{M} \right) \text{G} \tag{5.40}$$

for which a black hole formation is inevitable. This limiting field is not much larger than the maximum fields reported by Lattimer et. al. who studied different EoS.

| $f_0$ | $\epsilon_c$ | $m$ | $R$ | $B_c$ | $B_{pole}$ | $\mu$ | $\mid 1 - \lambda \mid$ |
|-------|--------------|-----|-----|-------|------------|-------|------------------------|
|       | MeV/fm$^3$ | $M_\odot$ | km | $(10^{17})$ G | $(10^{17})$ G | $(10^{35})$ Gaussian | $(10^{-2})$ |
| 0.000 | 1436.267 | 1.937 | 10.468 | 0.000 | 0.000 | 0.000 | 4.109 |
| 1.000 | 1416.038 | 1.963 | 10.518 | 3.959 | 0.469 | 1.931 | 4.597 |
| 2.000 | 1246.328 | 2.000 | 10.854 | 7.881 | 0.995 | 4.394 | 4.893 |
| 2.500 | 1144.644 | 2.038 | 11.094 | 9.929 | 1.324 | 6.042 | 5.240 |

Table 5.4: Properties of magnetized stars for the maximum mass configuration

| $\epsilon_c$ | $f_0$ | $m$ | $R$ | $B_c$ | $B_{pole}$ | $\mu$ | $\mid 1-\lambda \mid$ |
|---|---|---|---|---|---|---|---|
| $MeV/fm^3$ | | $M_\odot$ | km | $(10^{17})$G | $(10^{17})$ G | $(10^{35})$ Gaussian | $(10^{-2})$ |
| 186.273 | 0.000 | 0.519 | 13.166 | 0.000 | 0.000 | 0.000 | 0.073 |
| | 1.000 | 0.530 | 13.226 | 0.810 | 0.709 | 1.064 | 0.199 |
| | 2.000 | 0.575 | 13.465 | 1.749 | 0.170 | 2.546 | 0.785 |
| | 2.500 | 0.629 | 13.731 | 2.332 | 0.244 | 3.771 | 2.258 |
| 350.000 | 0.000 | 1.275 | 13.257 | 0.000 | 0.000 | 0.000 | 0.716 |
| | 1.000 | 1.300 | 13.367 | 1.844 | 0.242 | 3.028 | 0.974 |
| | 2.000 | 1.416 | 13.776 | 4.029 | 0.582 | 7.222 | 2.042 |
| | 2.500 | 1.562 | 14.211 | 5.535 | 0.879 | 10.89 | 3.294 |
| 375.000 | 0.000 | 1.341 | 13.230 | 0.000 | 0.000 | 0.000 | 0.880 |
| | 1.000 | 1.369 | 13.332 | 1.975 | 0.263 | 3.159 | 1.114 |
| | 2.000 | 1.478 | 13.674 | 4.391 | 0.643 | 7.482 | 1.809 |
| | 2.500 | 1.610 | 14.014 | 6.075 | 0.973 | 11.07 | 2.826 |
| 400.000 | 0.000 | 1.397 | 13.186 | 0.000 | 0.000 | 0.000 | 0.989 |
| | 1.000 | 1.426 | 13.284 | 2.072 | 0.277 | 3.237 | 1.238 |
| | 2.000 | 1.534 | 13.606 | 4.601 | 0.677 | 7.607 | 1.982 |
| | 2.500 | 1.662 | 13.916 | 6.352 | 1.018 | 11.13 | 2.998 |
| 425.000 | 0.000 | 1.447 | 13.132 | 0.000 | 0.000 | 0.000 | 1.085 |
| | 1.000 | 1.476 | 13.226 | 2.163 | 0.291 | 3.290 | 1.359 |
| | 2.000 | 1.582 | 13.528 | 4.798 | 0.706 | 7.669 | 2.145 |
| | 2.500 | 1.705 | 13.807 | 6.607 | 1.057 | 11.09 | 3.145 |
| 450.000 | 0.000 | 1.492 | 13.071 | 0.000 | 0.000 | 0.000 | 1.184 |
| | 1.000 | 1.521 | 13.159 | 2.250 | 0.303 | 3.323 | 1.475 |
| | 2.000 | 1.626 | 13.441 | 4.983 | 0.733 | 7.683 | 2.308 |
| | 2.500 | 1.742 | 13.692 | 6.843 | 1.091 | 10.99 | 3.286 |
| 475.000 | 0.000 | 1.534 | 13.002 | 0.000 | 0.000 | 0.000 | 1.268 |
| | 1.000 | 1.563 | 13.087 | 2.334 | 0.314 | 3.339 | 1.583 |
| | 2.000 | 1.659 | 13.344 | 5.056 | 0.739 | 7.576 | 2.331 |
| | 2.500 | 1.775 | 13.572 | 7.064 | 1.120 | 10.84 | 3.421 |
| 500.000 | 0.000 | 1.572 | 12.929 | 0.000 | 0.000 | 0.000 | 1.345 |
| | 1.000 | 1.547 | 13.002 | 2.392 | 0.321 | 3.324 | 1.604 |
| | 2.000 | 1.693 | 13.247 | 5.216 | 0.759 | 7.522 | 2.473 |
| | 2.500 | 1.804 | 13.450 | 7.273 | 1.147 | 10.67 | 3.547 |
| 1498.705 | 0.000 | 1.935 | 10.346 | 0.000 | 0.000 | 0.000 | 2.548 |
| | 1.000 | 1.962 | 10.380 | 4.024 | 0.471 | 1.844 | 4.793 |
| | 2.000 | 1.992 | 10.369 | 8.297 | 1.007 | 3.746 | 5.254 |
| | 2.500 | 2.016 | 10.351 | 10.655 | 1.334 | 4.728 | 5.556 |

Table 5.5: Properties of magnetized stars for different values of $\epsilon_c$ and $f_o$
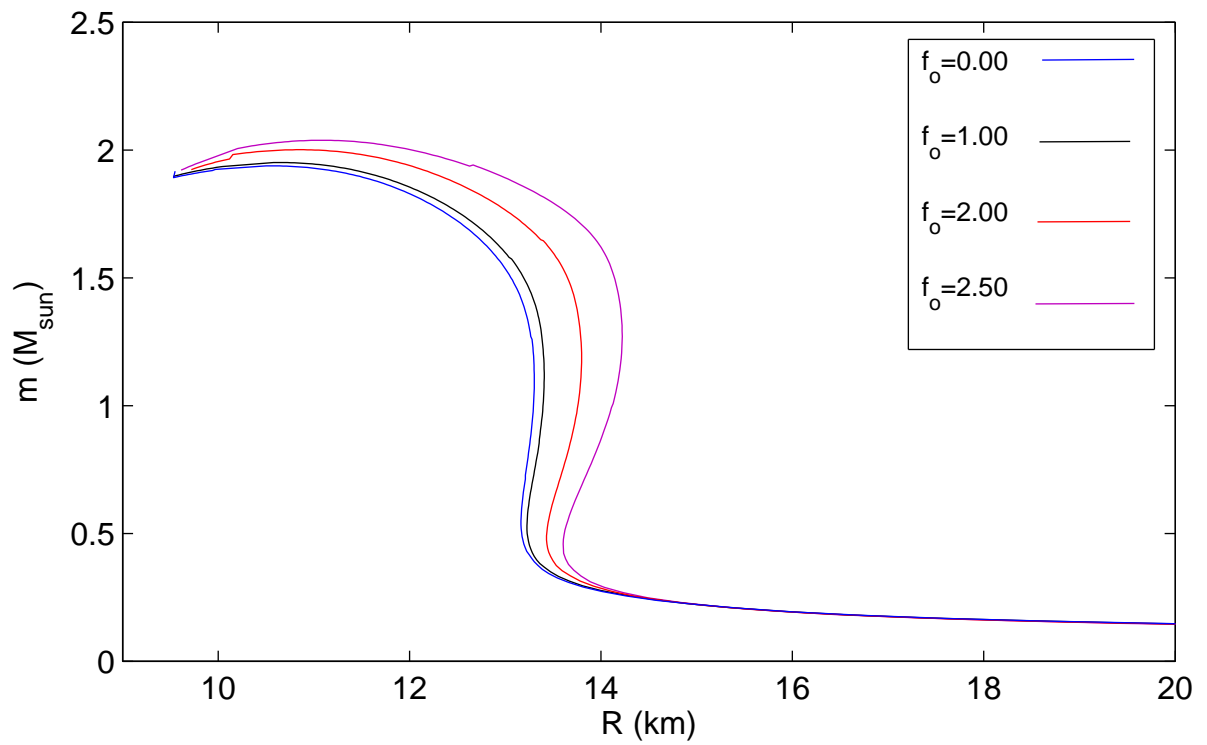
Figure 5.24: Mass vs circumferencial radius for different current functions.



Figure 5.25: Mass vs central energy density for different current functions.

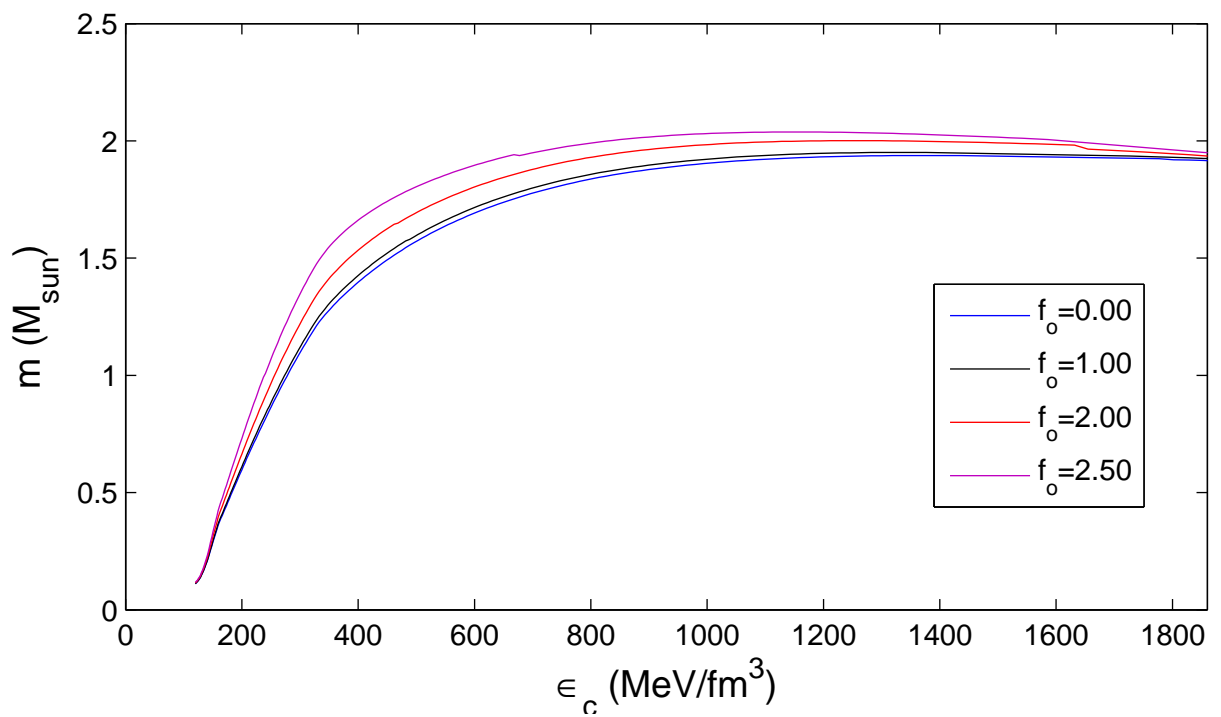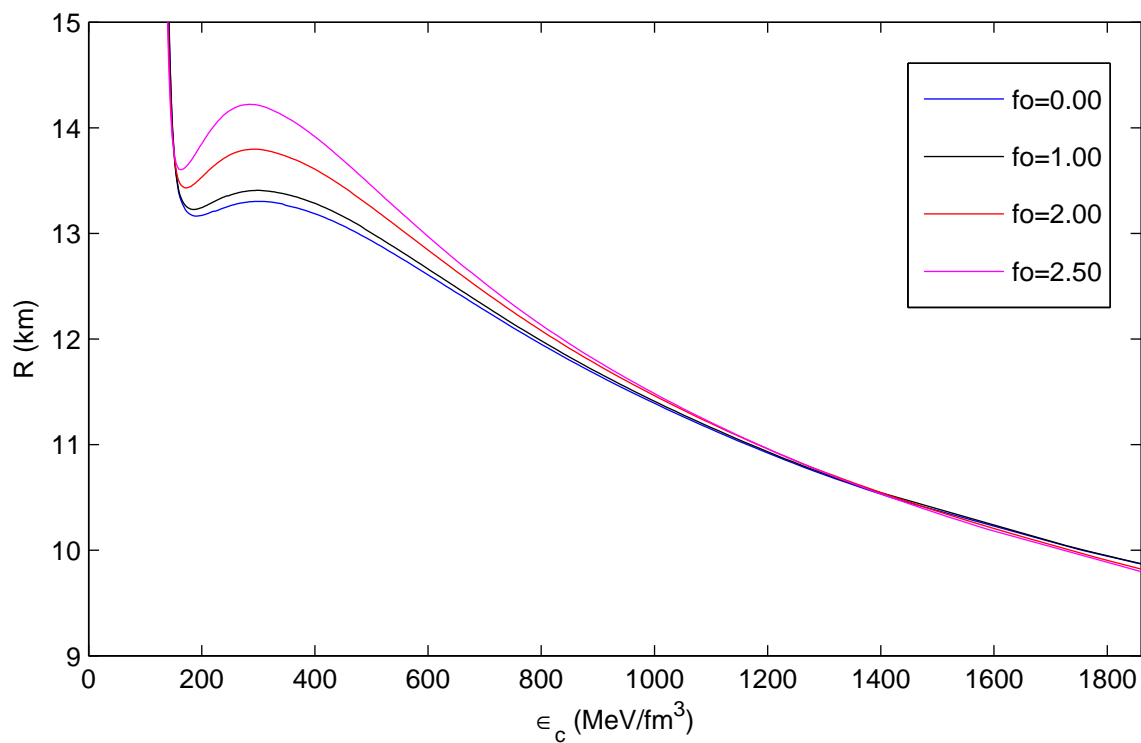Figure 5.26: Circumferential radius vs central energy density for different current functions.
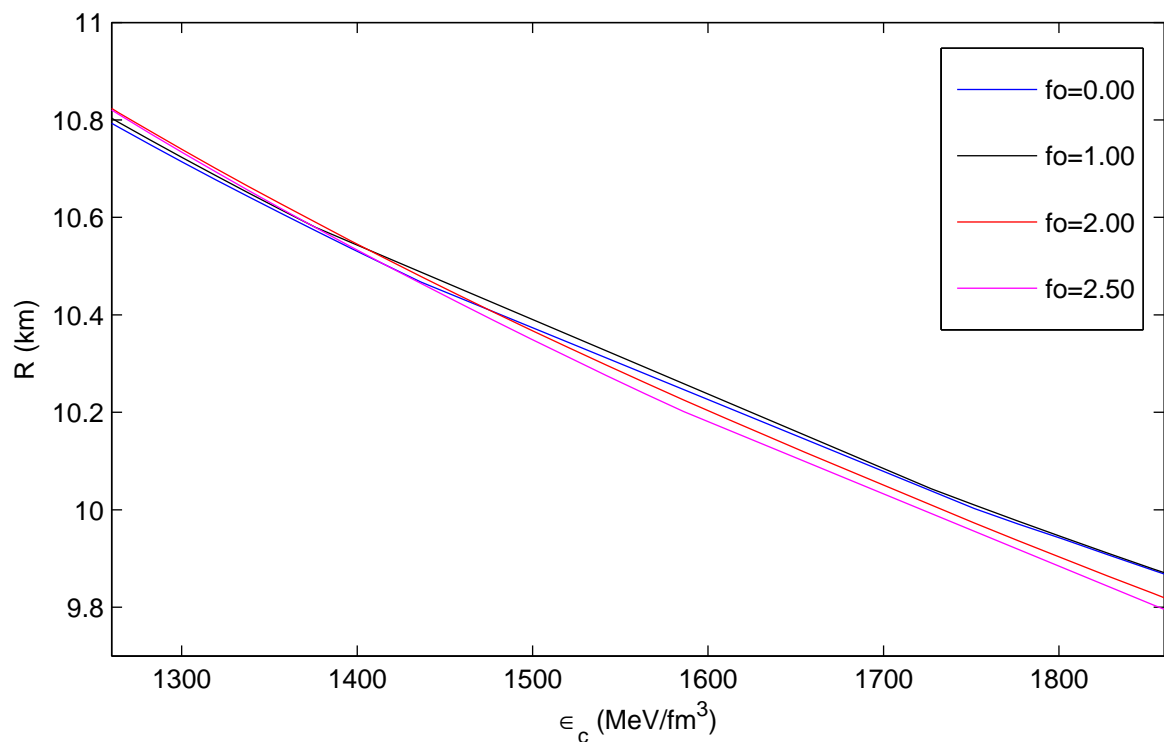


Figure 5.27: Circumferential radius vs central energy density for different current functions. This plot is a zoom of figure 5.26. It shows that from around $\epsilon_c = 1500\text{MeV/fm}^3$ the stars with higher magnetic field, corresponding to $f_o = 2.00$ and $f_o = 2.50$, have smaller radius.

# Chapter 6

# Conclusions

The three main fronts of compact star research are the microscopical composition and equation of state, relativistic structure, and evolution. The purpose of this research was to study, within a totally general relativistic framework, the effects of magnetic fields in the structure of neutron stars, i.e. how a magnetic field affects the spacetime geometry of these compact objects. We started by studying the formal general relativity aspects involving the equations that describe a perfect fluid coupled with a poloidal magnetic field using two different approaches, the first one uses Weyl spherical coordinates considered by Herrera et. al. [23] to describe an anisotropic relativistic fluid and the second one is based in the study of Shapiro et al. [19] who derived the field equations for a rotating neutron star. We introduced three quantities, namely $W$, $\Pi$ and $\sigma$, and derived the conservation equations of a magnetized neutron star. Comparing with the equations presented by Herrera et. al. we concluded that these quantities could be identified as the electromagnetic energy density, anisotropy and the shear stress expirienced by the fluid, respectively [18].

Inspired by the work of Shapiro et. al. [19], the field equations describing a perfect fluid coupled with a poloidal magnetic field were derived. The results show that the electromagnetic effects are only present in the source associated with the metric potential $\rho$ and in the equation defining the metric potential $\alpha$. When the equations are written in terms of the 4-potential $A_\phi$, the source $S_\rho$ can be written as a superposition of the source coming from the perfect fluid contribution $S_\rho^{PF}$ and the electromagnetic source $S_\rho^{EM}$. No direct contribution

from the electromagnetic field is present in the source of the metric potential $\gamma$.

With the physical interpretation for the introduced quantities $W$, $\Pi$ and $\sigma$ in mind, we wrote the field equations for the metric potentials $\rho$ and $\alpha$ in terms of these three quantities. The right hand side of the equation associated to the metric potential $\rho$, corresponding to the source $S_\rho$, shows the electromagnetic influence in the term $2W$ which appears as a sum of the energy density and pressure of the fluid. Moreover, the factor 2 appears again in the expression of the gravitational mass in chapter IV, in which another approach was used to study the neutron star structure and where the term $E^{EM}$ definitely represents the electromagnetic energy density. These results allow us to conclude two important points: one is the fact that the quantity $W$ can be understood as the electromagnetic energy density as is concluded in [18]. The second point is, we confirm the conclusions of Papapetrou in 1947 [26] who studied the static solution of the equations of the gravitational field for an arbitrary charge distribution, the factor 2 appears as a fundamental property of electro-gravitational field and hence is independent on the coordinates choice. Later, in 1960 Bonnor [27] studied the contribution to the gravitational mass of a circular wire carring a steady current. Bonnor showed that to obtain a physically reasonable solution, within general relativity, for the field of a loop steady current, it is necessary to endow the wire with a gravitational mass which corresponds to the energy of the magnetic field created. The result of Bonnor was the gravitational mass is twice the magnetic energy $M = 2W$ (see equation (7.16) in reference [27]). In the present work, we have studied the contribution of the electromagnetic energy to the gravitational mass for a perfect fluid coupled with a poloidal magnetic field and our results are in agreement with the conclusions of Papapetrou and Bonnor.

In the Shapiro approach no source is associated to the metric potential $\alpha$ because the method used by the authors to solve this metric function does not imply a Poisson equation. Writing the expression that defines $\alpha$ in terms of the 4-potential, the electromagnetic effects appear as an addition of the equation found by Shapiro et. al. [19] if is considered a non rotating fluid. But more interesting issues arise when this expression is written in terms of the introduced quantities. First of all, no influence of $W$ is present in the equation. Secondly, the quantities $\Pi$ and $\sigma$ appear as the electromagnetic effects in the equation of $\alpha$. For the metric

considered, $\alpha$ is the factor associated to the coordinates $r$ and $\theta$ which are the directions where the symmetry is broken. In our system the breaking of spherical symmetry is due to the poloidal magnetic field which has two components $B_r$ and $B_\theta$, quantities $\Pi$ and $\sigma$ are written in terms of these components. We can conclude that $\Pi$ is related to anisotropy (two different components of the magnetic field) and $\sigma$ is related to the shear stress experienced by the fluid. These two quantities are responsible to breaking the symmetry of the system.

Having in mind the future numerical solution, in chapter III we studied the relativistic virial theorem, but instead of the usual derivation from a conservation law, this important theorem was derived from a projection of the Einstein field equations in the hypersurface $\Sigma_t$ thanks to the $3+1$ formalism. The equations presented in this chapter are based in the pioneer work of Bonazzola and Gourgoulhon [41] who derived a relativistic generalization of the virial theorem for any stationary and asymptotically flat spacetime. The result of this work is a virial integral which consists of a term related to the gravitational field source (such as energy density, pressure, electromagnetic field, etc.), a term taking into account second derivatives of the metric potential $\nu$, which plays the role of the gravitational potential in the Newtonian limit and finally, a term associated with the extrinsic curvature. The motivation to present the virial theorem in a chapter of this work was twofold: first, the usefulness as a consistency check of numerical solutions of the Einstein equations and secondly the fact that in the works in which we based to model numerically the solutions found in chapter V, the virial integral looks unclear for the reader.

In chapter IV, we presented the theoretical formalism describing rotating and highly magnetized neutron stars using a full axially symmetric treatment, we wrote the Einstein-Maxwell equations in terms of a flat space elliptic operator and denoted the source as the terms containing matter, electromagnetic and non linear terms in the metric potentials. The hydrostatic equilibrium equations were derived within the assumption of infinite conductivity matter and the relevant physical quantities describing the system were derived. We found that the formalism of stationary neutron stars with poloidal magnetic fields consists of a closed system of eleven variables (four metric variables, energy density, pressure, two components of the electromagnetic potential, two components of the electromagnetic current,

and the heat function); eleven equations (four Poisson equations for the metric variables, two Poisson equations for the components of the electromagnetic potential, a relation between these components, the equation of state, the relation between the heat function, energy density and pressure, the first integral of the equations of hydrostatic equilibrium, and the restriction on the electromagnetic current); three input parameters (angular velocity, total electric charge, and the maximum density); and one input current function.

The discussions developed in chapter IV, aided us in constructing the numerical solution presented in chapter V, where we studied both rotating neutron stars without magnetic field and magnetized neutron stars without rotation, modelled as a perfect fluid coupled with a poloidal magnetic field in stationary configurations. As focus was the study of magnetic field effects in the structure of neutron stars, the microscopical composition used to describe neutron star matter was based on a traditional model of EoS known as G300 which supposes that the neutron stars are composed by hadrons and studies the system in the framework of field theory of interacting nucleons, hyperons and mesons.

To describe global properties of a rotating neutron star without magnetic field we calculated the total gravitational mass, the circumferential radius, the angular velocity, angular momentum and two quantities that contribute to the total gravitational mass, the first one depends on matter and the kinetic energy, and the second measures the contribution of the extrinsic curvature to the total energy of the system. The results show that the rotational effects increase the spherical configuration mass in 18.5% for the maximum rotation studied and change the star´s surface from the spherical to ellipsoidal shape.

To describe magnetized neutron stars without rotation with constant current functions we calculated the total gravitational mass, the circumferential radius, the magnetic field at the center, magnetic field in the pole, the magnetic moment and two quantities that contribute to the total gravitational mass, the first one expresses the perfect fluid contribution, and the second measures the contribution of the electromagnetic energy to the total mass. The results show that for a star with the lowest value of the current function, which means lower magnetic fields, the deviations from the spherically symmetric configuration are not significant. In fact, for the maximum mass configuration the magnetic field increases

the spherical mass only in 2.6%, hence the spherical perturbation method would be used to describe these magnetized neutron stars. This perturbation approach was followed by Ioka et. al. [74] who considered poloidal and toroidal magnetic fields with meridional flow.

When the current function is set at $f_o = 2.50$, the contribution of the electromagnetic energy increases the mass in 28.7% for a star with central energy density equal to 350 MeV/fm$^3$ which corresponds to a magnetic field at the pole of $8.79 \times 10^{16}$ G. For this case the shape of the star´s surface has a clear deviation from spherical symmetry, showing the effects of the electromagnetic energy.

The electromagnetic effects become more dramatic for a star with a magnetic field in the center of $1.240 \times 10^{18}$ G, for this case not only the shape of the star´s surface is affected but also the magnetic force pushes a sufficient amount of mass off-center, showing the transition to a toroidal topology. For the maximum mass configuration, the results showed that for stars with central magnetic field $\sim 10^{18}$ G electromagnetic effects increase the mass in 10.1% with respect to the configuration without magnetic field.

The pressure contours studied suggest similar effects in the magnitude of the pressure between rotating and nonmagnetized neutron stars with high central densities and nonrotating neutron stars with high magnetic fields and lower central densities.

Another important point to be mentioned is that besides the expressions for the gravitational mass for a rotating star with no magnetic field and the magnetized star without rotation, suggest an analogy between the roles of the energy density coming from the extrinsic curvature and the electromagnetic contribution in the gravitational mass, the results show that the distribution through the star of these gravitational sources are different, while the extrinsic curvature energy density has its largest values near and even beyond to the star's surface, the electromagnetic energy density maximum values are near the center of the star.

The mass-radius and mass-central energy density relations for the stellar sequences show that for stars with values of the current functions $f_o = 2.00$ and $f_o = 2.50$, the deviation from the spherical symmetry is more dramatic, this allows us to conclude that it is not appropriate to adopt the spherical perturbation approach for these stars and hence the full axially symmetric treatment used in this work brings the suitable description for these

highly magnetized neutron stars. As expected we see that as the magnetic fields increase the maximum mass and the radius also increase. Similar results can be found in Lattimer et. al. [71], actually the largest maximum mass founded by our study is similar to that reported by Lattimer, although in our work the magnetic field at center and in the pole are smaller than that reported by Lattimer. This result indicates the role of the microscopical composition of the matter in magnetized neutron stars, while Lattimer considered the presence of quarks, the EoS adopted in this work only considers hadrons.

An interesting effect that we found was that for lower central energy densities the radius increases with magnetic field, but for stars with central energy density between $(1500-1860)$ MeV/fm$^3$ the radius of the stars with higher magnetic field are smaller, even compared with the spherically symmetric configurations. This effect is not present for stars with $f_o = 1.00$ whose radii have similar values compared to the nonmagnetized stars.

In summary, in chapter V we showed results of the numerical solution describing rotating and highly magnetized neutron stars considering the static configurations. The code that allowed us to found the numerical solution combined the methods used by Shapiro et. al. [19] and Lattimer et. al. [71]. Our method is on par with that of the other authors.

***A few topics to be considered for future investigations:***

- Investigate if the factor two present in the gravitational mass expression for the electromagnetic energy, i.e. $2W$, for a perfect fluid coupled with a poloidal magnetic field and discussed in chapter II, (identified by Papapetrou [26] as a *fundamental property of the static electro-gravitational field*) appears in the case of non poloidal magnetic field, for example toroidal configurations.

- Study the relation between the extrinsic curvature contribution to the total gravitational mass as well its contour plot near to the Kepler frequency.

- Compare the effects of the extrinsic curvature in the orbits of different kind of particles with the results founded by Alfradique et. al. [75].

- Compare the redshift effects of the magnetic fields founded in our solution with the results reported by Troconis et. al. [76] who adopted the analytical solution for the

metric proposed by Bonnor [50] and measures the redshift effect for neutron stars with magnetic field at the center $\sim 10^{16}$ G.

- As we saw in chapter V, after the value $f_o = 3.26$ for a star with central density equal to 350MeV/fm$^3$, convergence cannot be achieved. In that sense, the transition to a toroidal topology is suggestive of possible dynamical outcomes that may be considered for future works.

- Investigate the effects of the microscopical composition in the extrinsic curvature and electromagnetic energy distribution considering more realistic equations of state.

- The magnetic field evolution, non constant current functions, the magnetic field role in the cooling processes and the consequences in the neutron star structure are other issues that can be considered as the next step of the present work.

# Chapter 7

# Appendix

## 7.1 Appendix of chapter II

Thinking in future works devoted to find numerical solutions of the equations presented in chapter II, we are going to write Einstein field equations in terms of dimensionless coordinate $s$ which is related to radial coordinate $r$, through

$$r = R\left(\frac{s}{1-s}\right) \tag{7.1}$$

so if $s = 0 \Rightarrow r = 0$ and $s = 1 \Rightarrow r \longrightarrow \infty$ and in this way we cover all $r$ coordinate domain. In terms of $s$ we have that

$$\nabla f . \nabla g = \frac{(1-s)^2}{R^2}\left[(1-s)^2 f_{,s}g_{,s} + \frac{(1-\mu^2)}{s^2}f_{,\mu}g_{,\mu}\right] \tag{7.2}$$

$$S_\gamma(s,\mu) = e^{\gamma/2}\left\{16\pi e^{2\alpha}P + \frac{\gamma}{2}\left[16\pi e^{2\alpha}P - \frac{(1-s)^2}{2R^2}\left((1-s)^2(\gamma_{,s})^2 + \frac{(1-\mu^2)}{s^2}(\gamma_{,\mu})^2\right)\right]\right\} \tag{7.3}$$

Nonetheless, equation (7.3) has dimension of $\frac{1}{[L]^2}$, so our dimensionless effective source $\widetilde{S}$ will be define as

$$
\begin{aligned}
\widetilde{S}_\gamma(s,\mu) &= r^2 S_\gamma(s,\mu) \\
&= R^2 \frac{s^2}{(1-s)^2} S_\gamma(s,\mu) \\
&= e^{\gamma/2} \left\{ 16\pi e^{2\alpha} \widetilde{P} + \frac{\gamma}{2} \left[ 16\pi e^{2\alpha} \widetilde{P} - \frac{1}{2} \left( s^2 (1-s)^2 (\gamma_{,s})^2 + (1-\mu^2)(\gamma_{,\mu})^2 \right) \right] \right\}.
\end{aligned}
\tag{7.4}
$$

where the dimensionless quantity $\widetilde{C}$ is defined as

$$
\begin{aligned}
\widetilde{C} &= r^2 C \\
&= R^2 \frac{s^2}{(1-s)^2} C
\end{aligned}
\tag{7.5}
$$

then $\widetilde{P} = r^2 P$, $\widetilde{\rho}_0 = r^2 \rho_0$ and $\widetilde{\rho}_i = r^2 \rho_i$.

The expression for $S_\rho(s,\mu)$ is

$$
\begin{aligned}
S_\rho(s,\mu) &= e^{\gamma/2} \left[ 8\pi e^{2\alpha}(\rho_0 + \rho_i + P) + \frac{(1-s)^3}{R^2} \frac{\gamma_{,s}}{s} - \frac{\mu}{R^2} \frac{(1-s)^2}{s^2} \gamma_{,\mu} + \right. \\
&\quad + \left. \frac{\rho}{2} \left( 16\pi e^{2\alpha} P - \frac{1}{2} \nabla\gamma . \nabla\gamma - \frac{(1-s)^3}{R^2} \frac{\gamma_{,s}}{s} + \frac{\mu}{R^2} \frac{(1-s)^2}{s^2} \gamma_{,\mu} \right) \right] + \\
&\quad + e^{\gamma/2} \frac{e^{-(\gamma-\rho)}}{R^2(1-\mu^2)} \frac{(1-s)^2}{s^2} 2\nabla A_\phi . \nabla A_\phi,
\end{aligned}
\tag{7.6}
$$

The expression for the dimensionless source (or effective source) $\widetilde{S}_\rho(s,\mu)$ is

$$
\begin{aligned}
\widetilde{S}_\rho(s,\mu) &= r^2 S_\rho(s,\mu) \\
&= R^2 \frac{s^2}{(1-s)^2} S_\rho(s,\mu) \\
&= e^{\gamma/2} \Bigg[ 8\pi e^{2\alpha}(\widetilde{\rho}_0 + \widetilde{\rho}_i + \widetilde{P}) + s(1-s)\gamma_{,s} - \mu\gamma_{,\mu} + \\
&\quad + \frac{\rho}{2}\left( 16\pi e^{2\alpha}\widetilde{P} - \frac{1}{2}R^2\frac{s^2}{(1-s)^2}\nabla\gamma.\nabla\gamma + \right. \\
&\quad - \left. s(1-s)\gamma_{,s} + \mu\gamma_{,\mu} \right) \Bigg] + e^{\gamma/2}\frac{e^{-(\gamma-\rho)}}{(1-\mu^2)}2\nabla A_\phi.\nabla A_\phi,
\end{aligned} \tag{7.7}
$$

where $\nabla\gamma.\nabla\gamma$ and $\nabla A_\phi.\nabla A_\phi$ are given by (7.2) and we have to remember the dimensions of quadripotential in our coordinates are $[A_\phi] = [Lenght]$, so the final term of (7.7) is dimensionless.

The dimensionless introduced quantities, i.e. dimensionless energy, anisotropy and shear stress are given by

$$
\begin{aligned}
\widetilde{W}(s,\mu) &= r^2 W(s,\mu) \\
&= R^2 \frac{s^2}{(1-s)^2} W(s,\mu) \\
&= R^2 \frac{s^2}{(1-s)^2}\frac{1}{16\pi}\frac{e^{-(\gamma-\rho)}e^{-2\alpha}}{R^2(1-\mu^2)}\frac{(1-s)^2}{s^2}2\nabla A_\phi.\nabla A_\phi \\
&= \frac{1}{16\pi}\frac{e^{-(\gamma-\rho)}e^{-2\alpha}}{(1-\mu^2)}2\nabla A_\phi.\nabla A_\phi,
\end{aligned} \tag{7.8}
$$

$$
\begin{aligned}
\widetilde{\Pi}(s,\mu) &= r^2\Pi(s,\mu) \\
&= R^2 \frac{s^2}{(1-s)^2}\Pi(s,\mu) \\
&= R^2 \frac{s^2}{(1-s)^2}\left\{ -\frac{1}{8\pi}\frac{e^{-(\gamma-\rho)}e^{-2\alpha}}{R^2(1-\mu^2)}\frac{(1-s)^2}{s^2}\left[ \nabla A_\phi.\nabla A_\phi - \frac{2(1-\mu^2)}{R^2}\frac{(1-s)^2}{s^2}(A_{\phi,\mu})^2 \right]\right\} \\
&= -\frac{1}{8\pi}\frac{e^{-(\gamma-\rho)}e^{-2\alpha}}{(1-\mu^2)}\left[ \nabla A_\phi.\nabla A_\phi - \frac{2(1-\mu^2)}{R^2}\frac{(1-s)^2}{s^2}(A_{\phi,\mu})^2 \right],
\end{aligned} \tag{7.9}
$$

$$
\begin{aligned}
\widetilde{\sigma}(s,\mu) &= r^2 \sigma(s,\mu) \\
&= R^2 \frac{s^2}{(1-s)^2} \sigma(s,\mu) \\
&= R^2 \frac{s^2}{(1-s)^2} \left\{ -\frac{1}{8\pi} \frac{2e^{-(\gamma-\rho)}e^{-2\alpha}}{R^4(1-\mu^2)^{1/2}} \frac{(1-s)^5}{s^3}(A_{\phi,s})(A_{\phi,\mu}) \right\} \\
&= -\frac{1}{8\pi} \frac{2e^{-(\gamma-\rho)}e^{-2\alpha}}{R^2(1-\mu^2)^{1/2}} \frac{(1-s)^3}{s}(A_{\phi,s})(A_{\phi,\mu}).
\end{aligned}
\tag{7.10}
$$

Taking into account (7.8) and (7.7) we write the expression for $\widetilde{S}_\rho(s,\mu)$ in terms of the dimensionless introduced quantities,

$$
\begin{aligned}
\widetilde{S}_\rho(s,\mu) &= e^{\gamma/2}\Bigg[ 8\pi e^{2\alpha}(\widetilde{\rho}_0 + \widetilde{\rho}_i + \widetilde{P} + 2\widetilde{W}) + s(1-s)\gamma_{,s} - \mu\gamma_{,\mu} + \\
&+ \frac{\rho}{2}\left( 16\pi e^{2\alpha}\widetilde{P} - \frac{1}{2}R^2 \frac{s^2}{(1-s)^2}\nabla\gamma.\nabla\gamma - s(1-s)\gamma_{,s} + \mu\gamma_{,\mu} \right)\Bigg].
\end{aligned}
\tag{7.11}
$$

Expression for $\widetilde{S}_\gamma$ is given by (7.4) and it does not depend on the possible physical quantities.

Finally, the equation for $\gamma$ in a dimensionless way is

$$
\begin{aligned}
\alpha_{,\mu} \;=\;& -\frac{1}{2}(\gamma_{,\mu}+\rho_{\mu}) - \{[1+s(1-s)\gamma_{,s}]^2(1-\mu^2)+[\mu-(1-\mu^2)\gamma_{,\mu})]^2\}^{-1} \times \qquad (7.12)\\
\times\;& \Big[ -\frac{1}{2}\{3\mu^2-4\mu(1-\mu^2)\gamma_{,\mu}+(1-\mu^2)^2(\gamma_{,\mu})^2\}(\gamma_{,\mu}+\rho_{,\mu}) + \\
-\;& \frac{1}{2}s(1-s)\gamma_{,s}[1+s(1-s)\gamma_{,s}](1-\mu^2)(\gamma_{,\mu}+\rho_{,\mu}) + \frac{1}{2}\mu s(1-s)[1+s(1-s)\gamma_{,s}](\gamma_{,s}-\rho_{,s}) + \\
-\;& s(1-s)[1+s(1-s)\gamma_{,s}](1-\mu^2)(\gamma_{,s\mu}+\gamma_{,s}\gamma_{,\mu}) \\
+\;& \frac{1}{2}s(1-s)[1+s(1-s)\gamma_{,s}](1-\mu^2)(\gamma_{,s}\gamma_{,\mu}-\rho_{,s}\rho_{,\mu}) \\
+\;& \frac{1}{2}[\mu-(1-\mu^2)\gamma_{,\mu}][3\mu\rho_{,\mu}+s(1-s)\rho_{,s}] \\
-\;& \frac{1}{2}[\mu-(1-\mu^2)\gamma_{,\mu}]\{s^2(1-s)[(1-s)\gamma_{,ss}-2\gamma_{,s}]-(1-\mu^2)\gamma_{,\mu\mu}\} + \\
-\;& \frac{1}{4}R^2\frac{s^2}{(1-s)^2}[\mu-(1-\mu^2)\gamma_{,\mu}]\left\{\nabla\gamma.\nabla\gamma+\nabla\rho.\nabla\rho-\frac{2(1-\mu^2)(1-s)^2}{R^2s^2}[(\gamma_{,\mu})^2+(\rho_{,\mu})^2]\right\}\Big] + \\
+\;& \{[1+s(1-s)\gamma_{,s}]^2(1-\mu^2)+[\mu-(1-\mu^2)\gamma_{,\mu})]^2\}^{-1} \times \\
\times\;& e^{-(\gamma-\rho)}\left[\frac{[\mu-(1-\mu^2)\gamma_{,\mu}]}{(1-\mu^2)}\left[\nabla A_\phi.\nabla A_\phi-\frac{2(1-\mu^2)(1-s)^2}{R^2s^2}(A_{\phi,\mu})^2\right] + \\
+\;& \frac{2(1-s)^3[1+s(1-s)\gamma_{,s}]}{R^2s}(A_{\phi,s})(A_{\phi,\mu})\right].
\end{aligned}
$$

Using equations (7.9) and (7.10) we write,

$$
\begin{aligned}
\alpha_{,\mu} \;=\;& -\frac{1}{2}(\gamma_{,\mu}+\rho_{\mu}) - \{[1+s(1-s)\gamma_{,s}]^2(1-\mu^2)+[\mu-(1-\mu^2)\gamma_{,\mu})]^2\}^{-1} \times && (7.13)\\[4pt]
\times\;& \Big[ -\frac{1}{2}\{3\mu^2-4\mu(1-\mu^2)\gamma_{,\mu}+(1-\mu^2)^2(\gamma_{,\mu})^2\}(\gamma_{,\mu}+\rho_{,\mu})+ \\[4pt]
-\;& \frac{1}{2}s(1-s)\gamma_{,s}[1+s(1-s)\gamma_{,s}](1-\mu^2)(\gamma_{,\mu}+\rho_{,\mu})+ \\[4pt]
+\;& \frac{1}{2}\mu s(1-s)[1+s(1-s)\gamma_{,s}](\gamma_{,s}-\rho_{,s})+ \\[4pt]
-\;& s(1-s)[1+s(1-s)\gamma_{,s}](1-\mu^2)(\gamma_{,s\mu}+\gamma_{,s}\gamma_{,\mu}) \\[4pt]
+\;& \frac{1}{2}s(1-s)[1+s(1-s)\gamma_{,s}](1-\mu^2)(\gamma_{,s}\gamma_{,\mu}-\rho_{,s}\rho_{,\mu})+ \\[4pt]
+\;& \frac{1}{2}[\mu-(1-\mu^2)\gamma_{,\mu}][3\mu\rho_{,\mu}+s(1-s)\rho_{,s}]+ \\[4pt]
-\;& \frac{1}{2}[\mu-(1-\mu^2)\gamma_{,\mu}]\{s^2(1-s)[(1-s)\gamma_{,ss}-2\gamma_{,s}]-(1-\mu^2)\gamma_{,\mu\mu}\}+ \\[4pt]
-\;& \frac{1}{4}R^2\frac{s^2}{(1-s)^2}[\mu-(1-\mu^2)\gamma_{,\mu}]\left\{\nabla\gamma.\nabla\gamma+\nabla\rho.\nabla\rho-\frac{2(1-\mu^2)(1-s)^2}{R^2 s^2}[(\gamma_{,\mu})^2+(\rho_{,\mu})^2]\right\}\Big]+ \\[4pt]
-\;& \{[1+s(1-s)\gamma_{,s}]^2(1-\mu^2)+[\mu-(1-\mu^2)\gamma_{,\mu})]^2\}^{-1}\times \\[4pt]
\times\;& \left\{8\pi e^{2\alpha}\left\{[\mu-(1-\mu^2)\gamma_{,\mu})]\,\widetilde{\Pi}(s,\mu)+(1-\mu^2)^{1/2}[1+s(1-s)\gamma_{,s}]\widetilde{\sigma}(s,\mu)\right\}\right\}.
\end{aligned}
$$

# Bibliography

[1] F. Weber, editor. *Pulsars as astrophysical laboratories for nuclear and particle physics*, 1999.

[2] W. Baade and F. Zwicky. Remarks on Super-Novae and Cosmic Rays. *Physical Review*, 46:76–77, July 1934.

[3] R. N. Manchester and J. H. Taylor. *Pulsars*. 1977.

[4] G. D. Birkhoff and R. E. Langer. *Relativity and modern physics*. 1923.

[5] J. R. Oppenheimer and G. M. Volkoff. On Massive Neutron Cores. *Physical Review*, 55:374–381, February 1939.

[6] R. C. Tolman. Effect of Inhomogeneity on Cosmological Models. *Proceedings of the National Academy of Science*, 20:169–176, March 1934.

[7] R. C. Tolman. Static Solutions of Einstein's Field Equations for Spheres of Fluid. *Physical Review*, 55:364–373, February 1939.

[8] R. W. Lindquist, R. A. Schwartz, and C. W. Misner. Vaidya's Radiating Schwarzschild Metric. *Physical Review*, 137:1364–1368, March 1965.

[9] L. Herrera, A. di Prisco, E. Fuenmayor, and O. Troconis. Dynamics of Viscous Dissipative Gravitational Collapse:. a Full Causal Approach. *International Journal of Modern Physics D*, 18:129–145, 2009.

[10] L. Herrera, A. di Prisco, J. Martin, J. Ospino, N. O. Santos, and O. Troconis. Spherically symmetric dissipative anisotropic fluids: A general study. *Phys.Rev.D*, 69(8):084026, April 2004.

[11] R. C. Duncan and C. Thompson. Formation of very strongly magnetized neutron stars - Implications for gamma-ray bursts. *Astrophysical Journal*, 392:L9–L13, June 1992.

[12] C. Thompson and R. C. Duncan. Neutron star dynamos and the origins of pulsar magnetism. *Astrophysical Journal*, 408:194–217, May 1993.

[13] S. A. Olausen and V. M. Kaspi. The McGill Magnetar Catalog. *Apj*, 212:6, May 2014.

[14] A. Melatos. Bumpy Spin-Down of Anomalous X-Ray Pulsars: The Link with Magnetars. *ApJl*, 519:L77–L80, July 1999.

[15] P. Chatterjee, L. Hernquist, and R. Narayan. An Accretion Model for Anomalous X-Ray Pulsars. *ApJ*, 534:373–379, May 2000.

[16] K. Makishima, T. Enoto, J. S. Hiraga, T. Nakano, K. Nakazawa, S. Sakurai, M. Sasano, and H. Murakami. Possible Evidence for Free Precession of a Strongly Magnetized Neutron Star in the Magnetar 4U 0142+61. *Physical Review Letters*, 112(17):171102, May 2014.

[17] C. Kouveliotou, G. J. Fishman, C. A. Meegan, W. S. Paciesas, J. van Paradijs, J. P. Norris, R. D. Preece, M. S. Briggs, J. M. Horack, G. N. Pendleton, and D. A. Green. The rarity of soft $\gamma$-ray repeaters deduced from reactivation of SGR1806 - 20. *Nature*, 368:125–127, March 1994.

[18] R. Negreiros, C. Bernal, V. Dexheimer, and O. Troconis. Many aspects of magnetic fields in neutron stars. *Accepted by Universe Journal*, January 2018.

[19] G. B. Cook, S. L. Shapiro, and S. A. Teukolsky. Spin-up of a rapidly rotating star by angular momentum loss - Effects of general relativity. *ApJ*, 398:203–223, October 1992.

[20] K. N. Singh, N. Pant, and O. Troconis. A new relativistic stellar model with anisotropic fluid in Karmarkar space-time. *Annals of Physics*, 377:256–267, February 2017.

[21] S. Bonazzola, E. Gourgoulhon, M. Salgado, and J. A. Marck. Axisymmetric rotating relativistic bodies: A new numerical approach for 'exact' solutions. *Astronomy and Astrophysics*, 278:421–443, November 1993.

[22] J.A. Wheeler, C. Misner, Thorne k.s., and Freeman W.H. *Gravitation*. 1973.

[23] L. Herrera, A. Di Prisco, J. Ibáñez, and J. Ospino. Axially symmetric static sources: A general framework and some analytical solutions. *Phys.Rev.D*, 87(2):024014, January 2013.

[24] H. Bondi. The contraction of gravitating spheres. In *Proceedings of the Royal Society A*, volume 0167 of *Mathematical, Physical and Engineering Sciences*, 1964.

[25] H. Komatsu, Y. Eriguchi, and I. Hachisu. Rapidly rotating general relativistic stars. I - Numerical method and its application to uniformly rotating polytropes. *MNRAS*, 237:355–379, March 1989.

[26] A. Papapetrou. *Proc. Roy Irish Acad.*, 51:191, 1947.

[27] W. Bonnor. *Proc. Phys. Soc.*, 76:891, 1960.

[28] E. Gourgoulhon. 3+1 Formalism and Bases of Numerical Relativity. *ArXiv General Relativity and Quantum Cosmology e-prints*, March 2007.

[29] L. Smarr and J. W. York, Jr. Kinematical conditions in the construction of spacetime. *Phys. Rev. D*, 17:2529–2551, May 1978.

[30] J. M. Bardeen. A Variational Principle for Rotating Stars in General Relativity. *ApJ*, 162:71, October 1970.

[31] J. M. Bardeen. Timelike and null geodesics in the Kerr metric. In C. Dewitt and B. S. Dewitt, editors, *Black Holes (Les Astres Occlus)*, pages 215–239, 1973.

[32] S. Chandrasekhar. The Post-Newtonian Equations of Hydrodynamics in General Relativity. *ApJ*, 142:1488, November 1965.

[33] G. W. Collins, II. *The virial theorem in stellar astrophysics*. 1978.

[34] S. Bonazzola. The Virial Theorem in General Relativity. *ApJ*, 182:335–340, May 1973.

[35] S. Bonazzola and J. Schneider. An Exact Study of Rigidly and Rapidly Rotating Stars in General Relativity with Application to the Crab Pulsar. *ApJ*, 191:273–290, July 1974.

[36] C. Vilain. Virial theorem in general relativity - Consequences for stability of spherical symmetry. *ApJ*, 227:307–318, January 1979.

[37] J. Katz. COMMENT: A note on Komar's anomalous factor. *Classical and Quantum Gravity*, 2:423–425, May 1985.

[38] A. Lichnerowicz. *Relativistic Hydrodynamics and Magnetohydrodynamics*. 1967.

[39] R. L. Arnowitt, S. Deser, and C. W. Misner. *Canonical analysis of general relativity*, page 127. 1962.

[40] A. Komar. Covariant Conservation Laws in General Relativity. *Physical Review*, 113:934–936, February 1959.

[41] E. Gourgoulhon and S. Bonazzola. A formulation of the virial theorem in general relativity. *Classical and Quantum Gravity*, 11:443–452, February 1994.

[42] J. Katz and A. Ori. Localisation of field energy. *Classical and Quantum Gravity*, 7:787–802, May 1990.

[43] R. Beig. Arnowitt-Deser-Misner energy and g $_{00}$. *Physics Letters A*, 69:153–155, December 1978.

[44] A. Ashtekar and A. Magnon-Ashtekar. On conserved quantities in general relativity. *Journal of Mathematical Physics*, 20:793–800, May 1979.

[45] B. Carter. Black hole equilibrium states. In C. Dewitt and B. S. Dewitt, editors, *Black Holes (Les Astres Occlus)*, pages 57–214, 1973.

[46] J. M. Bardeen and R. V. Wagoner. Relativistic Disks. I. Uniform Rotation. *ApJ*, 167:359, August 1971.

[47] S. Bonazzola and G. Maschio. Models of Rotating Neutron Stars in General Relativity. In R. D. Davies and F. Graham-Smith, editors, *The Crab Nebula*, volume 46 of *IAU Symposium*, page 346, 1971.

[48] M. Bocquet, S. Bonazzola, E. Gourgoulhon, and J. Novak. Rotating neutron star models with a magnetic field. *AAP*, 301:757, September 1995.

[49] J. Lense and H. Thirring. Über den Einfluß der Eigenrotation der Zentralkörper auf die Bewegung der Planeten und Monde nach der Einsteinschen Gravitationstheorie. *Physikalische Zeitschrift*, 19, 1918.

[50] W. B. Bonnor. Dragging of inertial frames by a charged magnetic dipole. *Physics Letters A*, 158:23–26, August 1991.

[51] L. Herrera and W. Barreto. Electromagnetic radiation produces frame dragging. *Phys.Rev.D*, 86(6):064014, September 2012.

[52] L. Herrera, G. A. González, L. A. Pachón, and J. A. Rueda. Frame dragging, vorticity and electromagnetic fields in axially symmetric stationary spacetimes. *Classical and Quantum Gravity*, 23:2395–2408, April 2006.

[53] T. G. Cowling. The stability of gaseous stars. *MNRAS*, 94:768–782, June 1934.

[54] H. Alfven. *Cosmical electrodynamics*. 1950.

[55] P. Goldreich and A. Reisenegger. Magnetic field decay in isolated neutron stars. *ApJ*, 395:250–258, August 1992.

[56] C. Kittel and H. Kroemer. *Thermal Physics*, volume 2. W. H. Freeman, 1980.

[57] A. Vidal. *Fisica Estadistica*. Universidad Central de Venezuela, Facultad de Ciencias, Escuela de Fisica, 3 edition, 2007.

[58] E. Gourgoulhon. An introduction to the theory of rotating relativistic stars. *ArXiv e-prints*, March 2010.

[59] C. Mysner and D. Sharp. *Phys. Rev.*, 136:B571, 1964.

[60]  R. P. Feynman. *Feynman lectures on physics. Volume 2: Mainly electromagnetism and matter.* 1964.

[61]  M. May and R. White. *Phys. Rev.*, 141:1232, 1966.

[62]  R. C. Tolman. On the Use of the Energy-Momentum Principle in General Relativity. *Physical Review*, 35:875–895, April 1930.

[63]  E. T. Whittaker. On Gauss' Theorem and the Concept of Mass in General Relativity. *Proceedings of the Royal Society of London Series A*, 149:384–395, April 1935.

[64]  L. Herrera, J. Ospino, A. di Prisco, E. Fuenmayor, and O. Troconis. Structure and evolution of self-gravitating objects and the orthogonal splitting of the Riemann tensor. *Phys. Rev. D*, 79(6):064025, March 2009.

[65]  R. M. Wald. *General relativity.* 1984.

[66]  C. W. Misner, K. S. Thorne, and J. A. Wheeler. *Gravitation.* 1973.

[67]  A. D'Aì, P. A. Evans, D. N. Burrows, N. P. M. Kuin, D. A. Kann, S. Campana, A. Maselli, P. Romano, G. Cusumano, V. La Parola, S. D. Barthelmy, A. P. Beardmore, S. B. Cenko, M. De Pasquale, N. Gehrels, J. Greiner, J. A. Kennea, S. Klose, A. Melandri, J. A. Nousek, J. P. Osborne, D. M. Palmer, B. Sbarufatti, P. Schady, M. H. Siegel, G. Tagliaferri, R. Yates, and S. Zane. Evidence for the magnetar nature of 1E 161348-5055 in RCW 103. *MNRAS*, 463:2394–2404, December 2016.

[68]  N. Rea, A. Borghese, P. Esposito, F. Coti Zelati, M. Bachetti, G. L. Israel, and A. De Luca. Magnetar-like Activity from the Central Compact Object in the SNR RCW103. *ApJl*, 828:L13, September 2016.

[69]  N. K. Glendenning. Neutron stars are giant hypernuclei? *ApJ*, 293:470–493, June 1985.

[70]  N. K. Glendenning. The hyperon composition of neutron stars. *Physics Letters B*, 114:392–396, August 1982.

[71] C. Y. Cardall, M. Prakash, and J. M. Lattimer. Effects of Strong Magnetic Fields on Neutron Star Structure. *ApJ*, 554:322–339, June 2001.

[72] M. Prakash, J. R. Cooke, and J. M. Lattimer. Quark-hadron phase transition in protoneutron stars. *Phys. Rev. D*, 52:661–665, July 1995.

[73] J. Zimanyi and S. A. Moszkowski. Nuclear equation of state with derivative scalar coupling. *Phys. Rev. C*, 42:1416–1421, October 1990.

[74] K. Ioka and M. Sasaki. Relativistic Stars with Poloidal and Toroidal Magnetic Fields and Meridional Flow. *ApJ*, 600:296–316, January 2004.

[75] V. A. P. Alfradique, O. N. Troconis, and R. P. Negreiros. Equatorial Geodesics Around the Magnetars. In *International Journal of Modern Physics Conference Series*, volume 45 of *International Journal of Modern Physics Conference Series*, page 1760050, 2017.

[76] O. Troconis, V. Alfradique, and R. Negreiros. About Bonnor Solution and Gravitational Redshift. In *International Journal of Modern Physics Conference Series*, volume 45 of *International Journal of Modern Physics Conference Series*, page 1760048, 2017.